Measurement of 6 by 6 Stiffness Matrix of the Knee Joint: Basis for Biomechanical Principles of Knee Surgery

by

Yukun Zhang

BS, Northwestern Polytechnical University, Xian, China, 2018

Submitted to the Graduate Faculty of the

Swanson School of Engineering in partial fulfillment

of the requirements for the degree of

Master of Science in Bioengineering

University of Pittsburgh

2020

UNIVERSITY OF PITTSBURGH

SWANSON SCHOOL OF ENGINEERING

This thesis was presented

by

Yukun Zhang

It was defended on

July 21, 2020

and approved by

Kevin M. Bell, PhD, Assistant Professor, Department of Orthopaedic Surgery and Bioengineering

Volker Musahl, MD, Professor, Department of Orthopaedic Surgery and Bioengineering

Thesis Advisor: Richard E. Debski, PhD, Professor, Department of Bioengineering

Measurement of 6 by 6 Stiffness Matrix of the Knee Joint: Basis for Biomechanical Principles of Knee Surgery

Yukun Zhang, MS

University of Pittsburgh, 2020

The knee is the largest joint in the human body and gets injured frequently because of its complex structural characteristics and the external load it carries. Stiffness is thought to be an important factor in musculoskeletal performance, either too much or too little stiffness may lead to injury. For the knee joint with 6 degrees of freedom, a 6 by 6 stiffness matrix, including both primary and secondary stiffness, can be built to improve the understanding of the load-carrying characteristics and structural properties of the knee. However, the quantifying of the stiffness matrix at different joint positions remains unclear. In some attempts to develop the stiffness matrix, linear elastic theory has always been assumed while the knee joint is a nonlinear system or the stiffness was measured separately on each degrees of freedom.

Therefore, the overall objective of this work was to develop a protocol to derive the 6 by 6 stiffness matrix of the porcine knee joint by using a robotic testing system and investigate the knee stiffness coefficients as a function of joint positions. Six intact porcine cadaveric knees were used. 45 joint positions at 30°, 60°, and 90° of flexion were chosen as the target position. At each joint position, force perturbation was performed by inputting additional loads on all directions and measuring the corresponding displacements of 6 DOFs to derive the compliance matrix. Then the stiffness matrix could be calculated by inverting the whole compliance matrix. This method overcame the two major limitations previously: 1. Measure the stiffness matrix by assuming the knee joint was a linear system; 2. Measure the nonlinear stiffness throughout the range of motion instead of building a matrix. Thus, the current work successfully quantified the stiffness matrix at

any desired joint positions. The primary stiffness from the stiffness matrices have been validated by literature and the quantification of secondary stiffness also has implications to knee function. The understanding of stiffness matrix and 6 by 6 joint biomechanics further provides an excellent foundation to pursue the improvement of the diagnostic procedure and surgical reconstruction of the knee joint.

Table of Contents

List of Tables

List of Figures

Preface

I would like to acknowledge my thesis advisor, Dr. Richard Debski, for all his support, guidance, and most importantly, for allowing me to perform my graduate research in Orthopaedic Robotics Laboratory. Specifically, when I first transferred from mechanical engineering to bioengineering, he gave many kind suggestions whenever I felt confused. In addition, I want to thank you for giving me the opportunity to continue to stay here for PhD study after this work. I will keep working hard and making contribution to our lab in the later few years.

I would also like to thank the remaining members of my thesis committee, Dr. Volker Musahl and Dr. Kevin Bell. Dr. Musahl has provided much valuable knowledge and advice from a clinical perspective. He inspired me with numerous clinical implications and future direction of this research. Dr. Bell has played a critical role in my thesis work with his expertise in the robotic testing system. He has tremendous input in the engineering area especially robotic protocol and biomechanics. Thank both of you for your generous effort and advice that you have given me.

Besides, thanks to all the colleagues in ORL. Calvin, you have a huge contribution to my work with help me to perform all my test on the robotic testing system. Every time you would sit there the whole day for adjusting the robot protocol and check if everything is in the safe range. I appreciate all your contribution to my graduate work. Gerald, you are the first person I met in this lab and always made people laugh, also helped me a lot academically. Hope you doing well in Philadelphia. Luke, you are like a big brother to me. Every time I had some questions the first person in my head was you and I would always feel that everything was clear after talking with you. And your smile always made my day. Satoshi Y. and Satoshi T., thank both of you for your

advice in engineering and clinical area. I look forward to my next trip to Japan. I wish the best to all of you.

Mentioning a few friends along the way… Yifei, as my roommate, I almost spent every day with you in these two years. We had a really good time and our apartment was always filled with laughter. Also, we had common hobbies in classical music and good corporation in many pieces though I was always the piano accompaniment for your violin. Yunxing, I always felt you knew everything and learned a lot from you in both academic and life aspects. My little basketball team, Captain Yang, Dongwen and Young, thanks for all the happy time we spent in basketball, beer and hotpot. Xiaochang, one of my greatest regrets is that it was too late to meet you. You took me into the world of rock music and I opened the door for you to classical. Though we spent very little time together, thank you for making my life brighter during this tough time. I sincerely bless you and hope you will have a promising future in your career.

Last but not least, I would like to thank my parents. I could never thank you enough for your selfless devotion this far. You gave me the best guidance, support, and encouragement in my life and education and always driven me further and further. Every time I hit the low point you will always be there to hearten me. And you would always support my decision on my education. I am so lucky to have such enlightened and open-minded parents like you. Thank you from the bottom of my heart.

1.0 Introduction and Background

Stability of the knee joint is maintained through a complex interplay of all the musculoskeletal components, including bony contact and soft tissue restraints. Stiffness matrix is an important factor represents the structural characteristics and will be the primary focus of this work. The structure and biomechanics of the osseous components and ligaments of the knee have been analyzed by many previous studies, and will be discussed in detail in Section 1.1 and 1.2. The definition and calculation of the stiffness matrix will be talked in Section 1.3. Even with all of the previous research, however, the measurement and implications of the 6 by 6 stiffness matrix of the knee joint has not been clarified.

1.1 Structure of the Knee

1.1.1 Human Knee

The knee is the largest joint in the human body and one of the most often injured joints because of its complex anatomic and structural characteristics [20]. It consists of three osseous components, femur, patella, and tibia (Figure 1.1). The femur is the longest bone in human body, which supports the weight of the body and allows motion of the leg [4]. Tibia, or shin bone, functions in supporting the powerful muscles that move the lower leg and stabilizing the ankle. Patella is the largest sesamoid bone in the body [9]. It acts as a fulcrum to increase the extensor

moment arm of the quadriceps [8]. These three bones together form two joints: the tibiofemoral joint and the patellofemoral joint [9], which comprise the knee.

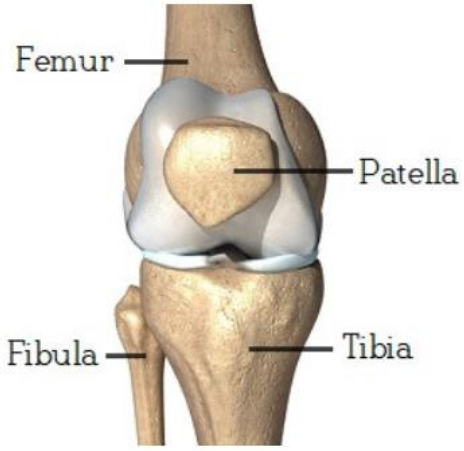

Figure 1.1 Osseous structure of knee joint [28]

The ligaments join the bones of the knee and provide stability to the knee structure by limiting movement. There are four major ligaments in the knee that connect the femur to the tibia: anterior cruciate ligament (ACL), posterior cruciate ligament (PCL) (Figure 1.2), medial collateral ligament (MCL), and lateral collateral ligament (LCL) (Figure 1.3). ACL originates from the medial wall of the lateral femoral intercondylar notch and inserts into the anterior intercondylar area of the tibial plateau [20]. It consists of two major bundles: the anteromedial (AM) and posterolateral (PL) bundle. Both bundles together contribute to the rotational and anteroposterior stability of the knee [20]. The AM bundle becomes tight during knee flexion whereas the PL bundle tightens in extension [12]. PCL inserts into the lateral wall of the medial femoral intercondylar notch and attaches to the posterior intercondylar area of the tibia [19, 20]. It also has two bundles: the anterolateral (AL) and the posteromedial (PM) bundle. In extension, the PM

bundle is tight and during flexion, the AL bundle tightens more [18, 21]. For the pair of the collateral ligament, the MCL has two layers, one deep and the other superficial layer. The superficial layer functions in primary static medial stability of the knee [17]. And the deep layer extends from the medial femoral condyle to the medial tibial condyle [20] and adheres to the medial meniscus [22]. LCL is a cordlike band that extends from the lateral epicondyle of the femur to the fibular head [22].

Figure 1.2 Cruciate ligaments of the knee [27]

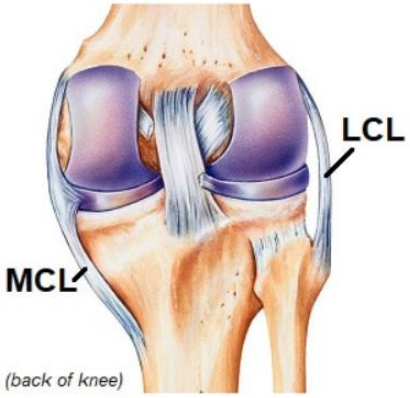

Figure 1.3 Collateral ligaments of the knee [26]

The meniscus is a fibrocartilage structure functions in absorbing shock between femur and tibia [22]. The meniscus is a smooth, lubricated tissue [10], which has medial and lateral, two half-moon-shaped structures located on the medial and lateral aspects of the tibial condyles [20] (Figure 1.4). The medial meniscus is C shaped, with its medial portion is firmly adherent to the deep fibers of the MCL. The anterior horn is attached to the tibia plateau and the posterior horn is attached to the intercondylar fossa of the tibia [10]. All these strong insertions make the medial meniscus is less mobile than the lateral and has a greater risk of injury [20]. The lateral meniscus is almost circular with an O shape. Both anterior and posterior horns are attached to the tibia. The lateral side of it is not attached to the LCL thus the lateral meniscus is more mobile than the medial meniscus [10] and the mobility protects it from injury.

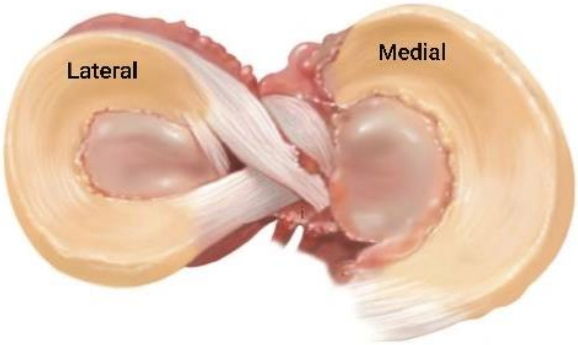

Figure 1.4 The superior aspect of the tibial plateau in an anatomic specimen [22]

1.1.2 Porcine Knee

Like the human knee joint, the porcine knee joint comprises the same osseous components and soft tissues that include four ligaments (ACL, PCL, MCL, and LCL), two meniscuses (medial

meniscus and lateral meniscus), and a patellar tendon [1]. Some previous studies demonstrated that there was some significant difference in the dimension between human and porcine knee. Not like the human knee can attain full extension, the minimum extension angles of the porcine was around 30 ~ 40 degrees [2, 69]. After normalization, the porcine ACL and PCL were significantly longer than the human counterpart. The human notch is proportionally significantly wider than the notch of the porcine knee. And the tibial insertion site of the ACL was split by the anterior lateral meniscus attachment in the porcine knees. Takroni and coworkers [3] compared human and porcine knee meniscus. They investigated that the circumference of human menisci was significantly longer than that of the pig. The porcine meniscal weight (medial: 5.0 g, lateral: 6.4 g) was significantly greater than the human (medial: 4.4 g, lateral: 4.9 g). The dimensions measured in the porcine meniscus were generally larger than human menisci with a significant difference in most categories.

1.2 Biomechanics of the Knee

The knee joint has six degrees of freedom for the movement of the tibia with respect to the femur in 3-D space. It has three translations: anterior-posterior (AP), medial-lateral (ML), and proximal-distal (PD), combined with the change of orientation through rotation about the axes of the three translations: varus-valgus (VV, about AP axis), flexion-extension (FE, about ML axis), and internal-external (IE, about PD axis).

Ligaments are the primary static stabilizers for the knee joint. The major function of the knee ligaments is to stabilize the knee, control normal kinematics, and prevent abnormal translations or rotations to avoid getting injuries of the soft tissues [20]. The ACL is the primary

restraint to anterior translation of the tibia with respect to the femur, and the remaining ligamentous and capsular structures provide only a small secondary restraint, contribute less than 3% of the restraining force of anterior tibial translation on femur [6]. For a human knee joint, the anterior-medial bundle is always taut in flexion, tested with anterior drawer, whereas the posterior-lateral bundle mostly tightens in extension and is tested with Lachman's test. The PCL is the primary structure resisting posterior translation of the tibia relative to the femur, providing 94% of the total restraining force at 30 and 90 degrees of knee flexion. None of the remaining ligamentous and capsular structures provide more than 2% of the restraining force of the posterior tibial translation on femur [6, 7]. Both cruciate ligaments also function as restraints to the rotation of the knee joint. When an anterior-directed shear load is applied to the tibiofemoral joint, the ACL produces an internal tibial rotation, whereas the PCL produces an external tibial rotation with the applied posterior tibial load [13]. Gollehon and coworkers [7] showed that isolated transaction of the PCL did not affect varus or external rotation of the tibia. However, when the PCL was sectioned after the LCL and deep ligament complex had been cut, a significant increase in varus rotation, posterior translation, and external rotation at all angles of knee flexion had been investigated. Wascher and associates [15, 24] measured force in the ACL and the PCL in the intact cadaveric knee under different loading conditions. They found the force in the ACL increases when anterior tibial force combined with internal tibial torque at full extension or valgus moment at knee flexion angles greater than 10 degrees. The combination of posterior tibial force, internal torque, and varus moment produced the greatest forces in the PCL.

Other studies have attempted to assess the primary function of the collateral ligaments. Warren and colleagues [23] demonstrated that after sectioning the long fibers of the MCL complex, a significant increase in valgus rotation and external rotation of the tibia could be investigated.

Grood and associates [11] stated that the long superficial portion of the MCL complex provided 57.4% restraining moment of the valgus rotation at 5 degrees of knee flexion angle, whereas ACL and PCL together provided 14.8%. At 25 degrees flexion angle, the valgus restraint would increase to 78.2%. They also demonstrated that the LCL provided 54.8% of the total varus restraint at 5 degrees knee flexion and 69.2% at 25 degrees. Gollehon and coworkers [7] found that the LCL and deep ligament complex function together as the principal structures resisting varus and external rotation of the tibia. Blankevoort and Huiskes [5] stated that both collateral ligaments acted as direct restraint to the axial rotation for external rotation of the tibia.

Though differences in size and full extension position were investigated between porcine knee and human knee [2], the porcine was still often used in biomedical studies as a valid animal model. Boguszewski and associates demonstrated that the porcine knee model could be used in the study for ACL function [63]. They found ACL was the primary restraint, accounting for 80-125% of anterior force, throughout the simulated anterior tibial motion in 2 mm increments from 0 mm to 10 mm. Xerogeanes and colleagues stated that porcine knee may be a preferred animal model for ACL experimental studies compared to goat and sheep knees [64]. During 50 and 100 N anterior tibial force at 90° of flexion, the only significant difference between human and porcine was the magnitude and direction of the *in situ* force in the PL bundle. An increased laxity in varus-valgus was found in the ACL injured porcine knee compared to the intact knee, but the laxity could be weakened by adding posterior tibial load [65]. Human knee showed the same characteristics that ACL functioned to restrain the varus and valgus rotation [66].

1.3 Stiffness Matrix

1.3.1 Stiffness

Stiffness refers to the ability of a material or structure to resist deformation when subjected to an applied force [51]. It is a characterization of the difficulty of elastic deformation of materials or structures, which is one of the most significant properties of a mechanism. The basic definition of stiffness is:

$$K = \frac{F}{u} \tag{1.1}$$

Or by Hooke's Law

$$F = Ku \tag{1.2}$$

where K is proportionality constant, and it describes the stiffness of a system. F is the applied load. u is the deformation created by the load. The load can be forces or moments applied on a structure and the deformation can be displacement or angles [51]. In terms of the knee joint, stiffness is a biomechanical parameter that describes the deformation of on bone with respect to another bone in response to an applied force or moment [48]. It is a combination of the stiffness contributed by ligaments, cartilage, tendons, muscles, and bone [62].

1.3.2 Stiffness Matrix

For a system that has multi-degree of freedom, a stiffness matrix can be built with several stiffness terms associated with these degrees of freedom. When a displacement on a pure axis is

applied to a multiple DOF structure, there would be a force on that direction in response to this pure displacement. The coefficient relates the applied displacement and the response force in the same direction is called the primary stiffness coefficient. At the same time, there would be several coupled forces on other axes following the applied displacement. The coefficient relates the force component and the displacement component in a different direction is called the secondary stiffness coefficient [44]. Some studies also called the secondary stiffness coefficients as the coupled stiffness coefficients [44, 45]. Broadly speaking, the stiffness matrix coefficients can map the applied loads with the displacements on all the DOFs of a structure [60].

For a structure that has 6 DOFs, the stiffness matrix [*K*] is:

$$\begin{bmatrix} F_1 \\ F_2 \\ F_3 \\ F_4 \\ F_5 \\ F_6 \end{bmatrix} = \begin{bmatrix} K_{11} & K_{12} & K_{13} & K_{14} & K_{15} & K_{16} \\ K_{21} & K_{22} & K_{23} & K_{24} & K_{25} & K_{26} \\ K_{31} & K_{32} & K_{33} & K_{34} & K_{35} & K_{36} \\ K_{41} & K_{42} & K_{43} & K_{44} & K_{45} & K_{46} \\ K_{51} & K_{52} & K_{53} & K_{54} & K_{55} & K_{56} \\ K_{61} & K_{62} & K_{63} & K_{64} & K_{65} & K_{66} \end{bmatrix} \times \begin{bmatrix} u_1 \\ u_2 \\ u_3 \\ u_4 \\ u_5 \\ u_6 \end{bmatrix} \tag{1.3}$$

where

$$F_i = K_{ij} u_j \quad i = 1-6, j = 1-6$$

The number 1-6 represent the 6 DOFs of the structure. The 6 coefficients of the diagonal, K_{11}, K_{22}, K_{33}, K_{44}, K_{55}, K_{66}, are the primary stiffness coefficients. The other 30 coefficients are secondary stiffness coefficients. K_{21} indicates that when a pure displacement u_1 in direction 1 is applied, the force in direction 2 would be $F_{21}=K_{21}\times u_1$. And K_{12} denotes the force in direction 2 in response to a unit displacement in direction 1, which has $F_{12}=K_{12}\times u_2$. According to the conservation of energy principle, $K_{21}=K_{12}$. Therefore, the whole stiffness matrix is symmetric under the assumption of linear elastic theory [44, 61]. $K_{ij}=K_{ji}$. However, for a biological knee joint

the stiffness matrix is not symmetric due to the contact with friction and nonlinear elastic characteristics of the structure [36].

1.3.2.1 Compliance Matrix

Same as stiffness matrix, the compliance matrix is made up of the compliance coefficients from a multi-degree of freedom system. For a structure that has 6 DOFs, the compliance matrix [C] is:

$$\begin{bmatrix} u_1 \\ u_2 \\ u_3 \\ u_4 \\ u_5 \\ u_6 \end{bmatrix} = \begin{bmatrix} C_{11} & C_{12} & C_{13} & C_{14} & C_{15} & C_{16} \\ C_{21} & C_{22} & C_{23} & C_{24} & C_{25} & C_{26} \\ C_{31} & C_{32} & C_{33} & C_{34} & C_{35} & C_{36} \\ C_{41} & C_{42} & C_{43} & C_{44} & C_{45} & C_{46} \\ C_{51} & C_{52} & C_{53} & C_{54} & C_{55} & C_{56} \\ C_{61} & C_{62} & C_{63} & C_{64} & C_{65} & C_{66} \end{bmatrix} \times \begin{bmatrix} F_1 \\ F_2 \\ F_3 \\ F_4 \\ F_5 \\ F_6 \end{bmatrix} \tag{1.4}$$

and

$$C_{11} = \frac{u_1}{F_1}, C_{21} = \frac{u_2}{F_1}, C_{31} = \frac{u_3}{F_1}$$

$$C_{41} = \frac{u_4}{F_1}, C_{51} = \frac{u_5}{F_1}, C_{61} = \frac{u_6}{F_1} \tag{1.5}$$

The diagonal of this compliance matrix is the primary compliance coefficient, which indicates the relationship between the force and displacements on the same direction. The other 30 items are secondary compliance coefficients.

1.3.2.2 Stiffness Matrix Calculation

In previous biomechanics studies, there were two major methods to derive stiffness matrix: stiffness method or compliance method.

For the stiffness method, a single known displacement u was input each time. Therefore in [u] only one displacement element is non zero. By measuring the forces in response to this single

displacement on all the directions, one column of the stiffness matrix related to the displacement could be calculated by $K_{ij}=F_i/u_j$ [45].

However, some studies stated that stiffness method is difficult experimentally because a displacement on one pure axis is unphysiological. Therefore, compliance method has been introduced [40, 41, 44], which is to measure the compliance coefficients and then take the invert of the whole compliance matrix to obtain the stiffness matrix. For the compliance method, a single force on one direction was input. By measuring the displacements that resulted from the application of force on all the DOFs, one column of the compliance matrix can be derived through $C_{ij}=u_i/F_j$. The whole compliance could be built up after inputting all the forces on all the DOFs [40, 41, 44]. The relationship between stiffness matrix and compliance matrix is:

$$[K] = [F] \times [u]^{-1} = ([u] \times [F]^{-1})^{-1} = [C]^{-1} \quad (1.6)$$

Thus, with the results of compliance matrix, stiffness matrix can be easily derived by taking the inverse of the whole compliance matrix. Errors will develop if stiffness matrix coefficients are just the reciprocal of the corresponding coefficients in compliance matrix [44].

Both of these two methods can be applied to discrete joint positions or a continuous displacement. To derive the stiffness matrix at discrete joint positions, a small force or displacement will be applied on one direction and measure the output displacement or force on six directions. Thus, stiffness matrix can be derived by performing a perturbation at one joint position. For the continuous method, the forces or displacements are inputted throughout the range of motion to obtain a load-displacement curve to depict the stiffness characteristics on one direction, which is a more common method to derive the nonlinear stiffness in previous studies [36, 45, 48, 56].

1.3.3 Robotic Testing System

Different experimental apparatus was used in previous studies to measure the 6 by 6 stiffness matrix [40, 45, 46] or the load-carrying characteristics of the knee joint [36, 48]. For the six-degree-of-freedom instrumented spatial linkage used for experimental measurement [40], the sensitivity of displacement was low with 0.5 mm or 0.5°. Thus, the small displacement less than that sensitivity would be assumed to be zero, which could cause inaccuracy. In addition, the precise orientation and position of Cartesian coordinate systems were difficult to locate, which can lead to error in the direction of applied loads.

In this current work, a novel robotic testing system [37] with six degrees of freedom will be used to measure the stiffness matrix of the knee joint. A widely accepted coordinate system for the knee joint [67, 68] was used for comparing procured results to other studies or clinical observation and reproducing the joint motion. The fixation clamps for the femur and tibia were connected to lower and upper mechanism separately. The compliance of the system was 0.001 mm/N in vertical and longitudinal directions and 0.003 mm/N in lateral direction. The displacement repeatability was 0.001 ± 0.003 mm in vertical direction, 0.005 ± 0.007 mm in longitudinal direction and 0.084 ± 0.027 mm in lateral direction under a load of 500 N applied to the clamps. Overall, the performance of this robotic system should be better with a lower compliance and displacement error and it will be more easily to quantify stiffness matrix.

2.0 Motivation: Research Question and Hypothesis

Knee is the largest joint in the human body and gets injured frequently because of its complex structural characteristics and the external load it carries. A thorough understanding of the locomotion and biomechanics of the knee is very important to several fields, including knee reconstruction, knee modeling, rehabilitation and physical therapy [49]. Stiffness is thought to be an important factor in musculoskeletal performance, either too much or too little stiffness may lead to injury [34]. And for a multi-degree of freedom structure like the knee joint, a stiffness matrix can be built to describe the structural characteristics of the total 6 motions. Both primary and secondary stiffness coefficients will be used to describe the load-displacement change of all the degrees of freedom. Thus, the study of knee stiffness matrix would improve our understanding of the load-carrying characteristics of the knee, which is a basic biomechanical principle for diagnostical and surgical procedure, as well as the design of knee replacement devices.

2.1 Motivation for Specific Aims

Stiffness is a structural property that indicates the resistance of the deformation in response to an applied force or moment [51]. The stability of the knee joint is maintained by all the components of the knee, including the osseous structure and soft tissues. And the stiffness contributed by all the structures of the knee joint together composes the stiffness matrix of the whole knee joint [62], which represents the load-displacement characteristics and stability of the knee on 6 DOFs. Stiffness matrix measured for a human knee could be used to establish a 3-D

structural model of the knee joint and allow the study of particular structural elements, such as examining the role of ACL graft in ACL reconstruction on joint motion and tissue forces [40], by assuming linear elastic theory. However, the knee joint has nonlinear structural characteristics and the stiffness coefficients are highly nonlinear. The value of both primary and secondary stiffness is different as the initial orientation of the knee joint is varied, which identifies the knee as a nonlinear coupled structural system, and both the nonlinear nature and shifts in the minimum stiffness position can be quantitatively observed by using stiffness method [45]. On AP direction, the human knee with an intact ACL has both low and high stiffness regions as the anterior load is increased and the primary stiffness of anterior load-displacement curve could be different at different flexion angles [36]. From the load-displacement curve on medial-lateral direction, when the tibia is displaced medially or laterally, cruciate ligaments would contribute to resisting the applied medial-lateral displacement. The ACL resists medial tibial motion and the PCL prevents the lateral displacement of the tibia [29, 46]. And on internal-external and varus-valgus direction, the torsional joint stiffness would increase as the magnitude of applied torque increased [38, 48] and there is a significant difference in torsional joint stiffness between genders [38] and right-left knee [35].

Besides the stiffness matrix of the human knee joint, the lower-limb multi-joint (knee and ankle) stiffness matrix plays an important role in functional activities such as walking [39]. The bending-torsional dynamic stiffness matrix calculated for aerofoil cross-section can be used to compute the natural frequencies and mode shapes [59]. Stiffness matrix of the human thoracic spine can be used to build mathematical models of the human spine structure, which can be applied to predict the biomechanical behavior of the spine [44]. Also, stiffness matrix of the external fixator is quantified and interpreted to evaluate the axial compliance of the fixators and facilitate

rapid and successful healing of bone fractures [41]. The load-displacement curve of the porcine on tibial anterior-posterior translation and internal-external rotation also has a nonlinear nature [56].

Even with all of the research about load-displacement and stiffness matrix of the knee joint that has been performed, the role of the whole stiffness matrix played in the knee joint is still not clear. Most previous studies only focus on the primary stiffness coefficients [36, 38, 48] and not all of the degrees of freedom [35, 39, 48], while the knee is actually a system with 6 degrees of freedom. The 6×6 Cartesian stiffness matrix is generally asymmetric if the forces and moments resulted from the linear elastic coupling is non-zero[58]. Some studies measured the whole stiffness matrix by assuming the linear elastic theory [40, 41, 44]. And the measurement protocol of the nonlinear coupled stiffness matrix of the human knee joint was only applicable to some specific joint positions with a fixed flexion angle [45]. The goal of this research is to develop a protocol to derive the 6 by 6 stiffness matrix of the knee joint and investigate the stiffness coefficients as a function of joint position. The protocol of the stiffness matrix measurement would work for any knee joint position. The long-term goal is to have the ability to assess the 6-DOF stiffness of knee in the intact, injured and reconstructed states. The motivation is that stiffness matrix of the knee could promise a better understanding of the structural characteristics of the knee, which is important in knee reconstruction and modeling.

With the measurement of stiffness at different joint positions which are very common in knee injuries, the difference in stiffness between the normal knee joint position and high-risk injury position could be investigated. Also, the stiffness data is significant for knee reconstruction to make the knee after reconstruction restore the structural characteristics back to the intact knee by comparing the stiffness matrix. Previous studies of biomechanics always compared the loads or displacements of an intact knee and the knee without parts of soft tissues [29, 46, 43]. By

comparing both the primary and secondary stiffness coefficients of the intact and ligament-deficient knee, the contribution of the ligament to the biomechanics of the knee could be investigated. And stiffness matrix data could be applied to establish a knee model to predict the biomechanical behavior of the knee [40], which is very useful in clinical diagnosis and knee structural characteristics research. Changing the stiffness of the knee model can be used for simulating the ligament injuries instead of cutting off ligaments from the cadaver for more cost-efficient.

2.2 Research Questions

For the current work, either using the stiffness method or compliance method, the stiffness coefficients are mostly derived from a continuous load-displacement curve on only one degree of freedom by taking the slope at one point. Thus, the stiffness coefficient only represents the stiffness of one position on one direction with no choice of the positions on other DOF. The method of measuring the stiffness matrix of a specific joint position which is a combination of different displacement of several DOF is not clear. Also, there is no good interpretation of the secondary stiffness coefficients, the implication of the secondary stiffness and its effect on the stability of the knee has not been clarified. This leads to the following research questions:

1. How can the nonlinear stiffness matrix be built at any specific position of the knee joint?

2. How do the primary and secondary stiffness coefficients change as a function of joint positions?

2.3 Specific Aims

These questions will be answered with the following specific aims:

Specific Aim 1: Develop a protocol to derive the 6 by 6 stiffness matrix of the porcine knee joint using a robotic testing system.

Specific Aim 2: Investigate the knee stiffness coefficients as a function of joint positions from 30° to 90° of flexion.

3.0 Measurement of The Stiffness Matrix

3.1 Introduction

The purpose of this study is to develop a protocol to derive the stiffness matrix at several specific joint positions, then investigate the stiffness coefficients as a function of different joint positions. Two methods have been reported in the literature, including the stiffness method [45] and compliance method [40, 41, 44]. To better control the forces and moments for not breaking the soft tissues of the knee joint, the compliance method has been chosen.

Some other studies derived the load-displacement curve on some directions and calculate the stiffness by taking the slope of the curve [35, 36, 38, 48], which was also the most common method previously implemented. A continuous displacement would also be applied to the knee joint in this study to see the difference between stiffness coefficients derived from the protocol in this study and that derived from the load-displacement curve.

3.2 Robotic Testing System

A robotic testing system (MJT Model FRS 2010, Chino, Japan) has been used [37], which has two different movable mechanisms. The femur was attached to the femur clamp, which was connected relative to the lower mechanism with one translational axis. And the upper mechanism consists of two translational axes and three rotational axes, which were connected to the clamp for the tibia and a universal force/moment sensor (UFS, ATI Delta IP60 (SI-660-60), Apex, NC).

Through the six-movement axes from both upper and lower mechanisms, all the six degrees of freedom of the knee joint can be manipulated, which is controlled by a LABVIEW Program (Technology Services Inc., Chino, Japan) and operated in hybrid velocity impedance control. For both femur and tibia, the z-axis is defined from the insertion sites of the MCL to that of the LCL. The positive direction of the y-axis is the proximal direction. The x-axis is defined to be perpendicular to both the y- and z-axes, where the anterior direction is positive. The repeatability for position and orientation of the robotic testing system is less than 0.015 mm and 0.01° [33]. The orthogonal configuration of the translational axes provides a low clamp-to-clamp compliance (0.001 mm/N in vertical and longitudinal directions, 0.003 mm/N in lateral direction) to be appropriate for mechanical testing of the knee joint.

3.2.1 Specimen Preparation

Six fresh-frozen porcine cadaveric knees (Specimen ID: PK191114, PK200204, PK200624, PK200626, PK200630, PK200702) were used in this study. Specimens were stored in -22 degrees Celsius were thawed overnight at room temperature before testing. All the soft tissues were kept intact. ACL transection was performed on one specimen (PK200702) to compare the stiffness matrix derived from both intact and ACL-deficient knee. During the experimental protocol, specimens were kept moist with spraying saline on the whole knee joint every half an hour.

3.2.2 Experimental Setup

The porcine knee joint was mounted on the six degrees of freedom robotic testing system (Figure 3.1). The femur was fixed to the lower plate and the tibia was secured to the tibia clamp

on the upper plate through a 6-DOF UFS. Two metal rods were drilled into femur and tibia to the clamp to avoid internal-external rotation of the two bones within clamps during test. The insertion site of MCL and LCL with respect to UFS was measured and recorded into the robotic system to locate the axis of flexion-extension. The proximal-distal direction was vertical to the plate. After reaching 30° of flexion, passive path, where forces and moments in 6 DOFs were adjusted to 0, was considered as initial state of joint positions.

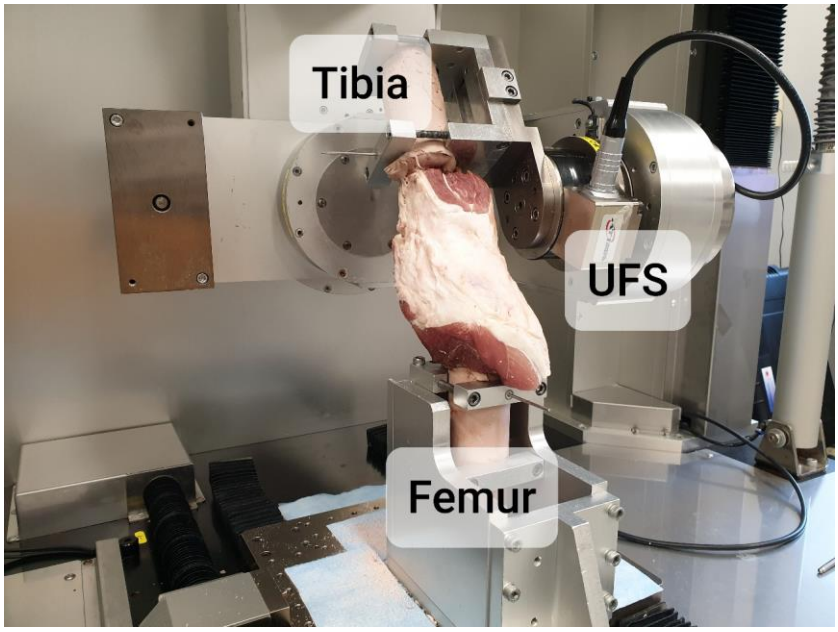

Figure 3.1 A porcine knee mounted in the robotic testing system at flexion 30°

3.3 Method of Measurement

From the previous studies, two major methods were used to derive stiffness matrix: stiffness method and compliance matrix [40, 41, 44, 45]. In the robotic testing system, the basic difference between these two methods is the input. The stiffness method is using position control,

which inputs a single displacement and measuring the output loads. However, in compliance method, a single force or moment is inputted and the output displacements are measured, which is force control. For this study, force control was chosen rather than position control to ensure the forces and moments are in the safe load condition, which is 100N for translation forces and 5N·m for rotation moments. Adding additional force is safer than additional displacement because the force can be controlled. Thus, the compliance method has been selected.

3.4 Protocol of Measurement

Different from the previous literature [36, 45, 46, 48], inputting a continuous displacement to derive a load-displacement curve which covers the whole range of motion on that direction and then calculate the stiffness from the curve, this study tried to develop a protocol to derive the stiffness matrix at any joint positions by using the robotic testing system.

3.4.1 Choice of Joint Positions

The porcine knee joint cannot reach the full extension position like the human knee, so three flexion angles, 30°, 60°, and 90° were selected. At each flexion angle, several joint positions were chosen as the target joint positions to derive the stiffness matrix. On each degree of freedom, the joint positions were decided by adding an additional displacement on that DOF based on the position of the passive path, which is the position satisfied the minimum force and moment. At each flexion angle, the joint positions are listed in Table 3.1:

Table 3.1 Joint positions at each flexion angle

AP	Passive path, PP +3mm, PP +5mm, PP -3mm, PP -5mm
PD	Passive path, PP +0.5mm, PP -0.5mm
ML	Passive path, PP +2mm, PP -2mm
VV	Passive path, PP +1deg, PP -1deg
IE	Passive path, PP +3deg, PP +5deg, PP -3deg, PP -5deg

PP – passive path

AP – anterior-posterior

PD – proximal-distal

ML – medial-lateral

VV – varus-valgus

IE – internal-external

All the magnitude of the displacements was selected to confirm the joint positions cover most of the range of motion on that direction and at the same time in a safe range. For the translational directions, joint positions with a force beyond 100 N would be considered to have a higher risk to get the soft tissues injured during the test. For the rotational directions, the load boundary was set to 5 N·m. Therefore, the additional joint positions were chosen to ensure the force or moment was within 100 N or 5 N·m respectively to keep the knee joint in an intact state during the test. On PD, ML and VV directions, two additional displacements were chosen as the extreme positions. On AP and IE direction, four joint positions were selected because some previous data showed that the load-displacement curve of these two DOFs was more nonlinear [36, 46, 48]. The full joint position list for this work is provided in Appendix Table 1.

3.4.2 Robotic Protocol

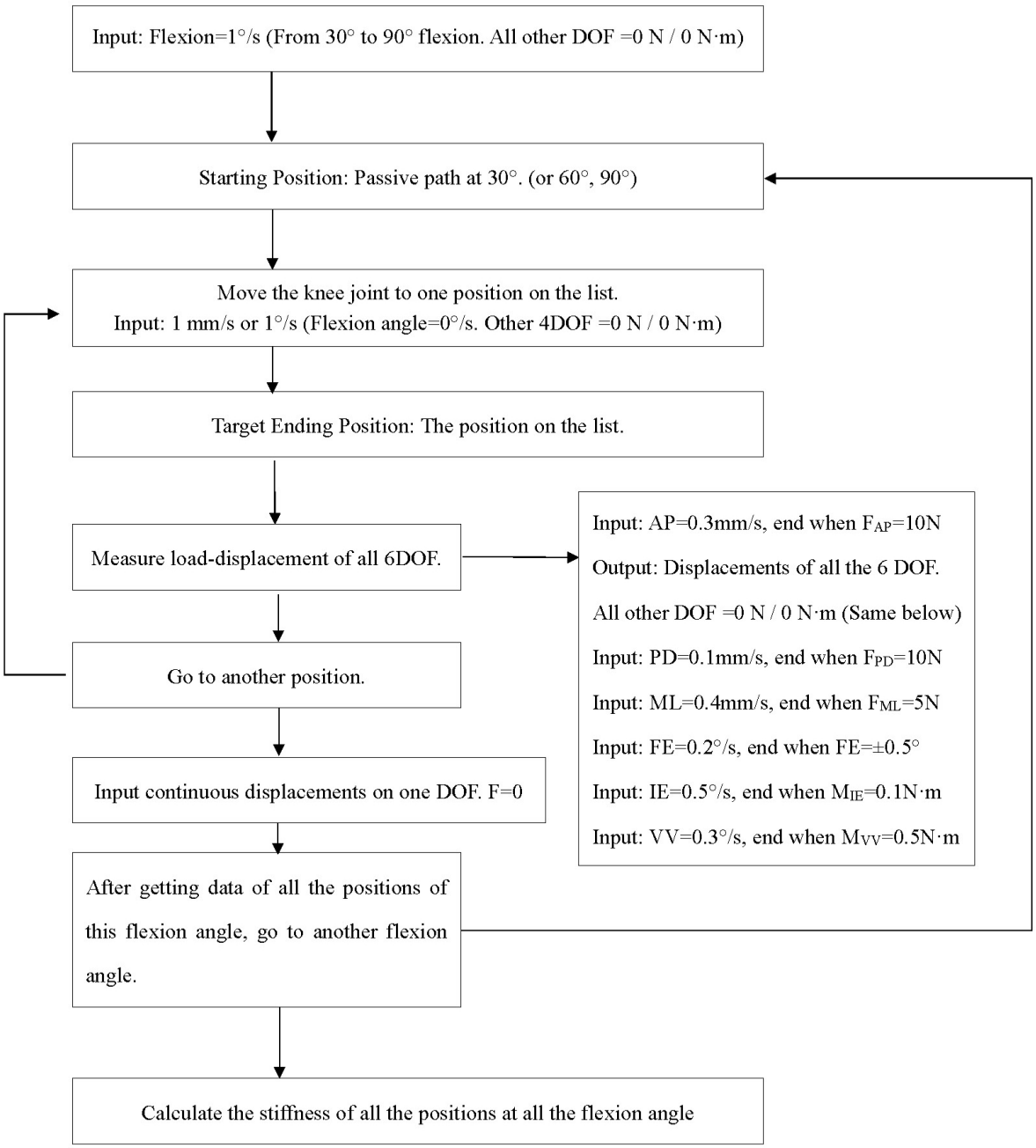

Figure 3.2 Robotic protocol flow chart of the measurement of stiffness matrix

The robotic protocol presented above has been implemented to measure the stiffness matrix at different joint positions. The passive path of each flexion angle (30°, 60°, and 90°) was first determined by moving the tibia in 1° increment of flexion per second while the forces and moments in the other DOFs stayed 0. The starting position was the passive path at each flexion angle and the 45 target ending positions were listed in Appendix Table 1. After reaching the target position by inputting 1mm/s or 1°/s on one DOF, the compliance matrix was measured by doing a perturbation on all 6 DOFs at that position. Force control was used when measuring the compliance matrix by adding a small additional force or moment on one direction at one time, then the six output displacements in response to that input load could be measured, therefore six load-displacement curves can be derived. By repeating this procedure for each of the six DOF, the 36 compliance coefficients could be derived. The values of the additional loads were chosen to ensure the corresponding displacements change are within 1 mm or 1° because the measurement of a stiffness matrix was performed at a desired joint position. On flexion-extension direction, position control rather than force control was selected to ensure that the flexion angle stays at target joint position during the measurement of the compliance matrix. In the preliminary test, an additional 0.3N·m moment applied on flexion-extension direction would move the tibia to a flexion angle far from the target joint position. To keep the flexion angle when measuring the compliance coefficients, additional displacements on flexion-extension direction were inputted to the tibia around 30° (or 60°, 90°) flexion. Still, only one moment and six displacements would change so even with position control on FE direction, force control can still be assumed for the matrix calculation.

The magnitudes of the force boundary and velocity of measuring the load-displacement curve in Figure 3.2 were decided from the preliminary test to identify the knee joint was moving

both under a safe condition and around the target joint position. For each perturbation, the forces or moments would be inputted five times. The first four times served as preconditioning cycle to the whole knee joint and the compliance coefficients were calculated by taking the slope of the fifth load-displacement curve derived from linear regression. In addition to the force perturbation around each joint position, a continuous displacement covered the range of motion was applied on one direction at one time and the corresponding force on the same direction was recorded. The load-displacement curve derived from the continuous displacement could be also used to calculate the primary stiffness by taking the slope. The primary stiffness coefficients derived from both methods would be investigated to compare the difference between the protocol in this study and the more traditional method in previous literature [36, 45, 46, 48].

3.5 Data Analysis

3.5.1 Stiffness Matrix at Each Joint Position

Compliance matrices were obtained at all the 45 joint positions for each knee joint, which include 36 coefficients in each of them. Each compliance coefficient was calculated from the load-displacement curve by linear regression. For a coefficient of determination R^2 lower than 0.60 or the displacement change during the additional force or moment smaller than 0.1mm or 0.2°, the compliance term was set to zero. These two criteria, which always been observed at the same time, were set due to the observation of several linear regression models. When R^2 was lower than 0.6 the linear regression model usually had a weaker prediction and goodness-of-fit. And a displacement even smaller than the robotic repeatability was also inaccurate and was assumed to

be zero. Take the additional AP load at 30° flexion passive path of the first specimen (PK191114) as an example (Table 3.2),

Table 3.2 Additional ±10N F_{AP} at 30° flexion passive path (Specimen ID: PK191114)

	AP (mm)	PD (mm)	ML (mm)	VV (deg)	IE (deg)	FE (deg)	F_{AP}(N)
Position	1.57	0.09	-1.43	-0.88	7.52	-30.02	0.38
From	1.55	0.15	-0.93	-0.53	3.78	-30.43	10.11
To	0.46	0.156	-0.98	-0.56	1.90	-30.66	-10.00
R^2	0.97	0.012	0.33	0.006	0.91	0.90	
C	0.063	0	0	0	0.115	0.014	

R^2 – coefficients of determination

C – compliance coefficients

the first row is the knee joint position of all six DOFs at passive path of 30° flexion. After reaching to that target position, an additional force on anterior-posterior direction F_{AP} was inputted from 10.1N to -10.0N and the six displacements in response to this force were measured. By linear regression, compliance coefficients related to F_{AP} were calculated as one column of the compliance matrix. The whole compliance matrix can be derived after the additional force or moment was inputted on six directions. The compliance matrix at 30 flexion of the first specimen is:

$$C_{Flex30} = \begin{bmatrix} 0.063 & 0.002 & 0.006 & 0 & 0.001 & -0.002 \\ 0 & 0.006 & -0.010 & 0 & 0 & 0 \\ 0 & -0.007 & 0.054 & 0.001 & -0.003 & 0 \\ 0 & -0.003 & 0.021 & 0 & -0.002 & 0 \\ 0.115 & -0.002 & -0.027 & 0.001 & 0.017 & 0 \\ 0.014 & 0 & -0.004 & 0 & 0.002 & 0.003 \end{bmatrix} \quad (3.1)$$

Then the stiffness matrix at this joint position can be calculated by taking inverse of the whole compliance matrix:

$$K_{Flex30} = \begin{bmatrix} 20.6 & -15.8 & -3.4 & -6.8 & -4.0 & 11.7 \\ -19.9 & 263.8 & 47.6 & 17.0 & 10.6 & 1.9 \\ -8.3 & 43.1 & 41.1 & 30.3 & 4.9 & -3.0 \\ -312.0 & 457.9 & -1593.6 & 4573.4 & 216.3 & -372.0 \\ -165.4 & 226.2 & 42.6 & 148.9 & 101.5 & -90.8 \\ -19.3 & 27.3 & 6.4 & 22.5 & -25.3 & 290.5 \end{bmatrix} \quad (3.2)$$

The definition of direction and units of the stiffness matrix are shown as below:

$$K = \left[\begin{array}{ccc:ccc} K_{11} & K_{12} & K_{13} & K_{14} & K_{15} & K_{16} \\ K_{21} & K_{22} & K_{23} & K_{24} & K_{25} & K_{26} \\ K_{31} & K_{32} & K_{33} & K_{34} & K_{35} & K_{36} \\ \hdashline K_{41} & K_{42} & K_{43} & K_{44} & K_{45} & K_{46} \\ K_{51} & K_{52} & K_{53} & K_{54} & K_{55} & K_{56} \\ K_{61} & K_{62} & K_{63} & K_{64} & K_{65} & K_{66} \end{array}\right]$$

Figure 3.3 Stiffness matrix

1-AP 2-PD 3-ML 4-VV 5-IE 6-FE

$$unit = \begin{bmatrix} \frac{N}{mm} & \frac{N}{deg} \\ \frac{N \cdot mm}{mm} & \frac{N \cdot mm}{deg} \end{bmatrix} \quad (3.3)$$

The diagonal of the stiffness matrix is the primary stiffness coefficients. Take the first column as an example, K_{11} is the primary stiffness on AP direction, all the other five coefficients are the secondary stiffness that connects the displacement on AP to the forces or moments on other DOFs as defined by number. When an anterior displacement u on the tibia was applied, the force on PD direction in response to u is $F_{PD} = K_{21} \times u_{AP} = -19.9 \times u_{AP}$; the moment on varus-valgus direction caused by u_{AP} is $M_{VV} = K_{41} \times u_{AP} = -312.0 \times u_{AP}$. The data were statistically analyzed using one-way ANOVA and Tukey's HSD post-hoc test at a confidence level of 95% to show difference in stiffness coefficients among different joint positions. Multiple linear regression model was used to fit the stiffness coefficients as a function of joint positions.

3.5.2 Primary Stiffness Derived from Load-displacement Curve

To compare the stiffness coefficients derived from this study with those from the method of previous literature, load-displacement curves that cover the range of motion on each DOF were used to calculate the primary stiffness. For each flexion angle, position control was used to translate or rotate the tibia throughout all target joint positions and forces/moments were measured. Fourth order polynomial was used to fit the data. Figure 3.4 shows the load-displacement curve fitting on AP direction at 30° flexion. Primary stiffness coefficients can be derived by taking the slope of the curve at the same AP position in Section 4.1.1, where in this case is 1.57mm of anterior translation (passive path position on AP direction).

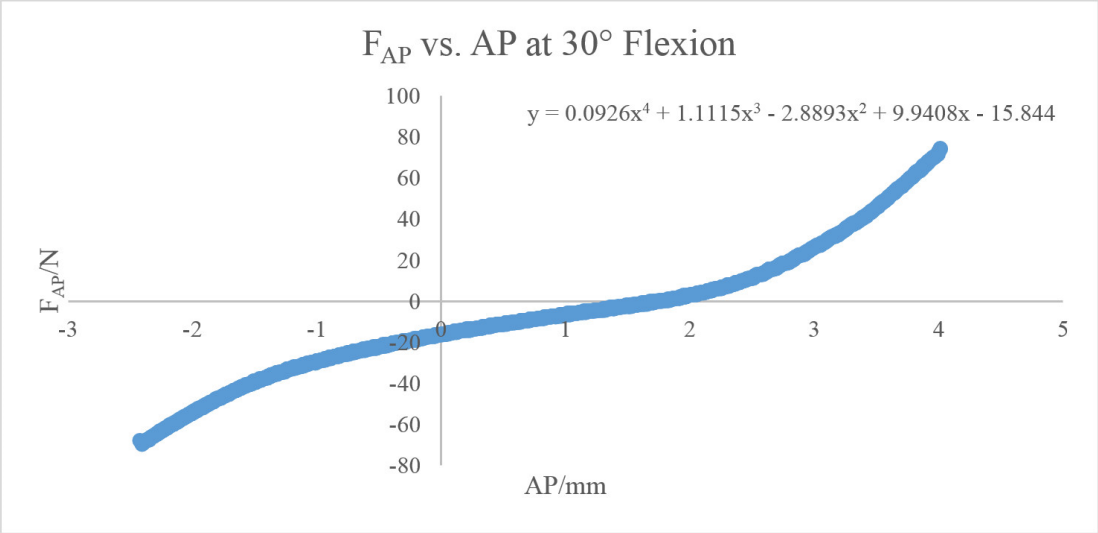

Figure 3.4 Load-displacement curve on anterior-posterior direction at 30° flexion (Specimen ID: PK191114)

4.0 Results

4.1 Comparison of Primary Stiffness on Same DOF

The joint positions were chosen by inputting displacement on one direction each time at different flexion angles. The first comparison was the primary stiffness at different joint positions on the same direction, which could indicate the change of stiffness value as a function of joint position and indicate the stiffer joint positions for each DOF.

4.1.1 Primary Stiffness of AP

The primary stiffness on anterior-posterior direction, K_{AP}, as a function of different AP positions and flexion angles for six specimens was depicted in Figure 4.1. “PP” on the x axis referred to the passive path. “AP+1.5”, “AP+3”, “AP-1.5”, and “AP-3” implied different translations on AP direction, with anterior translation as positive direction. K_{AP} on the y axis referred to the primary stiffness on AP direction with unit of N/mm. Each box and whisker chart included maximum, third quartile, median, first quartile, minimum, outlier and average (“X” in the middle of the box) values of K_{AP} for all specimens. Thus, the range and average of stiffness values at different joint positions could be investigated and compared. The curves of K_{AP} for each independent specimen were shown in Appendix Figure 1 – 3.

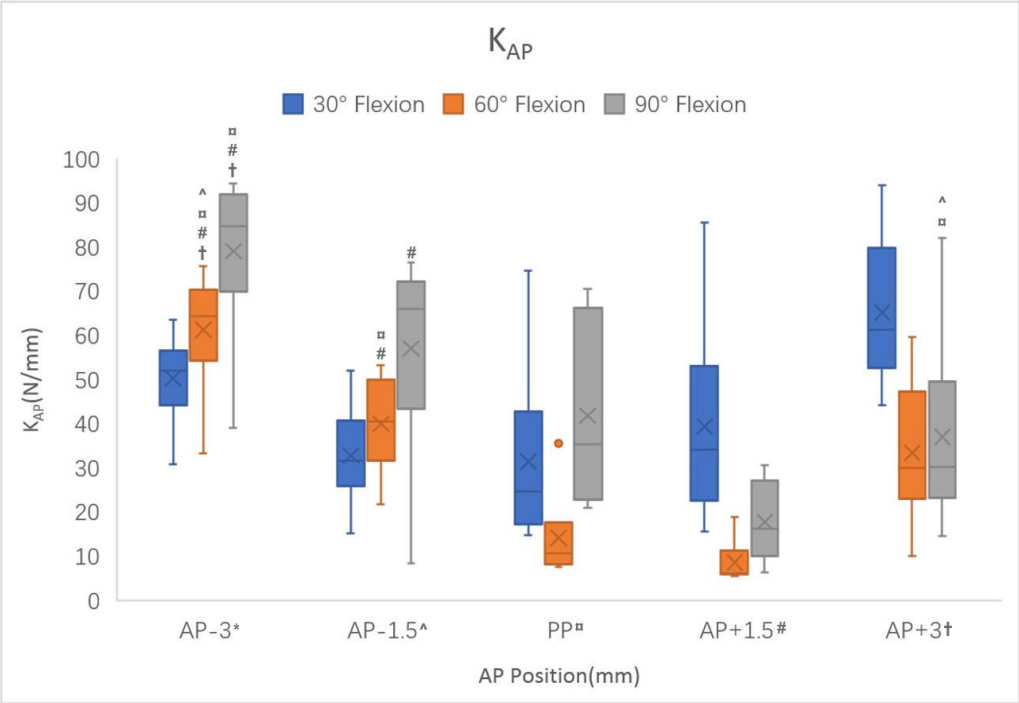

Figure 4.1 K_{AP} at different anterior-posterior positions: whisker represents range and X represents average. * indicates significant difference from AP-3. ^ indicates significant difference from AP-1.5. ¤ indicates significant difference from PP. # indicates significant difference from AP+1.5. † indicates significant difference from AP+3.

At 30° of flexion, K_{AP} was greater when the tibia was moving 3mm anteriorly with respect to the passive path position, with an average stiffness of 62.2 ± 17.4 N/mm and a range from 44.2 to 94.1 N/mm. K_{AP} at passive path and AP-1.5mm of 30° flexion were significantly smaller than that of AP+3mm position with an average of 31.5 ± 22.1 N/mm and 32.9 ± 12.0 N/mm respectively. One specimen (ID: PK200204) showed higher value of K_{AP} at flexion 30° than that other specimens, especially at passive path, +1.5mm anterior and +3mm anterior positions. Though the flexion angle in this study was chosen at 30° flexion, for porcine knee the full extension position usually occurs at 30° – 40° flexion angles. One possible reason for a higher K_{AP} value was that 30° flexion was a hyperextension joint position for that specimen.

At 60° and 90° of flexion, when the tibia was translating posteriorly, especially at AP-3mm position, K_{AP} would be greater than those of anterior translation positions. At AP -3mm posterior translation position, K_{AP} at 60° of flexion, from 33.4 to 75.8 N/mm with an average of 61.3 ± 13.3 N/mm, was significantly greater than the rest four AP positions. The average for K_{AP} at 90° flexion was 79.1 ± 18.5 N/mm with a range from 39.2 to 94.5 N/mm, which was significantly greater than that of passive path, AP+1.5mm and AP+3mm positions. At AP-1.5mm posterior translation position, K_{AP} at 60° of flexion was also significantly higher than that of passive path and AP+1.5mm positions. Therefore, at higher flexion angles, the knee joint on AP direction was stiffer when the tibia was translated posteriorly than moving anteriorly.

Between different flexion angles at AP-3mm position, K_{AP} at 90° of flexion was significantly greater than that of 30° flexion. At both AP+1.5mm and AP+3mm positions, K_{AP} at 30° flexion was significantly greater than that of 60° flexion. No significant difference was observed for other joint positions.

4.1.2 Primary Stiffness of IE

The primary stiffness on internal-external direction, K_{IE}, as a function of different IE positions and flexion angles for six specimens was shown in Figure 4.2. “PP” on the x axis referred to the passive path. “IE+3”, “IE+5”, “IE-3”, and “IE-5” signified different translations on IE direction, with internal rotation as positive direction. K_{IE} on the y axis referred to the primary stiffness on IE direction with unit of N·mm/deg. The comparison of K_{IE} between each specimen was depicted in Appendix Figure 4 – 6.

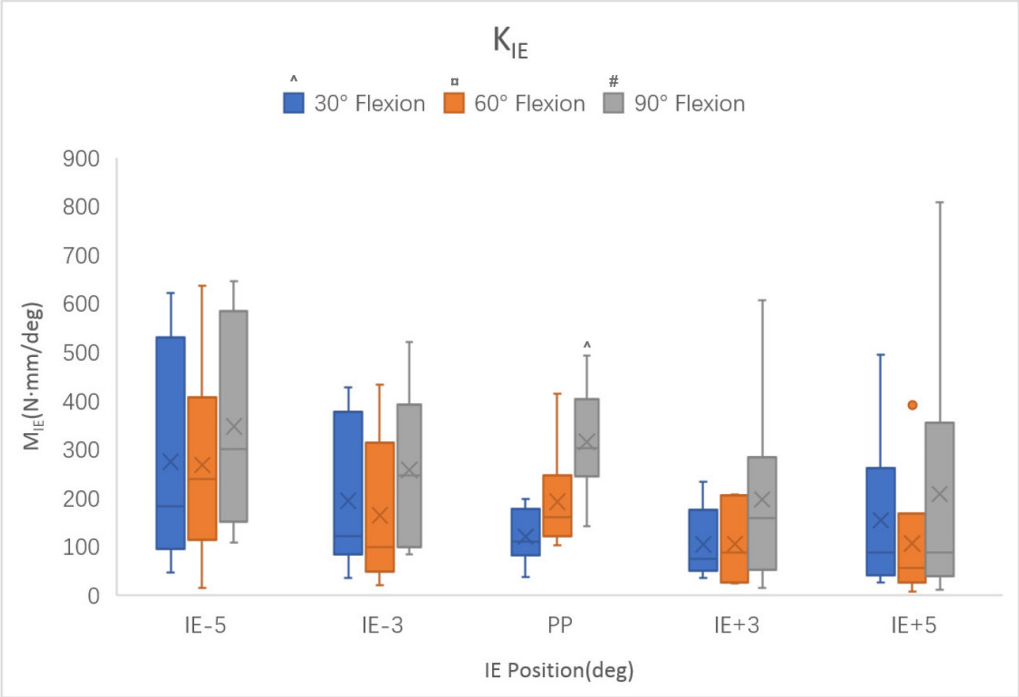

Figure 4.2 K_{IE} at different internal-external positions: whisker represents range and X represents average. ^ indicates significant difference from 30°. ¤ indicates significant difference from 60°. # indicates significant difference from 90°

Within each flexion angle, no significant difference was investigated between different IE positions. However, most specimens showed a higher value of K_{IE} when the tibia was rotating externally with respect to the passive path, especially at 30° (average: 234.7 ± 193.7 N·mm/deg) and 60° (average: 216.4 ± 189.2 N·mm/deg) of flexion, except one specimen (ID: PK200624) which was stiffer when the tibia rotated internally. The reason for an opposite result was that specimen was rotating internally during flexion (passive path on IE at 90° flexion was 26° internal rotation) while the joint position data showed that the other five specimens all rotated externally with the increase of flexion angle. Overall, at 30° and 60° of flexion, the tibia was stiffer on IE direction when it was rotating externally than internally. For different flexion angles, K_{IE} at passive path position of 90° flexion was significantly greater than that of 30° flexion.

4.1.3 Primary Stiffness of ML

The primary stiffness on medial-lateral direction, K_{ML}, was derived at different ML positions at 30°, 60°, and 90° of flexion for six specimens. (Figure 4.3) "PP", "ML+2", and "ML-2" represented passive path and two different translations on ML direction, with lateral translation as positive direction. K_{ML} on the y axis referred to the primary stiffness on ML direction with unit of N/mm. The comparison of K_{ML} between each specimen was shown in Appendix Figure 7 – 9.

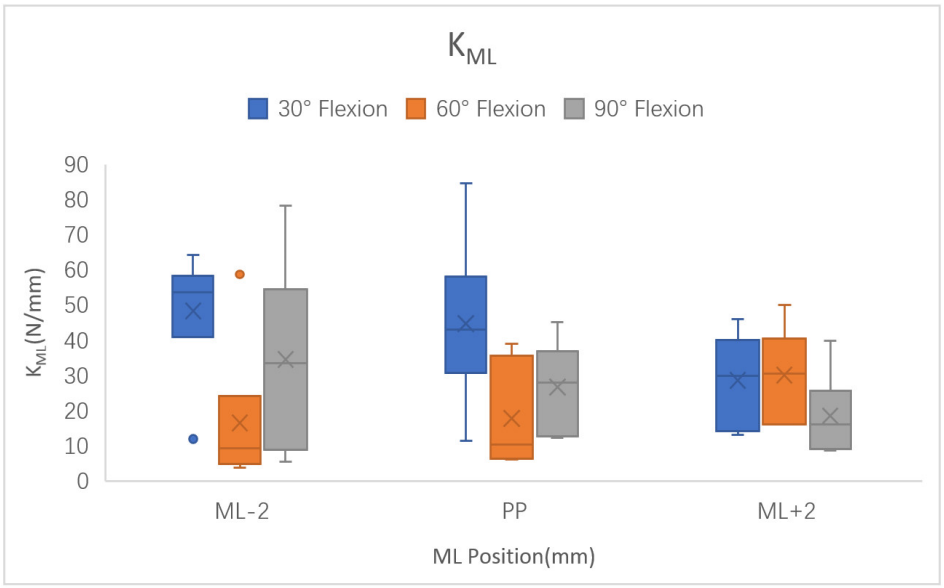

Figure 4.3 K_{ML} at different medial-lateral positions: whisker represents range and X represents average. No significant difference was observed among different joint positions

Unlike anterior-posterior and internal-external direction with higher mobility and laxity, medial-lateral did not show much difference in the primary stiffness at different joint positions. No significant difference was investigated between different ML translation positions or flexion angles. An overall comparison indicated that K_{ML} at 30° of flexion, with an average of 40.6 ± 19.8

N/mm and range from 11.3 to 84.6 N/mm, was significantly greater than that of 60° (average of 21.4 ± 17.0 N/mm, range from 3.8 to 58.8 N/mm).

4.1.4 Primary Stiffness of PD

The primary stiffness on proximal-distal direction, K_{PD}, was derived at passive path, proximal translation of +0.5mm, and distal translation of -0.5mm at 30°, 60°, and 90° of flexion for six specimens. (Figure 4.4) K_{PD} on the y axis referred to the primary stiffness on PD direction with unit of N/mm. The comparison of K_{PD} between each specimen was shown in Appendix Figure 10 – 12.

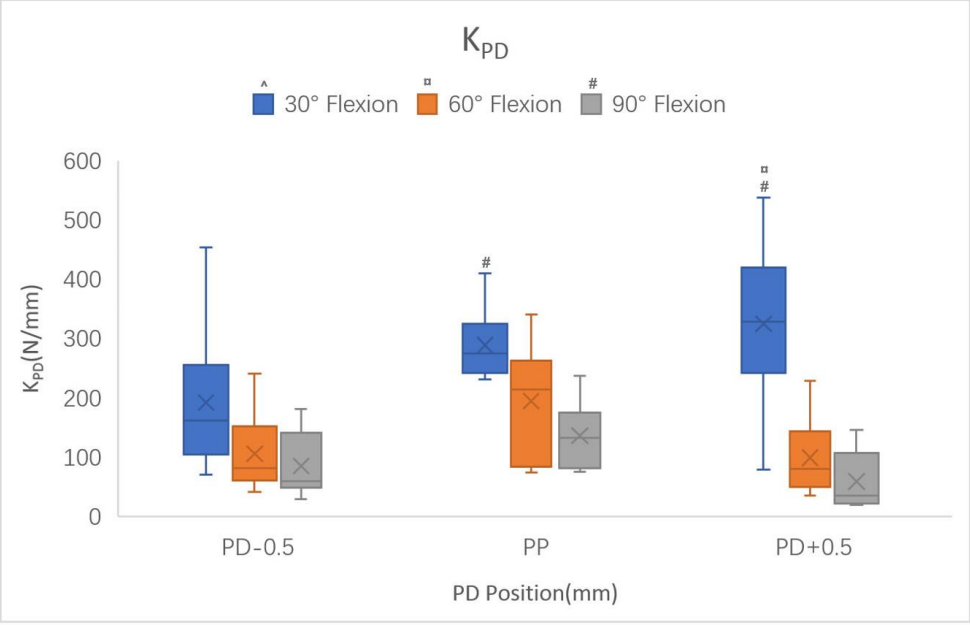

Figure 4.4 K_{PD} at different proximal-distal positions: whisker represents range and X represents average. ^ indicates significant difference from 30°. ¤ indicates significant difference from 60°. # indicates significant difference from 90°

Though within the same flexion angle no significant difference was observed, difference between different flexion angles at the same PD translation was found. At the passive path position, K_{PD} at 30° of flexion, with an average of 289.2 ± 64.2 N/mm and a range from 231.7 to 410.6 N/mm, was significantly greater than that of 90° flexion with an average of 136.6 ± 59.1 N/mm and a range from 75.6 to 237.9 N/mm. When the tibia was translating 0.5mm proximally, K_{PD} at 30° of flexion, with an average of 325.1 ± 148.3 N/mm, was significantly different with that of both 60° (average: 99.6 ± 68.9 N/mm) and 90° flexion (average: 59.4 ± 51.2 N/mm). At the position of PD-0.5mm, K_{PD} at 30° of flexion was still greater than 60° and 90° though there was no significant difference. Thus, the knee joint on proximal-distal direction will be stiffer at 30° flexion than 60° and 90°.

4.1.5 Primary Stiffness of VV

The primary stiffness on varus-valgus direction, K_{VV}, as a function of different VV positions and flexion angles was shown in Figure 4.5. Joint positions on VV direction were chosen at passive path position, valgus -1° rotation and varus +1° rotation at different flexion angles. K_{VV} with the unit of N·mm/deg was presented on y axis. The comparison of K_{VV} between each specimen was shown in Appendix Figure 13 – 15.

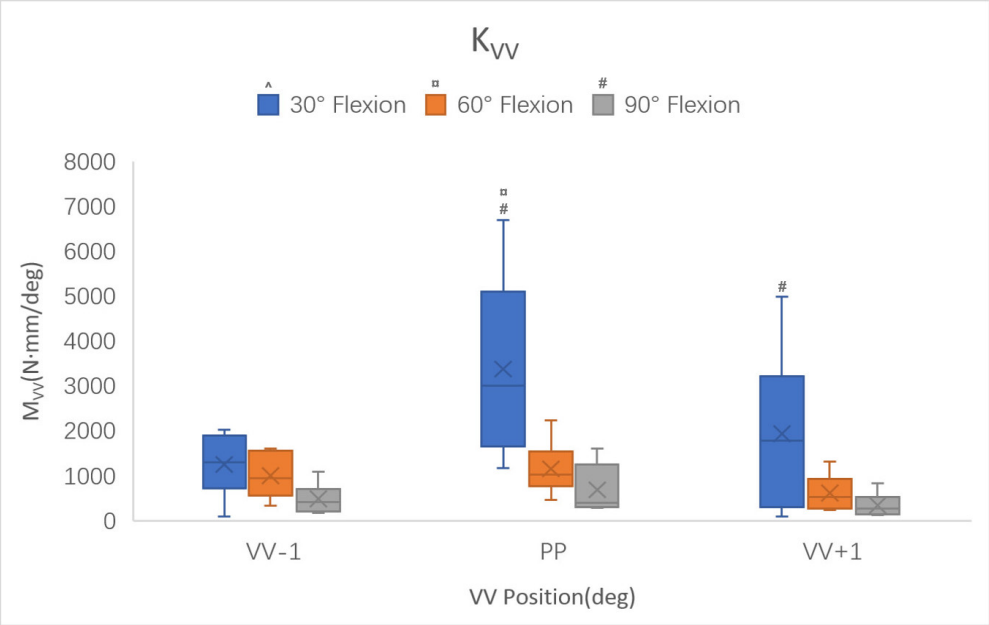

Figure 4.5 K_{VV} at different varus-valgus positions: whisker represents range and X represents average. ^ indicates significant difference from 30°. ¤ indicates significant difference from 60°. # indicates significant difference from 90°

Similar characteristics to the stiffness on PD direction was investigated on VV direction. At the passive path position, K_{VV} at 30° (with an average of 3375.3 ± 2010.2 N·mm/deg and a range from 1166.5 to 6695.5 N·mm/deg) of flexion was significantly greater than that of 60° (1159.2 ± 605.5 N·mm/deg) and 90° (692.7 ± 548.0 N·mm/deg). When the tibia rotated varus of 1°, the stiffness value of 30° (1941.2 ± 1785.4 N·mm/deg) flexion was significantly greater than that of 90° (344.7 ± 264.3 N·mm/deg). Overall, the joint positions at 30° flexion had a greater value of K_{VV}.

4.1.6 Conclusion for Primary Stiffness on the Same DOF

On anterior-posterior and internal-external directions, the porcine knee joint showed more laxity with significant difference between various joint positions within the same flexion angle. However, when the tibia was moving posteriorly or externally, the knee joint would become stiffer compared to anterior or internal displacement. On medial-lateral, proximal-distal, and varus-valgus DOFs, the porcine knee joint was stiffer at 30° of flexion. No significant difference was investigated among joint positions under the same flexion angle.

4.2 Comparison of Primary Stiffness on Different DOF

To investigate the stiffness on different directions of the knee joint, the primary stiffness coefficients of the three translational and three rotational DOFs at different joint positions were compared, which could indicate the stiffer directions.

4.2.1 Primary Stiffness of Translational DOFs

The primary stiffness of the three translational DOFs, K_{AP}, K_{PD} and K_{ML}, was compared at different joint positions (Figure 4.6 - Figure 4.8). All the joint positions on AP, PD, and ML directions including passive path positions were chosen, and the stiffness values were directly taken from the stiffness matrix. At 30° of flexion, (Figure 4.6) K_{PD} (with an average of 288.6 ± 98.9 N/mm and a range from 70.6 to 538.3 N/mm) throughout all the joint positions was significantly greater than that of K_{AP} (with an average of 38.8 ± 21.8 N/mm and a range of 7.7 –

94.1 N/mm) and K_{ML} (with an average of 45.9 ± 23.2 N/mm and a range from 70.6 to 538.3 N/mm). At 60° (Figure 4.7) and 90° (Figure 4.8) of flexion, K_{PD}, with an average of 184.1 ± 98.7 N/mm and 146.5 ± 85.1 N/mm respectively, was still significantly greater than K_{AP} and K_{ML}. No significant difference was observed between K_{AP} and K_{ML}. Therefore, proximal-distal was the stiffest direction among all the three translational DOFs. Bony contact during the motion on PD direction was considered as the primary reason.

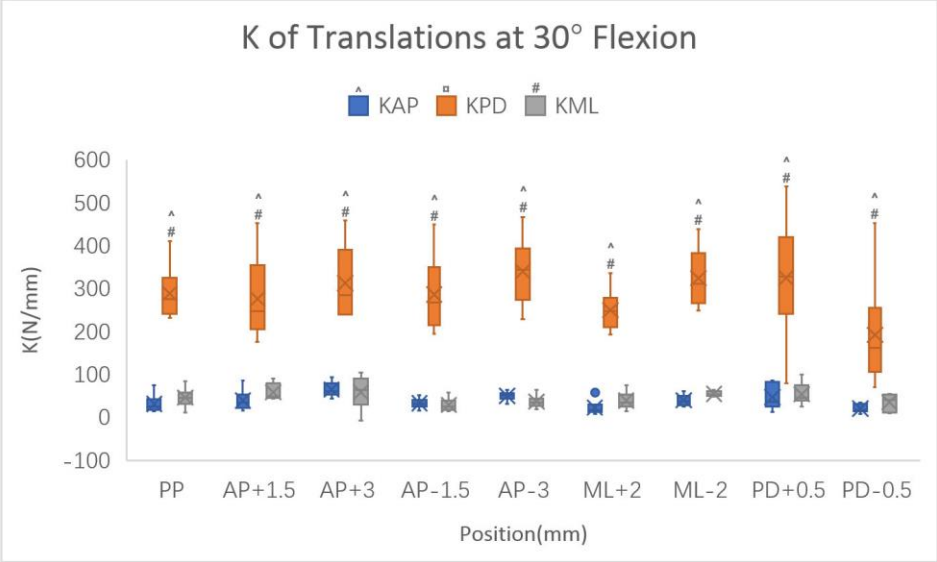

Figure 4.6 Primary stiffness of translational DOFs at 30° of flexion: whisker represents range and X represents average. ^ indicates significant difference from K_{AP}. ¤ indicates significant difference from K_{PD}. # indicates significant difference from K_{ML}

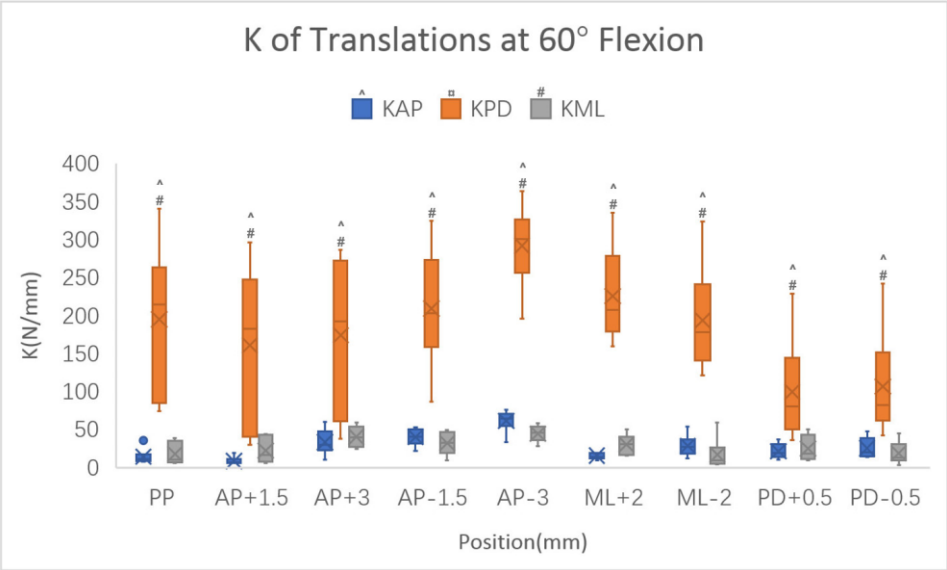

Figure 4.7 Primary stiffness of translational DOFs at 60° of flexion: whisker represents range and X represents average. ^ indicates significant difference from K_{AP}. ¤ indicates significant difference from K_{PD}. # indicates significant difference from K_{ML}

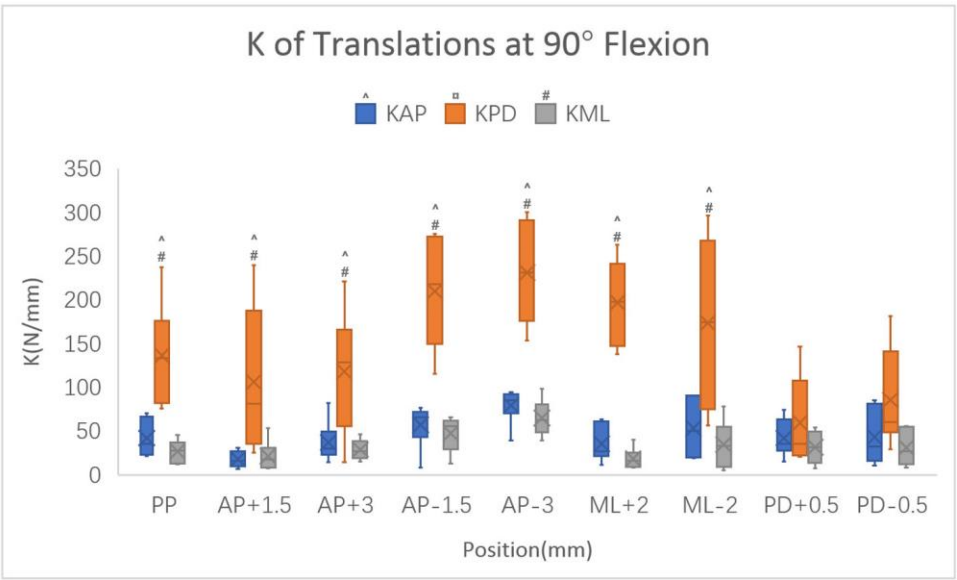

Figure 4.8 Primary stiffness of translational DOFs at 90° of flexion: whisker represents range and X represents average. ^ indicates significant difference from K_{AP}. ¤ indicates significant difference from K_{PD}. # indicates significant difference from K_{ML}

4.2.2 Primary stiffness of Rotational DOFs

The primary stiffness values of the three rotational directions, K_{VV}, K_{IE}, and K_{FE} were compared at different VV and IE joint positions including passive path position (Figure 4.9 – Figure 4.11). At 30° of flexion, (Figure 4.9) K_{VV} at all the rotational positions was greater than K_{IE} and K_{FE} with an average of 2735.2 N·mm/deg and a range from 362.2 to 8274.7 N·mm/deg, while the average for K_{IE} and K_{FE} was 228.9 and 300.4 N·mm/deg respectively. At 60° and 90° of flexion, K_{VV} with an average of 1170.7 and 713.7 N·mm/deg respectively was smaller than that of K_{VV} at 30°, but still significantly greater than K_{AP} and K_{ML}. There was no significant difference between K_{AP} and K_{ML} at any flexion angle. Thus, on the rotational DOFs, varus-valgus is the stiffest direction especially at 30° of flexion. Bony contact was considered as the major reason due to the compression between femur and tibia during varus-valgus motion.

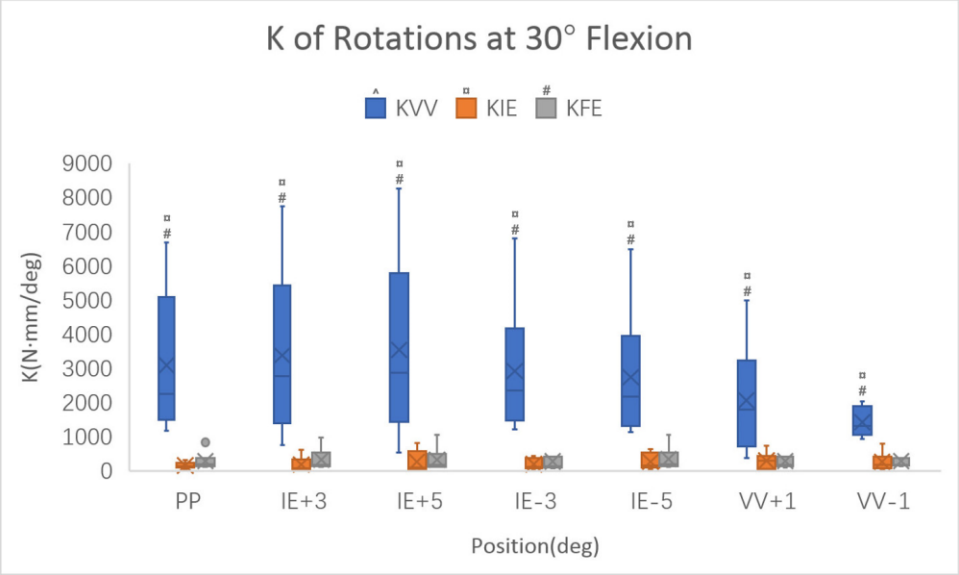

Figure 4.9 Primary stiffness of rotational DOFs at 30° flexion: whisker represents range and X represents average. ^ indicates significant difference from K_{VV}. ¤ indicates significant difference from K_{IE}. # indicates significant difference from K_{FE}

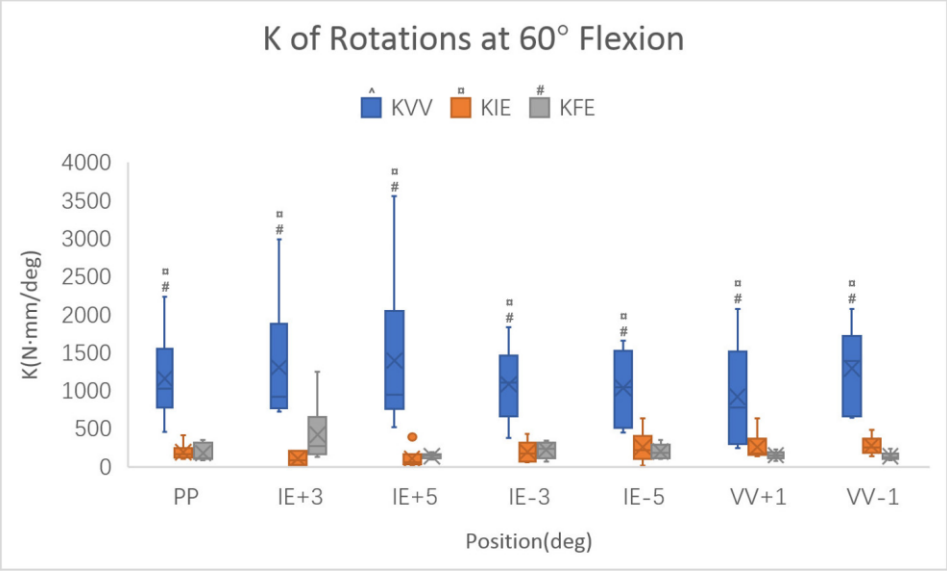

Figure 4.10 Primary stiffness of rotational DOFs at 60° flexion: whisker represents range and X represents average. ^ indicates significant difference from K_{VV}. ¤ indicates significant difference from K_{IE}. # indicates significant difference from K_{FE}

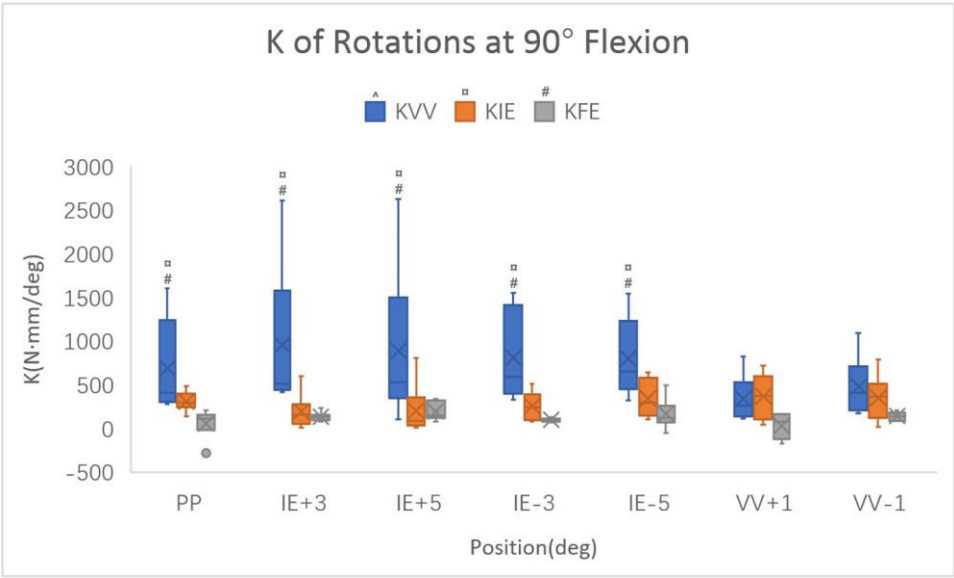

Figure 4.11 Primary stiffness of rotational DOFs at 90° flexion: whisker represents range and X represents average. ^ indicates significant difference from K_{VV}. ¤ indicates significant difference from K_{IE}. # indicates significant difference from K_{FE}

4.2.3 Conclusion for Primary Stiffness on Different DOFs

For the translational DOFs, proximal-distal direction is the stiffest one throughout all the translated positions at 30°, 60° and 90° of flexion. For the rotational DOFs, varus-valgus is the stiffest direction among all flexion angles, especially at 30° of flexion.

4.3 Comparison of Primary Stiffness from Two Methods

4.3.1 Perturbation vs. Continuous Curve

Besides the method of measuring stiffness matrix in the current work, a more common method in the previous studies was also used to measure the primary stiffness to compare the values derived from both methods. The comparisons of primary stiffness values at all 45 joint positions of specimen PK191114 were listed (Table 4.1 to Table 4.15). The results for the rest specimens were listed in Appendix C. The protocol in this study was to measure the whole stiffness matrix around each desired joint position (Section 4.1.1) thus it was noted as "perturbation". And the stiffness calculated from the load-displacement curves (Section 4.1.2) was noted as "continuous" in the tables. The stiffness matrices were derived from 45 joint positions and the same positions were chosen on the load-displacement curve to compare the values. Differences were observed and in most cases the stiffness value from perturbation was greater than that from the load-displacement curve.

Table 4.1 K_{AP} (N/mm) from both methods at 30° flexion of specimen ID: PK191114

	Passive Path	AP +1.5mm	AP+3mm	AP-1.5mm	AP-3mm
Perturbation	20.8	35	44.2	30.3	48.7
Continuous	10.5	18.2	53.0	13.7	34.1

Table 4.2 K_{IE} (N·mm/deg) from both methods at 30° flexion of specimen ID: PK191114

	Passive Path	IE+3deg	IE+5deg	IE-3deg	IE-5deg
Perturbation	102.0	56.3	81.5	110.6	111.3
Continuous	15.8	36.8	73.3	37.2	69.0

Table 4.3 K_{ML} (N/mm) from both methods at 30° flexion of specimen ID: PK191114

	Passive Path	ML+2mm	ML-2mm
Perturbation	41.4	13.1	11.9
Continuous	9.5	21.1	16.9

Table 4.4 K_{PD} (N/mm) from both methods at 30° flexion of specimen ID: PK191114

	Passive Path	PD+0.5mm	PD-0.5mm
Perturbation	265.1	381.0	70.6
Continuous	50.2	409.5	47.2

Table 4.5 K_{VV} (N·mm/deg) from both methods at 30° flexion of specimen ID: PK191114

	Passive Path	VV+1deg	VV-1deg
Perturbation	4559.3	1439.0	1502.6
Continuous	694.9	2189.0	613.6

Table 4.6 K_{AP} (N/mm) from both methods at 60° flexion of specimen ID: PK191114

	Passive Path	AP +1.5mm	AP+3mm	AP-1.5mm	AP-3mm
Perturbation	7.6	5.6	10.2	35.1	62.5
Continuous	1.5	2.7	4.3	12.9	40.9

Table 4.7 K_{IE} (N·mm/deg) from both methods at 60° flexion of specimen ID: PK191114

	Passive Path	IE+3deg	IE+5deg	IE-3deg	IE-5deg
Perturbation	104.3	61.7	34.2	21.8	146.9
Continuous	3.0	15.8	93.6	117.4	189.2

Table 4.8 K_{ML} (N/mm) from both methods at 60° flexion of specimen ID: PK191114

	Passive Path	ML+2mm	ML-2mm
Perturbation	6.1	16.2	3.8
Continuous	2.6	18.1	4.4

Table 4.9 K_{PD} (N/mm) from both methods at 60° flexion of specimen ID: PK191114

	Passive Path	PD+0.5mm	PD-0.5mm
Perturbation	74.1	55.3	91.0
Continuous	24.6	26.3	93.0

K_{VV} at Flexion 60 (N·mm/deg)

Table 4.10 K_{VV} (N·mm/deg) from both methods at 60° flexion of specimen ID: PK191114

	Passive Path	VV+1deg	VV-1deg
Perturbation	460.1	244.4	640.5
Continuous	227.1	280.3	709.4

Table 4.11 K_{AP} (N/mm) from both methods at 90° flexion of specimen ID: PK191114

	Passive Path	AP +1.5mm	AP+3mm	AP-1.5mm	AP-3mm
Perturbation	23.6	6.4	30.9	69.0	91.1
Continuous	5.0	7.3	12.4	14.7	55.5

Table 4.12 K_{IE} (N·mm/deg) from both methods at 90° flexion of specimen ID: PK191114

	Passive Path	IE+3deg	IE+5deg	IE-3deg	IE-5deg
Perturbation	373.0	149.2	126.8	348.8	563.2
Continuous	37.0	9.1	209.1	301.4	337.0

Table 4.13 K_{ML} (N/mm) from both methods at 90° flexion of specimen ID: PK191114

	Passive Path	ML+2mm	ML-2mm
Perturbation	27.7	8.6	5.5
Continuous	3.16	17.21	-1.80

Table 4.14 K_{PD} (N/mm) from both methods at 90° flexion of specimen ID: PK191114

	Passive Path	PD+0.5mm	PD-0.5mm
Perturbation	83.8	20.4	63.2
Continuous	35.4	35.0	51.6

Table 4.15 K_{VV} (N·mm/deg) from both methods at 90° flexion of specimen ID: PK191114

	Passive Path	VV+1deg	VV-1deg
Perturbation	282.0	121.5	182.2
Continuous	246.1	359.0	85.0

4.4 Secondary Stiffness

Unlike the primary stiffness coefficients can build a connection between applied forces and the displacements on the same direction, the secondary stiffness coefficients can map the loads and displacements on the different directions. For instance, when a doctor performing the Lachman test, the doctor will pull the patient's tibia anteriorly. The secondary stiffness coefficients can tell us what are the forces or moments on other directions in response to that anterior displacement of the tibia, which can have many implications for knee function or clinical use.

4.4.1 Secondary Stiffness of AP – IE

According to the definition of stiffness matrix in Figure 3.3, K_{51} is the secondary stiffness between anterior-posterior and internal-external directions, which implies that when a displacement on AP direction (u_{AP}) was inputted, the moment on IE direction (M_{IE}) in response to this AP displacement would be:

$$M_{IE} = K_{51} \times u_{AP} \tag{4.1}$$

The unit was N·mm/mm. K_{51} and the primary stiffness of IE direction K_{IE} were taken from the stiffness matrices at AP positions of all flexion angles. (Figure 4.12, Figure 4.13) For passive path,

AP+1.5mm and AP+3mm positions, K_{51} has a small value with an range from -363.2 to 271.1 N·mm/mm and no difference was investigated among the three flexion angle, which indicated that the effect of anterior translation to internal-external direction was small when the tibia was translating anteriorly. When the tibia was moving posteriorly, at AP-1.5mm of 60° flexion, K_{51} was greater with the range of -54.7 – 1010.6 N·mm/mm. And at 90° of flexion when the tibia was moving 3mm posteriorly with respect to the passive path position, K_{51} was greater with a range from -1173.8 to 202.7 N·mm/mm than that of the anterior translation positions. The primary stiffness on internal-external (Figure 4.13) and anterior-posterior (Figure 4.1) directions was also greater at the same joint positions with a higher K_{51} value. Thus, at the positions with a higher stiffness of each independent direction, a greater secondary stiffness between these directions was always observed.

At 90° of flexion throughout all the anterior-posterior translation, most secondary stiffness coefficients had a negative value, which indicated that when the tibia was translating anteriorly there would be an external moment in response to that anterior displacement. The LCL insertion site on the femur of the porcine knee is more anterior than the MCL. Therefore, when the tibia was moving anteriorly, the LCL was tight and pulled the tibia in an external way.

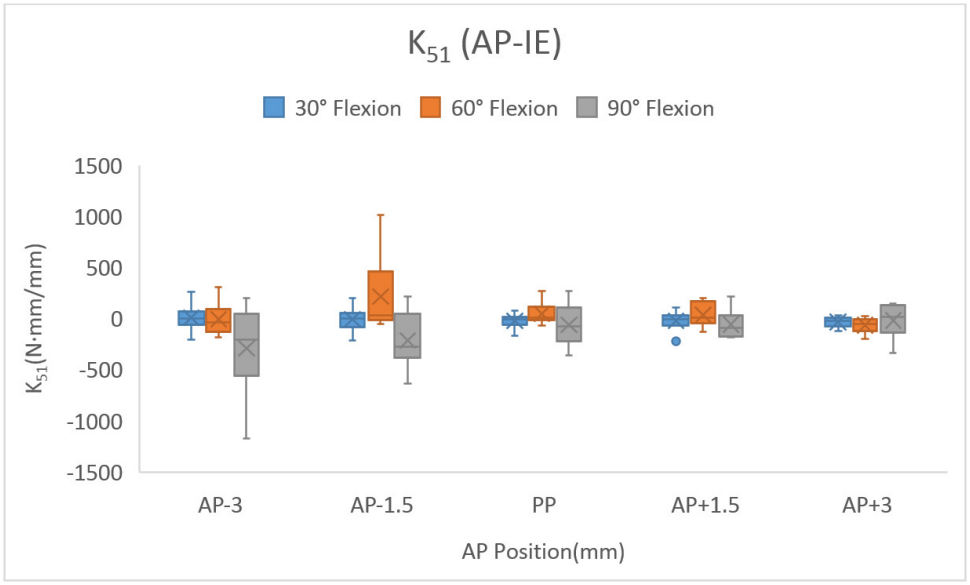

Figure 4.12 K_{51} at different AP positions: whisker represents range and X represents average. No significant difference was observed among different flexion angles

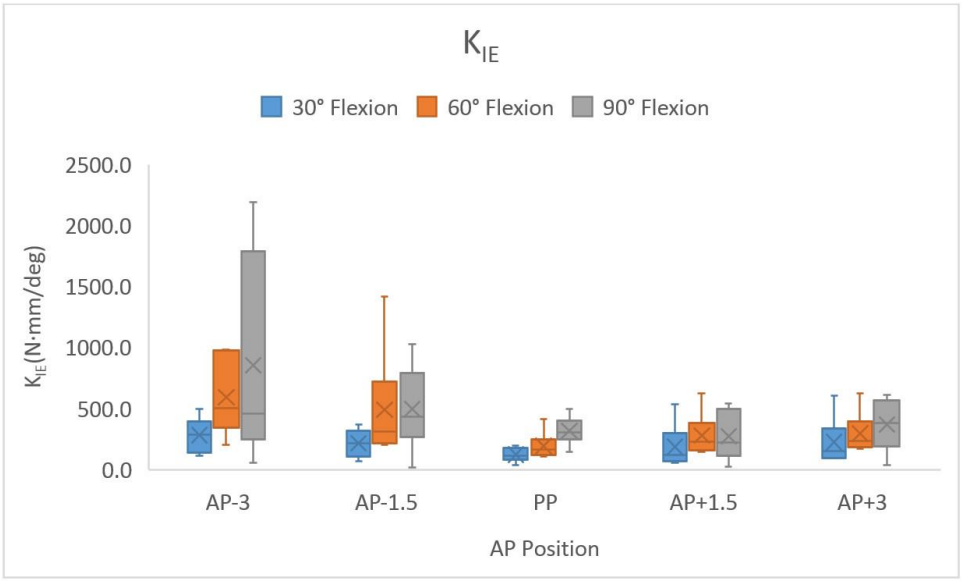

Figure 4.13 K_{IE} at different AP positions: whisker represents range and X represents average. No significant difference was observed among different flexion angles

4.4.2 Secondary Stiffness of AP–VV

K_{41} is the secondary between anterior-posterior and varus-valgus directions, which specifies that the moment on VV direction (M_{VV}, N·mm) can caused by a displacement on AP direction (u_{AP}, mm):

$$M_{VV} = K_{41} \times u_{AP} \tag{4.2}$$

The unit of K_{41} is N·mm/mm. Figure 4.14 depicted K_{41} as a function of AP joint positions at 30°, 60° and 90° of flexion. K_{VV} was also taken from the stiffness matrix at the same joint positions (**错误!未找到引用源。**). Similar conclusion that K_{VV} was greater at 30° of flexion could been observed. When the tibia was translating anteriorly, specifically at AP+3mm, K_{41} was greater than that of both higher flexion angles and more posterior positions with a range from -3017.6 to 0 N·mm/mm. Significantly greater value of the primary stiffness on AP direction K_{AP} was also investigate at the same joint position in 4.1.1. Therefore, at this joint position, the translation on AP direction had more effect on VV direction. The negative values of K_{41} demonstrated that an external moment would occur due to the anterior translation of the tibia at this joint position.

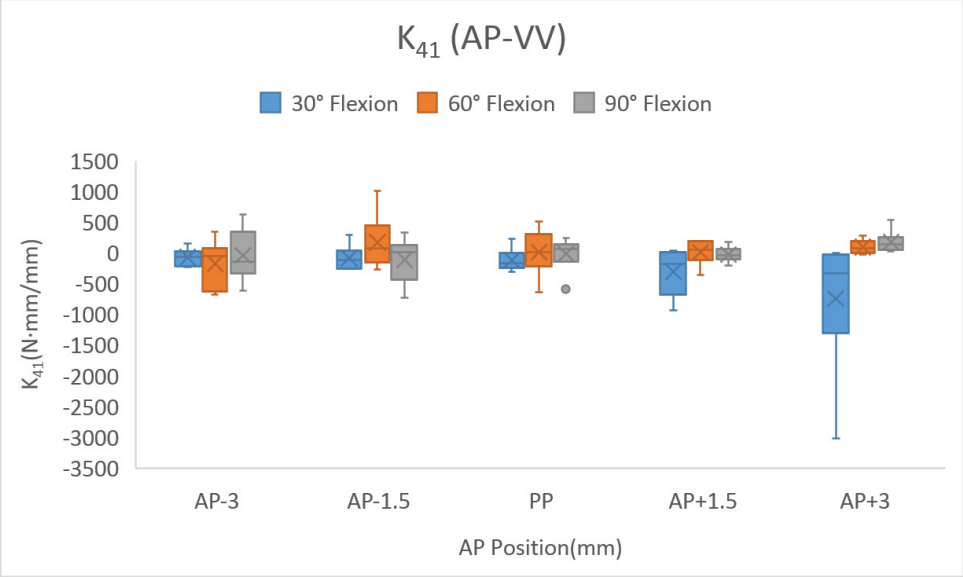

Figure 4.14 K_{41} at different AP positions: whisker represents range and X represents average. No significant difference was observed among different flexion angles

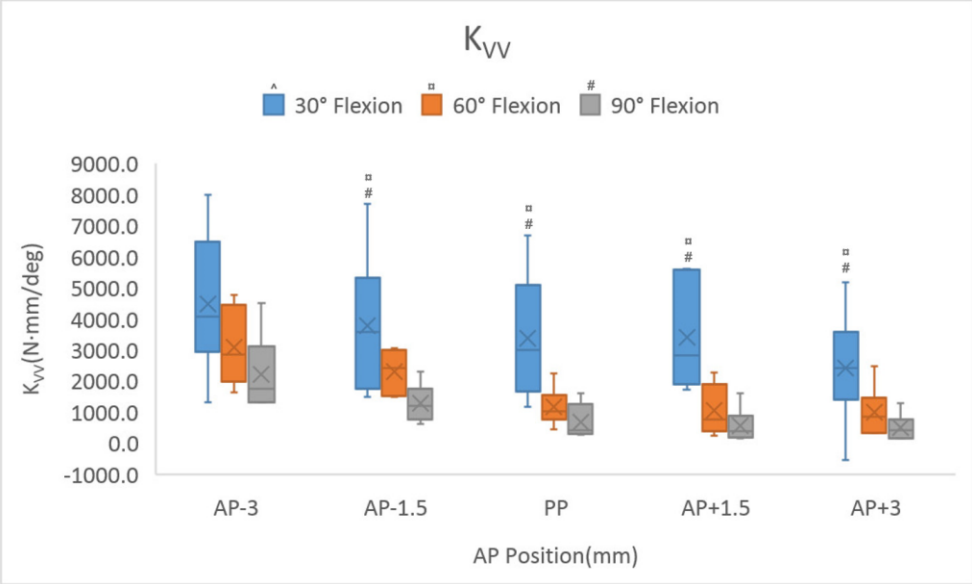

Figure 4.15 K_{VV} at different AP positions: whisker represents range and X represents average. ^ indicates significant difference from 30°. ¤ indicates significant difference from 60°. # indicates significant difference from 90°

4.4.3 Secondary Stiffness of ML – VV

When the tibia was translating on medial-lateral direction, the effect on varus-valgus direction could be known by the secondary stiffness between these two directions: K_{43}. The moment on VV direction (M_{VV}, N·mm) caused by ML displacement (u_{ML}, mm) was:

$$M_{VV} = K_{43} \times u_{ML} \tag{4.3}$$

K_{43} (N·mm/mm) and K_{VV} (N·mm/deg) at different displacement of ML was collected from stiffness matrices(Figure 4.16, **错误!未找到引用源。**). At the full extension position of 30° flexion with a higher value of K_{VV} and K_{ML} (as discussed in Figure 4.3), K_{43} was also greater than that of the other two flexion angles. When the tibia was translating 2mm medially, K_{43} at 30° of flexion (with an average of -1404.7 ± 482.6 N·mm/mm and a range from -2743.6 to 13.9 N·mm/mm) was significantly greater than 60° and 90°. In addition, most secondary stiffness has a negative value throughout the range of motion on ML direction, which indicated that a valgus moment would be generated to the tibia in response to lateral translation. When a lateral force was applied to the tibia at a distal end, with considering the length of the tibia as a moment arm, that lateral force would turn into a valgus moment. Therefore, the displacement on lateral direction had more effect on valgus moment.

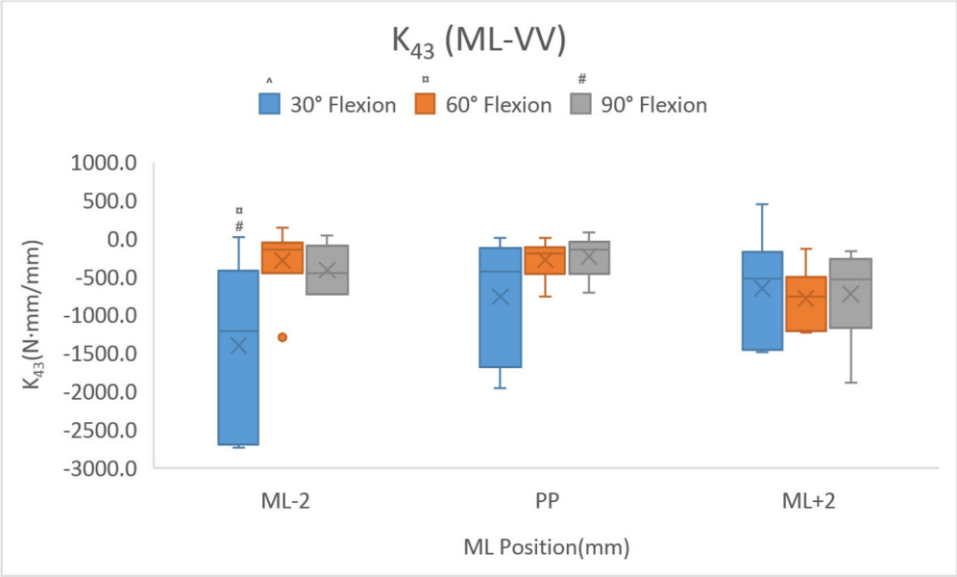

Figure 4.16 K_{43} at different ML positions: whisker represents range and X represents average. ^ indicates significant difference from 30°. ¤ indicates significant difference from 60°. # indicates significant difference from 90°

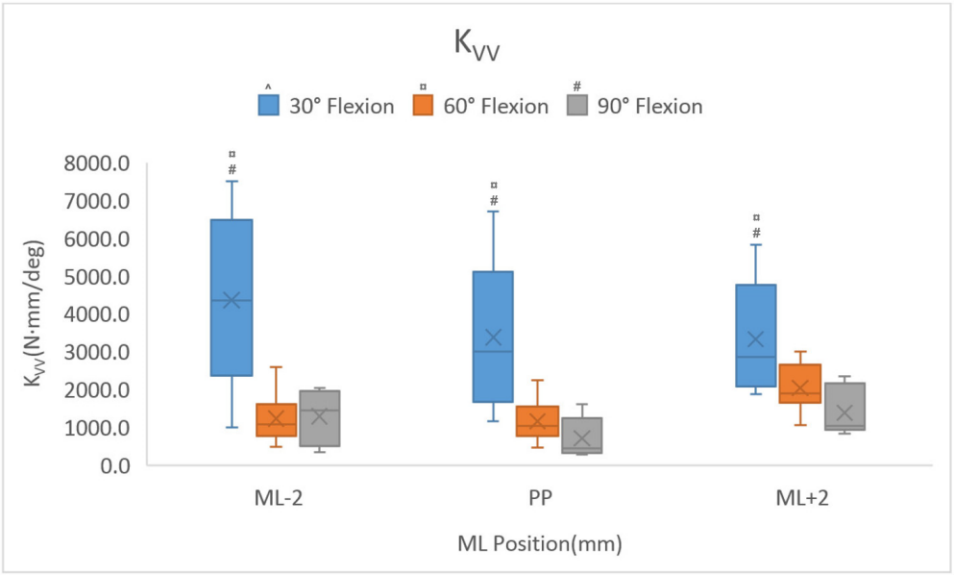

Figure 4.17 K_{VV} at different ML positions: whisker represents range and X represents average. ^ indicates significant difference from 30°. ¤ indicates significant difference from 60°. # indicates significant difference from 90°

4.4.4 Secondary Stiffness of PD – VV

From the discussion in previous sections (4.2), proximal-distal and varus-valgus were the stiffest two directions among the six. The secondary stiffness coefficient between these two directions was K_{42} (N·mm/mm):

$$M_{VV} = K_{42} \times u_{PD} \tag{4.4}$$

which implied the effect of displacement on PD direction on the VV moment (Figure 4.18). At 30°of flexion, the primary stiffness on PD and VV direction were both with higher values (Figure 4.4, Figure 4.19). In this case, the secondary stiffness between them also showed greater values at 30° of flexion. When the tibia was translating 0.5mm distally from the femur, K_{42} at 30° of flexion was significantly greater than that of 60° and 90° with an average of -1719.6 ± 1321.88 N·mm/mm and a range from -3599.9 to -638.3 N·mm/mm. Distal translation of the tibia would generate a varus moment at most PD joint positions. The higher secondary between PD and VV compared with other directions indicated more effect from the PD movement to the varus-valgus direction especially at a lower flexion angle.

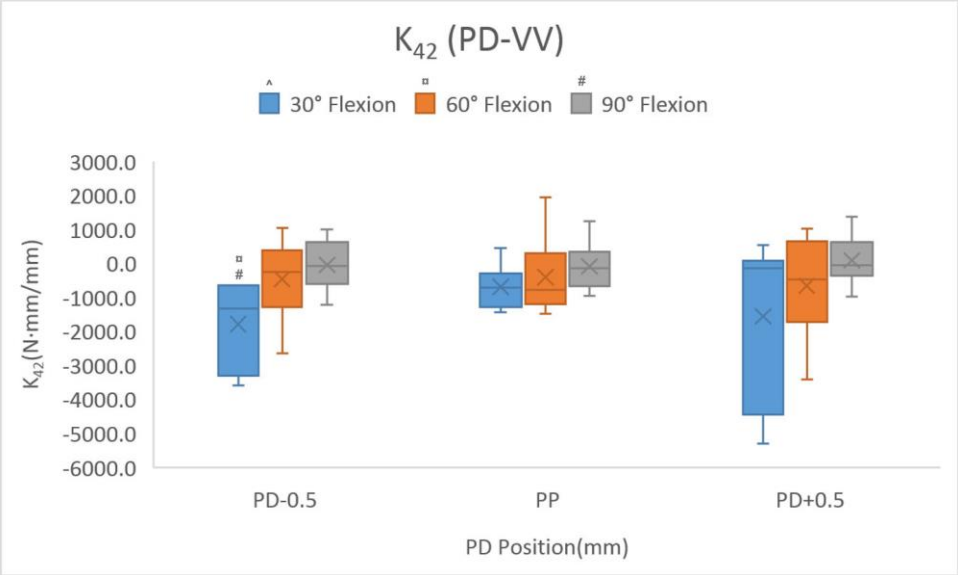

Figure 4.18 K_{42} at different PD positions: whisker represents range and X represents average. ^ indicates significant difference from 30°. ¤ indicates significant difference from 60°. # indicates significant difference from 90°

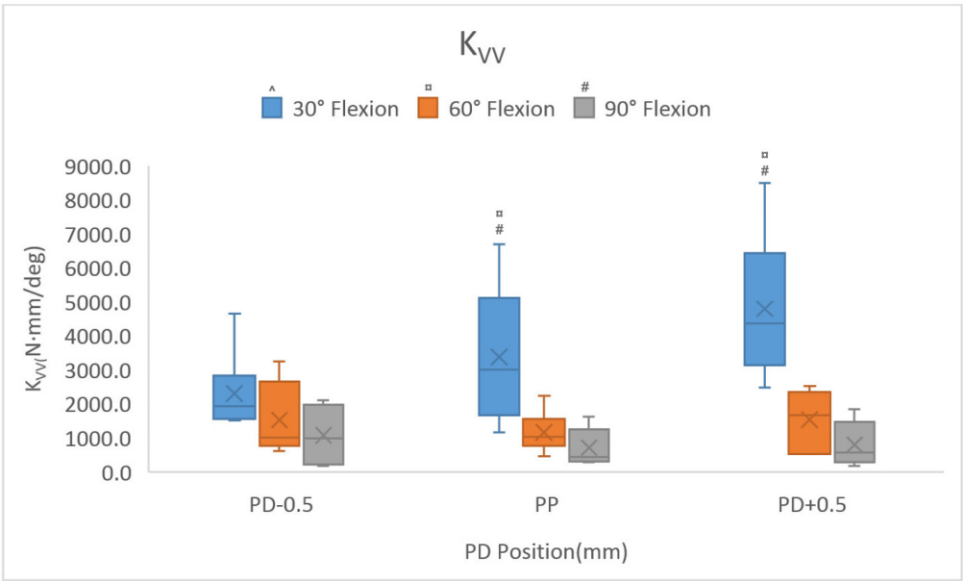

Figure 4.19 K_{VV} at different PD positions: whisker represents range and X represents average. ^ indicates significant difference from 30°. ¤ indicates significant difference from 60°. # indicates significant difference from 90°

4.4.5 Conclusion for Secondary Stiffness

Joint positions with higher secondary stiffness values always also had greater primary stiffness on the two directions separately. On anterior-posterior direction, the tibia has instability on internal-external direction with an external moment in response to the anterior displacement, especially when the tibia was translating posteriorly at higher flexion angles. However, an internal moment would generate by anterior displacement at a lower flexion when the tibia was moving anteriorly. When the was moving laterally with respect to the femur, a valgus load would be produced due to the lateral displacement.

4.5 Function of Joint Positions

The stiffness matrix in this current work was derived at each joint position with displacement on six directions. Thus, each stiffness coefficient in the matrix can be defined as a function of joint positions. Joint positions would be considered as the six independent variables and the stiffness coefficients was dependent variable. Therefore, with multiple linear regression, the function can be defined as:

$$K_{ij} = b_0 + b_{AP}u_{AP} + b_{PD}u_{PD} + b_{ML}u_{ML} + b_{VV}u_{VV} + b_{IE}u_{IE} + b_{FE}u_{FE} \qquad (4.5)$$

where K_{ij} is a single element in the stiffness matrix. b_0 is the intercept of this function. b_{AP}, b_{PD}, b_{ML}, b_{VV}, b_{IE} and b_{FE} are the coefficients of the joint displacements u at six different directions respectively. With the joint position of (u_{AP}, u_{PD}, u_{ML}, u_{VV}, u_{IE}, u_{FE}) as input, any stiffness terms in

the stiffness matrix could be calculated by Equation 4.5. As a result, a stiffness matrix as response variable could be predicted and built at any joint positions.

Multiple linear regression was applied to one specimen (specimen ID: PK191114) to fit the data into a function with joint positions as independent variables to calculate stiffness terms. 45 joint positions and corresponding stiffness coefficients was chosen. The primary stiffness on anterior-posterior direction as a function of joint position was:

$$K_{AP} = -51.7 - 7.0u_{AP} + 7.5u_{PD} - 5.5u_{ML} + 8.7u_{VV} + 0.69u_{IE} - 2.9u_{FE} \quad (4.6)$$

K_{AP} at any joint positions can be calculated through this equation. However, the R^2 value for this regression was 0.36, which indicated that the linearity and the ability to predict K_{AP} by joint positions was weak. The major reason was that during the measurement of stiffness matrix, the flexion angle was locked at 30°, 60° and 90° among 45 positions. The invariability of the flexion angle would weaken the goodness-of-fit of the model. Therefore, a new multiple linear model was built under 30° of flexion (full extension position with higher stiffness values):

$$K_{ij} = b_0 + b_{AP}u_{AP} + b_{PD}u_{PD} + b_{ML}u_{ML} + b_{VV}u_{VV} + b_{IE}u_{IE} \quad (4.7)$$

In this model only five independent variables were used to calculate K_{ij} because it was applied to the joint positions at 30° of flexion. Stiffness elements of this specimen (ID: 191114) could be predicted by Equation 4.7 for any joint position (u_{AP}, u_{PD}, u_{ML}, u_{VV}, u_{IE}, 30°). The 36 multiple linear regression models with coefficients of independent variables and R^2 values were listed in Table 4.16. Any joint positions at 30° of flexion could predict every stiffness element in the stiffness matrix. For instance,

$$K_{AP} = 41.5 - 2.9u_{AP} - 133.6u_{PD} - 25.5u_{ML} + 12.3u_{VV} + 0.6u_{IE} \quad (4.8)$$

$$K_{21} = -35.1 - 12.3u_{AP} + 157.7u_{PD} + 50.1u_{ML} - 36.4u_{VV} + 7.1u_{IE} \quad (4.9)$$

As a result, with the 36 equations of stiffness terms, the stiffness matrix (4.10) can be built:

$$\begin{bmatrix} K_{AP} & K_{12} & K_{13} & K_{14} & K_{15} & K_{16} \\ K_{21} & K_{PD} & K_{23} & K_{24} & K_{25} & K_{26} \\ K_{31} & K_{32} & K_{ML} & K_{34} & K_{35} & K_{36} \\ K_{41} & K_{42} & K_{43} & K_{VV} & K_{45} & K_{46} \\ K_{51} & K_{52} & K_{53} & K_{54} & K_{IE} & K_{56} \\ K_{61} & K_{62} & K_{63} & K_{64} & K_{65} & K_{FE} \end{bmatrix} \tag{4.10}$$

However, though these models were developed at 30° of flexion only, some of them still had a weak R^2 value (e.g. 0.33 for K_{PD}, 0.23 for K_{13}). Therefore, even taking no account of the flexion angles, linear regression still showed poor prediction for some stiffness terms. Future work can be done by building a nonlinear equation to fit the data and predict the stiffness matrix at different joint position. The predicted results can be validated by experimental data.

Table 4.16 Multiple linear regression models for stiffness calculation at 30° of flexion (specimen ID: PK191114)

Stiffness	b_0	b_{AP}	b_{PD}	b_{ML}	b_{VV}	b_{IE}	R^2
K_{AP}	41.5	-2.9	-133.6	-25.5	12.3	0.6	0.72
K_{21}	-35.1	-12.3	157.7	50.1	-36.4	7.1	0.88
K_{31}	-12.8	100.4	32.9	-18.0	5.2	-12.8	0.95
K_{41}	-1395.1	5.1	11349.9	1085.3	-78.7	-11.4	0.76
K_{51}	-1139.9	-412.1	10007.7	1817.5	-593.8	211.6	0.81
K_{61}	87.9	-44.2	-735.3	-113.5	-3.1	-17.4	0.53
K_{12}	-19.5	-3.8	85.4	22.7	-15.8	1.6	0.75
K_{PD}	271.1	-21.1	126.0	-39.9	88.9	7.4	0.33
K_{32}	18.6	33.7	-165.5	-52.5	7.7	-11.8	0.61
K_{42}	1291.0	-1801.7	-2966.7	172.8	485.7	544.1	0.61
K_{52}	854.1	46.7	-5270.9	-1024.6	605.3	-61.4	0.81
K_{62}	22.8	-99.4	368.2	97.7	-42.7	18.7	0.46
K_{13}	0.1	0.3	1.4	1.8	0.3	0.2	0.23
K_{23}	44.4	2.3	-64.2	4.0	-16.3	0.7	0.50
K_{ML}	27.9	8.8	9.4	-7.8	4.3	-1.9	0.30
K_{43}	-652.7	326.2	-4342.8	-745.1	219.6	-222.5	0.57
K_{53}	-24.1	-24.1	-24.1	-24.1	-24.1	-24.1	0.30
K_{63}	106.1	-207.8	-180.0	48.3	-113.8	2.6	0.34
K_{14}	-16.2	-2.8	45.2	7.1	-11.6	-0.2	0.74
K_{24}	62.1	10.8	-195.9	-96.3	134.5	-5.3	0.91
K_{34}	-7.0	-12.1	-16.3	20.4	-9.8	3.5	0.33
K_{VV}	3626.1	-2328.0	10033.0	3369.7	-1223.3	946.0	0.72
K_{54}	749.3	41.3	-3457.2	-596.7	334.2	-66.2	0.80
K_{64}	-253.9	444.6	751.5	-37.9	241.2	12.5	0.36
K_{14}	-16.2	-2.8	45.2	7.1	-11.6	-0.2	0.74
K_{15}	-2.0	-5.1	30.5	6.8	-0.1	1.7	0.53
K_{25}	13.5	8.8	-40.6	-12.1	11.4	-2.7	0.78
K_{35}	2.8	3.6	-19.6	-7.2	4.2	-1.0	0.78
K_{45}	356.0	-179.8	-922.5	148.0	-161.4	53.9	0.72
K_{IE}	440.7	-52.7	-1110.0	-131.8	120.6	-5.0	0.85
K_{65}	-53.9	19.1	67.5	14.0	-18.7	-3.5	0.61
K_{16}	10.5	12.0	-102.5	-21.4	1.1	-4.1	0.71
K_{26}	-1.4	-6.2	28.9	13.9	-15.0	3.0	0.69
K_{36}	-4.2	-7.4	61.7	23.1	-16.2	3.1	0.88
K_{46}	-891.3	127.3	6347.8	476.1	157.5	-52.6	0.73
K_{56}	-716.6	-192.5	5799.1	1046.4	-366.9	113.7	0.81
K_{FE}	385.3	-150.3	594.3	93.3	164.7	82.7	0.26

4.6 Stiffness Matrix of ACL Deficient Knee

In this current work, the anterior cruciate ligament of one specimen (ID: 200702) was cut to compare the stiffness matrix between intact and ACL-deficient knee. Because the ACL injury always occurred at the lower flexion angles with anterior translation of the tibia, ten joint positions were chosen in the comparison: the passive path position, +1.5 mm, +3 mm, -1.5 mm, and -3 mm on anterior-posterior direction at 30° and 60° of flexion angles. At a lower flexion angle, the ACL has more function when the tibia was translating on AP direction. Thus, the ten joint positions were AP joint positions at 30° and 60° of flexion. The stiffness matrices of the intact knee were derived from these joint positions first, then the ACL had been cut. Stiffness matrices of the ACL-deficient knee were measured at the same joint positions.

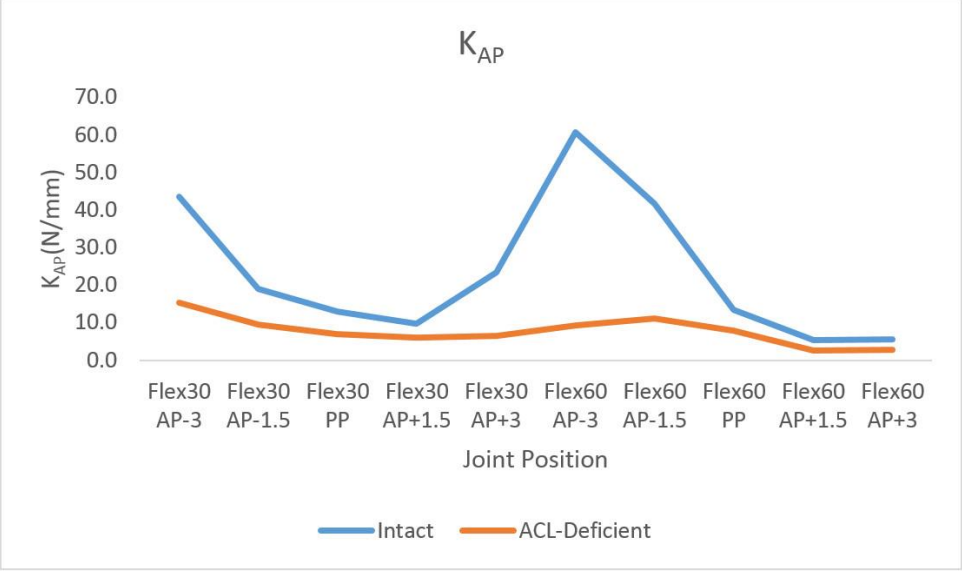

Figure 4.20 Primary stiffness on AP direction of both intact and ACL-deficient knee (ID: PK200702)

The primary stiffness on AP direction after cutting the ACL was smaller than that of the intact knee throughout all the joint positions (Figure 4.20). The major function of the ACL was to resist the anterior translation of the tibia with respect to the femur. For an ACL-deficient knee, the knee joint would lose the resistance from the ACL on AP direction during the measurement of stiffness matrix. Therefore, the primary stiffness of the ACL-deficient knee was smaller than that of the intact knee.

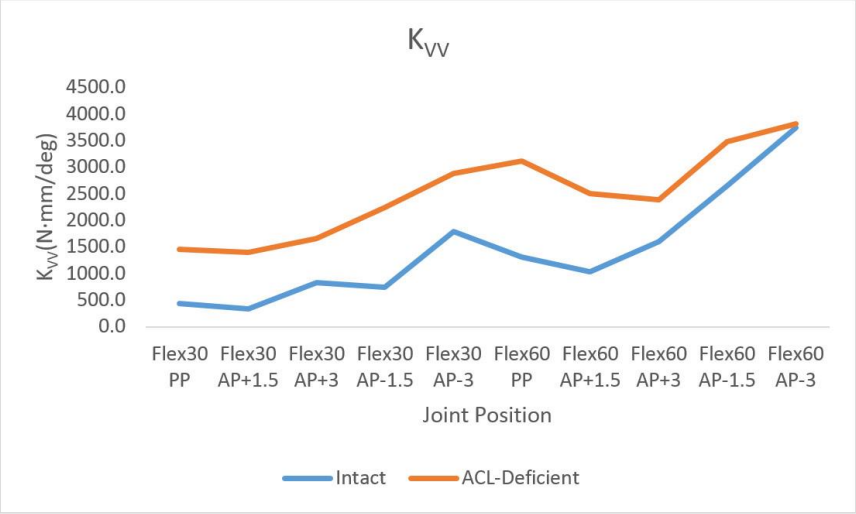

Figure 4.21 Primary stiffness on VV direction of both intact and ACL-deficient knee (ID: PK200702)

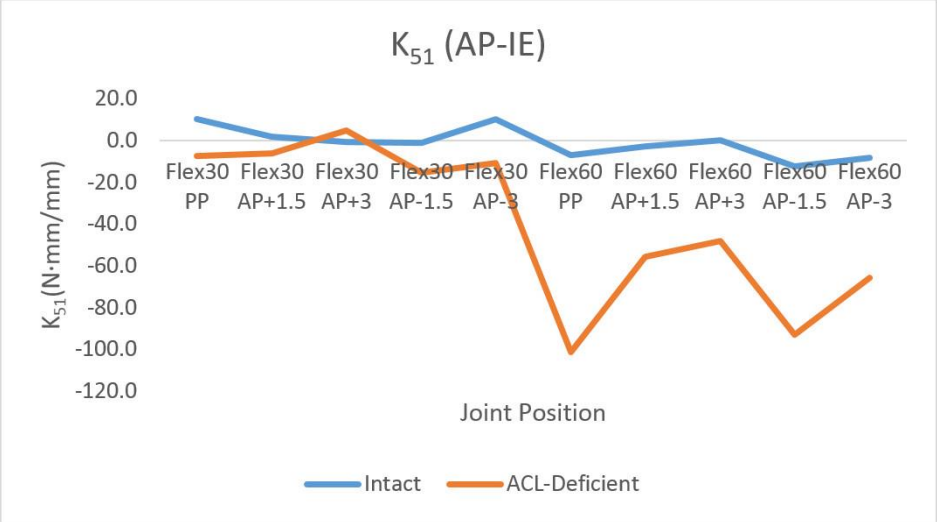

Figure 4.22 Secondary stiffness between AP and IE of both intact and ACL-deficient knee (ID: PK200702)

However, throughout all the joint positions, the primary stiffness on varus-valgus direction in the ACL-deficient knee was greater than the intact knee (Figure 4.21). Previous studies investigated that the stiffness on VV direction in the ACL-deficient knee was smaller than that of the intact knee [65], which was contradictory to the results in this study. Additionally, the secondary stiffness between AP and IE directions in the ACL-deficient knee was greater than the intact knee at 60° of flexion (Figure 4.22), which indicated that the effect of the anterior translation on the external moment was enhanced after cutting the ACL. Increase was also found in other stiffness coefficients of the ACL-deficient knee including both primary (K_{IE}) and secondary stiffness (K_{43}). (Appendix Figure 16 – 17) The ACL can prevent the tibia from translating anteriorly with respect to the femur, as well as provides rotational stability to the knee joint. A higher secondary stiffness between AP and IE indicated more instability on internal-external direction when the tibia was translating on AP direction. Therefore, the ACL-deficient knee showed higher secondary stiffness values compared with the intact knee. Nevertheless, the current work chosen ten joint positions on anterior-posterior direction with one specimen. Future work should be done on more specimens with more joint positions to have a better on the difference in stiffness matrix between intact and ACL-deficient knee.

5.0 Discussion

A protocol of robotic testing system was developed to derived the stiffness matrix at chosen joint positions of porcine knee have been derived by using a robotic testing system. Both primary and secondary stiffness coefficients associated with all the six DOFs established the matrix. The primary stiffness coefficients calculated by two methods were compared and the coefficients derived from the protocol of the current study were greater than those from a more traditional method. In addition, the secondary stiffness coefficients indicate that displacement applied on one DOF would cause forces or moments on other directions.

5.1 Cause of Difference between the Two Methods

In section 4.3, the primary stiffness values derived from both force perturbation and continuous displacement method showed quite difference and several reasons were considered. First, although the joint position on the calculated DOF are the same for both methods, there are some differences on the other five DOFs because of the different methods. Based on the results in Section 4.2, the different joint position on other DOFs may lead to change of stiffness. At some joint positions, a 4-5 degrees difference in internal-external direction or 1-2 mm difference in medial-lateral direction will occur, which can cause a difference in stiffness to the knee joint. Secondly, the stiffness calculation of the two methods is quite different. For the perturbation method, each stiffness coefficient is derived from the stiffness matrix, which is calculated by taking invert of the whole compliance matrix. Thus, all the 36 coefficients in the compliance matrix

will make contribution to the stiffness coefficients as coupled coefficients. However, in the continuous curve method, the primary stiffness is calculated by taking the slope of the load-displacement curve, which is the reciprocal of one compliance coefficient without the contribution of coupled coefficients. This difference implies that the primary stiffness obtained from the stiffness matrix will be higher than the values derived by taking slope of the load-displacement curve. The result shows that most comparisons were in accord with that expectation. Furthermore, the preconditioning in perturbation method was performed by inputting a small additional load and the joint was only moving around the chosen joint position. However, in continuous method, the preconditioning cycle was covered the whole range of motion of the knee joint. During each loading cycle, the internal structure of the soft tissues would change. As a result, the disparate cycle routine of the two methods can produce different mechanical properties of soft tissues, which will lead to difference in stiffness values. An example from specimen PK200206 at 30° of flexion could show the different mechanical properties between the two methods. When the tibia was translating from 1.983mm of anterior to 1.741mm of anterior, the anterior force was changing from 44N to 32N in the continuous method, however in perturbation method it was from 66N to 44N though the change of displacement were same. Thus, at this joint position the primary stiffness on AP direction derived from the perturbation method would be greater than that of the continuous method. Different joint positions at other DOFs and preconditioning method were both considered as reasons in this case.

5.2 Implications of Findings

5.2.1 Engineering

The data presented in the current work have many implications in the field of bioengineering, especially the area of experimental method and data analysis. The method of measuring knee stiffness matrix in this study is different with the common method in previous research. The previous work inputted a continuous load-displacement curve which could cover the whole range of motion. Each curve can provide one coefficient (primary or secondary) as a function of joint positions. However, when a continuous displacement was inputted on one DOF, only one column of the stiffness matrix could be derived. When the displacement was inputted on a different direction, the joint position would change. Thus, the continuous method in previous study can only developed several curves on each direction separately rather than a stiffness matrix to map all the DOFs. The method in the current study was doing a force perturbation on all the six DOFs after reaching the designed joint positions. With the additional force or moments on each direction and the outputted displacements on 6 DOFs, the compliance matrix with 36 elements could be built. Stiffness matrix with both primary and secondary coefficients can be derived by taking inverse of the compliance matrix. With the stiffness matrices at several chosen joint positions, the stiffness matrix map could be built to predict the structural characteristics at the positions which were not included in the experiment in the future work.

The data acquired in the current work have implications for mechanical properties of the knee joint at different joint positions. One stiffness matrix could offer 36 coefficients associated with six DOFs. These coefficients could not only show the stiffness on each direction independently, but also indicated the effect of motion on one direction to another. Therefore, one

stiffness matrix could help to determine the biomechanical properties on all the 6 DOFs. In addition, each coefficient was changing as a function of joint positions, which can be used to observe how the mechanical properties would change at different joint positions and its implications for knee function and biomechanics.

The stiffness matrix data can also be applied to establish the three-dimensional mathematical knee modelling. The use of stiffness matrix could promise a higher accuracy of the mechanical properties of the knee model. If the prediction of the mathematical model could be verified by the data from experiment, a solid knee model can be built for kinematic research. Changing the stiffness of the knee model to simulate the ligament injuries instead of cutting off ligaments from the knee cadaver is also an option to improve cost-efficient in a study.

5.2.2 Clinical

In addition to the implications in engineering area, the results presented in this study also have clinical relevance. The stiffness values at different joint positions of the porcine knee can indicate knee function. On AP direction, the knee was stiffer when the tibia was translating posteriorly. For this result, PCL tension pattern was considered as the major reason. Both AL and PM bundles would elongate more at higher flexion angles than extended position, as a result the elongated ligament became stiffer and had effect on the stiffness of the knee joint. The primary stiffness on medial-lateral direction was greater at 30° of flexion, where was a full extension position for the porcine knee joint, therefore the knee was stiffer than other flexion angles. Among different DOFs, proximal-distal and varus-valgus was stiffer than the other four directions especially at 30° of flexion. One possible reason for a higher value of K_{PD} and K_{VV} was bony contact. The stiffness on PD direction was measured by applying additional 10N force on both

proximal and distal directions. When the tibia was translating proximally, the tibia was pushing and compressing to the femur to cause a higher stiffness value due to the contact. And the joint position data from the robotic testing system implied that the tibia was moving more anteriorly and proximally during flexion (Table 5.1 is an example from specimen ID: PK191114), which could create more space and less bony contact between the femur and tibia. As a result, the primary stiffness on proximal-distal direction would decrease during flexion. For varus-valgus motion, bony contact still played a role due to the compressive force between femoral condyles and tibial plateau. Therefore, when the tibia was moving more anteriorly and proximally during flexion, K_{VV} decreased because of less bony contact and more space between the femur and tibia. And the bony contact between the tibia and femur during the measurement on these two directions leaded to a higher stiffness value.

Table 5.1 Passive path translational position on AP and PD directions at different flexion angles (Specimen ID: PK191114)

	30° of Flexion	60° of Flexion	90° of Flexion
AP (mm)	1.6	15.5	30.3
PD (mm)	0.1	3.5	11.4

Currently when clinicians perform a physical examination maneuver to assess the integrity of ACL, they would flex the patient's knee to a certain flexion angle then grasp and pull the tibia anteriorly to feel if there was an endpoint (e.g. Lachman test, anterior drawer, etc.). The stiffness data at different joint positions suggested that at some joint positions the stiffness of the knee is higher with the combination of flexion and external rotation. And a higher stiffness value indicates that the knee is harder to move, which could be helpful to find some joint positions easier to feel the endpoint when performing physical examination. If stiffness coefficients in the matrix can be

defined by a function of the joint positions as independent variables, stiffness characteristics of the untested positions could be derived. Joint positions with a higher stiffness value can be obtained from the function and then verified through experiment, which may also improve diagnostic procedure.

The secondary stiffness coefficients can be helpful in detecting joint positions which are easier to get injured with consideration of coupled loads. This current work suggests that some translational motion could generate a large moment on rotational directions. Therefore, the motion within a safe range on one direction may let the knee get injured from the moment of other directions. A comprehensive consideration with both primary and secondary stiffness should be made in post-operation exercise to avoid the ligament injuries. In addition, the concept of stiffness matrix includes the structural properties of the knee joint of 6 DOFs. The 36 stiffness coefficients of the knee joint can indicate the knee function and load-carrying characteristics on six directions. Thus, stiffness matrix can be used to assess if the knee after ligament reconstruction or total knee arthroplasty has totally restored knee biomechanics back to the intact state on all DOFs.

5.3 Comparison to Literature

Because such a method to quantify the nonlinear stiffness matrix for the knee joint has not been developed in the past, a direct comparison of the secondary stiffness to literature is difficult. However, the primary stiffness coefficients were compared to values reported in the literature. On anterior-posterior direction, the porcine knee was stiffer when the tibia was translating posteriorly than anteriorly by the same displacement with respect to the passive path position. When a previous work applied a 134 N force on both anterior and posterior directions of human knee, the

displacement on posterior direction was smaller than that of the anterior direction especially at higher flexion angles (60°: anterior 8.5mm/posterior 5.4mm, 90°: anterior 7.8mm/posterior 5.7mm), which indicated a higher stiffness value when the tibia was translating posteriorly [70].

For the rotational directions, the current work stated that the porcine knee was also stiffer when the tibia was rotating externally. Similar results were also found in a porcine study that the external tibia rotation (10°) was smaller than that of the internal tibia rotation (20°) under the same loading condition for porcine knee [56]. On varus-valgus direction, the primary stiffness had a higher value at 30° of flexion in this study. Previous work on porcine knee showed that at 30° of flexion, the primary stiffness on VV direction was 1515.2 N·mm/deg whereas at 60° of flexion it was 1020.4 N·mm/deg [65], which also indicated that K_{VV} was greater at 30° of flexion. Previous work on human knee also demonstrated that the primary stiffness on varus-valgus direction (with a range from around 0.8 to 6.2) was greater than that of internal-external direction (with a range from around 0.2 to 1.3 N·m/deg) [48]. This current work also concluded that the stiffness on varus-valgus direction of the porcine knee was significantly greater than that of internal-external direction.

5.4 Advancements and Limitations

5.4.1 Advancements

In the current work, a comprehensive analysis was performed in which an experimental method to describe the mechanical properties of the knee joint was developed. Previously, the

measurement of the stiffness of the knee joint has been performed by inputting a continuous displacement to cover the whole range of motion on one direction or assuming the linear elastic theory [35, 36, 38, 40, 41, 45, 48]. Nevertheless, in this study, a force perturbation at each joint position instead of the whole range of motion was performed to obtain the compliance. Therefore, a stiffness matrix could be quantified at each chosen joint position by taking inverse of the whole compliance matrix. The robotic testing system with high stiffness and repeatability could ensure accuracy of the measurement. Additionally, nonlinearity was observed in the stiffness coefficients as a function of joint positions, where the knee joint was indeed a nonlinear system.

In addition to experimental advancements, this study has demonstrated clear computational advancements as well. The stiffness coefficients of the current work were all directly taken from the stiffness matrix. Functions with joint positions as independent variables and stiffness coefficients as dependent variables could be built wo predict the stiffness performance at the untested joint positions. These stiffness terms can also be expanded by performing additional tests on more intact and ligament injury knee joints to determine the effect of ligament deficiency to the mechanical properties of the whole joint. With the need of research on a specified direction, the stiffness coefficients related to that direction could be directly found and be used in conjunction with knee movement to improve the overall understanding of the function and biomechanics of knee joint.

5.4.2 Limitations

In spite of the advancement to both the engineering and clinical area, there are several limitations that should be noted. The measurement of the stiffness matrix happened at each joint position by doing perturbations on six directions. However, after each perturbation, the joint

position would have some sort of change especially at the positions with a lower stiffness magnitude, which means the measurement was not performed around the exactly same position. Figure 5.1 shows an example of the measurement of stiffness matrix at 30° flexion and +1.5mm anterior displacement of specimen PK200204. From the load-displacement curve, at first the perturbation on AP direction was performed around 3° internal rotation on IR-ER direction, whereas it happened at 4° internal rotation when measuring the stiffness coefficients on FE direction in the end. That 1° difference of joint position on IR-ER direction may have effect to the stiffness value. The protocol made a big effort to ensure the joint position would stay same during each measurement, however the passive path was not controlled with the force control protocol.

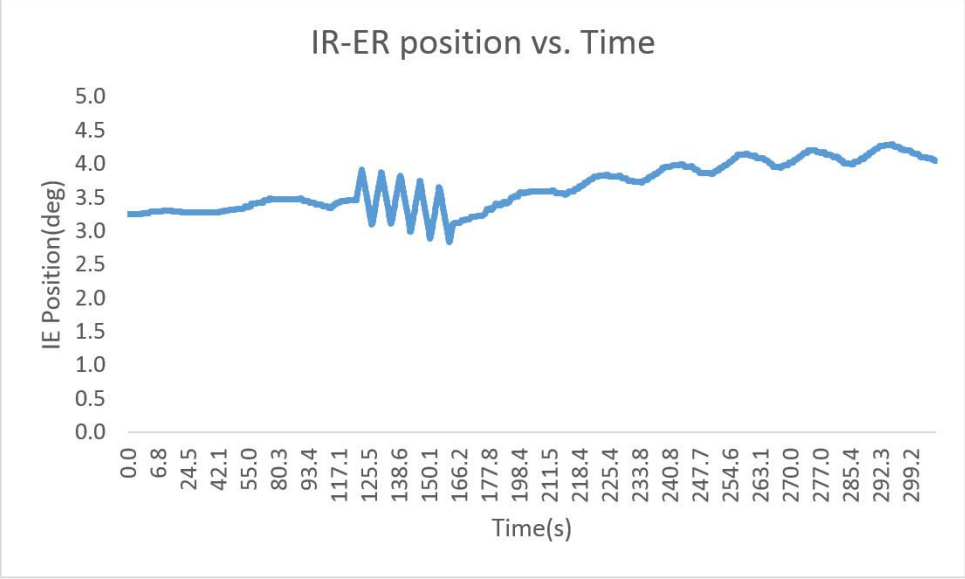

Figure 5.1 IE position (deg) during measuring the stiffness at 30° of flexion and +1.5mm of anterior (Specimen ID: PK200204)

Secondly, the experiment took far too long with 11-12 hours. Though saline was spraying on the knee joint every half hour, water still kept losing during the test. And the knee was clamped

and fixed at each flexion angle for 3-4 hours to measure stiffness at all the 15 joint positions. Therefore, the mechanical properties of the soft tissues may change after loading at one flexion angle for a long time.

In addition, maintaining the joint position and measuring the stiffness matrix cannot be performed at the same time perfectly. To keep the joint position as desired at each measurement, flexion angle was locked by using position control when the measurement of stiffness on other directions was performed for both perturbation and continuous method. However, there would be displacement on other directions (e.g. anterior translation, external rotation) during a normal flexion. Thus, the lock of flexion angle would lead to lose some displacements on other DOFs. As a result, the knee joint would be a littler stiffer than it supposed to be when the flexion angle was locked. Also, the results in this current study would only apply for this certain robotic testing system because the motion of this system is faster and could measure the small displacement of the knee joint while maintaining the joint position. If the same specimen was tested on another testing system the results would be different or inaccurate.

5.5 Future Direction

Most of the specimens used in the current study were intact porcine knees. In light of the stiffness matrix coefficients could demonstrate the knee function, future directions are suggested that more ligament injured knees should be tested to investigate the effect of the ligament injury to the stiffness coefficients and its connection with ligament function and mechanism of injuries. Still, stiffness matrices will be derived from the test of intact knee first and then one of the ligaments will be cut and test again. Comparison of the stiffness coefficients between the intact

and ligament deficient knee will be made to inspect the change of coefficients. More joint positions could be used in the test to map out the stiffness matrix as a function of joint positions to build a model with better goodness-of-fit to predict the structural characteristics at the joint positions which are not included in the experiment. Due to the limitation of the experimental time, joint positions in the current work were finite with displacements changing on only two directions each time. At different flexion angles, different joint positions were chosen by inputting displacements on one DOF at one time and the other DOFs are passive path. Based on the findings from current study, future work can focus on joint positions more prone to injuries. For instance, a higher risk of ACL injury may occur when the tibia has a movement of anterior translation, external rotation, and valgus at the same time. Stiffness matrix can be measured at such susceptible joint positions to analyses the biomechanical properties.

In addition to the joint positions, another certain future direction is to test on the cadaver of both intact or ligament deficient human knees. The porcine knee specimens in the current work could demonstrate the feasibility of this protocol to measure stiffness matrix and understand the 6 DOF phenomenon and its implications in knee function. The final aim will focus on apply the stiffness matrix concept into clinical sports medicine or orthopedics. Thus, same protocol will be performed on human knee cadavers and the chosen of joint positions will be reconsidered due to the different range of motion with porcine knee. Furthermore, bony morphology may be used to investigate the change of stiffness coefficients caused by different shape of the femur and tibia.

5.6 Summary

Stiffness matrix is an extremely complex concept which can evaluate the 6 DOFs structural properties of the knee joint, however the measurement of the stiffness matrix has not been standardized. Researchers have proposed assuming linear elastic theory to the knee joint or inputting a continuous displacement on each direction separately, which both have limitations. Therefore, the objective of this work was to develop a protocol to derive the 6 by 6 stiffness matrix of the porcine knee joint, and investigate the knee stiffness coefficients as a function of joint positions. Force perturbation was performed by inputting an additional force or moment on each direction and the displacements on six DOFs were measured to derive the compliance matrix with 36 elements. Then the whole compliance matrix was inverted for obtaining the stiffness matrix. The previous studies could only get the stiffness matrix by assuming the knee joint was a linear structure or measure the nonlinear stiffness throughout the range of motion instead of building a matrix. By using the novel method in the current work, a nonlinear stiffness matrix can be quantified at any joint position and the primary stiffness data has been validated by literature. In addition, primary stiffness coefficients were also collected from the load-displacement curve by inputting a continuous displacement on one direction to compare the stiffness values derived from both methods. The overall stiffness on anterior-posterior and internal-external directions was lower with larger range of motion, but when the tibia was moving posteriorly or externally, the porcine knee joint would become stiffer. On proximal-distal and varus-valgus directions the joint was stiffer, especially when the tibia was compressed to the femur at 30° of flexion. Difference was also investigated in the primary stiffness derived from the stiffness matrix and the load-displacement curve due to math calculation, different joint positions and preconditioning method. From the secondary stiffness coefficients, an anterior displacement could cause an external

moment on the tibia and the medial-lateral translation had effect on varus-valgus direction. With the stiffness coefficients at different joint positions, multiple linear regression model was built to fit the results into functions with stiffness as dependent variables and joint positions as independent variables to predict the stiffness matrix. Differences in the stiffness matrix were also investigated between the intact and ACL-deficient knee. The specimens used in the current work were all porcine knees. Thus, in the future studies of human knee, the protocol including joint positions and loading conditions may be adjusted and the results of stiffness change could show difference with that of the porcine knee.

Based on the findings in the current work, nonlinear stiffness matrix can be quantified at different joint positions of the knee joint. Before the conclusion of this work can be applied clinically, however, additional porcine knee joint with ligament injuries need to be tested at the same joint positions as the intact knee and the difference in stiffness matrix with a regular pattern between intact and injured knees should be investigated. Therefore, future direction includes using the measurement described in the current work to derive stiffness matrix at different joint positions of intact and injured knee, and suggest the clinically relevant joint positions where the primary and secondary stiffness both have higher values. This may allow for a more thorough understanding of the structural properties of the knee joint and accurate physical examinations by using these clinically relevant joint positions, which may eventually lead to an improve in surgical outcomes.

Appendix A Joint Positions

The table below are the 45 chosen joint positions in the current study. The detailed displacements on each DOFs are showed. A stiffness matrix was derived at each joint position.

Appendix Table 1 Joint Positions List

FE	IE	VV	AP	ML	PD
+30°	PP	PP	PP	PP	PP
+30°	+3°	PP	PP	PP	PP
+30°	+5°	PP	PP	PP	PP
+30°	-3°	PP	PP	PP	PP
+30°	-5°	PP	PP	PP	PP
+30°	PP	+1°	PP	PP	PP
+30°	PP	-1°	PP	PP	PP
+30°	PP	PP	+1.5mm	PP	PP
+30°	PP	PP	+3mm	PP	PP
+30°	PP	PP	-1.5mm	PP	PP
+30°	PP	PP	-3mm	PP	PP
+30°	PP	PP	PP	+2mm	PP
+30°	PP	PP	PP	-2mm	PP
+30°	PP	PP	PP	PP	+0.5mm
+30°	PP	PP	PP	PP	-0.5mm
+60°	PP	PP	PP	PP	PP
+60°	+3°	PP	PP	PP	PP
+60°	+5°	PP	PP	PP	PP
+60°	-3°	PP	PP	PP	PP
+60°	-5°	PP	PP	PP	PP
+60°	PP	+1°	PP	PP	PP
+60°	PP	-1°	PP	PP	PP
+60°	PP	PP	+1.5mm	PP	PP
+60°	PP	PP	+3mm	PP	PP
+60°	PP	PP	-1.5mm	PP	PP
+60°	PP	PP	-3mm	PP	PP
+60°	PP	PP	PP	+2mm	PP
+60°	PP	PP	PP	-2mm	PP
+60°	PP	PP	PP	PP	+0.5mm
+60°	PP	PP	PP	PP	-0.5mm
+90°	PP	PP	PP	PP	PP

Appendix Table 1 (continued)

+90°	+3°	PP	PP	PP	PP
+90°	+5°	PP	PP	PP	PP
+90°	-3°	PP	PP	PP	PP
+90°	-5°	PP	PP	PP	PP
+90°	PP	+1°	PP	PP	PP
+90°	PP	-1°	PP	PP	PP
+90°	PP	PP	+1.5mm	PP	PP
+90°	PP	PP	+3mm	PP	PP
+90°	PP	PP	-1.5mm	PP	PP
+90°	PP	PP	-3mm	PP	PP
+90°	PP	PP	PP	+2mm	PP
+90°	PP	PP	PP	-2mm	PP
+90°	PP	PP	PP	PP	+0.5mm
+90°	PP	PP	PP	PP	-0.5mm

PP – passive path

AP – anterior-posterior

PD – proximal-distal

ML – medial-lateral

VV – varus-valgus

IE – internal-external

Appendix B Stiffness Coefficients at Different Joint Positions of Each Specimen

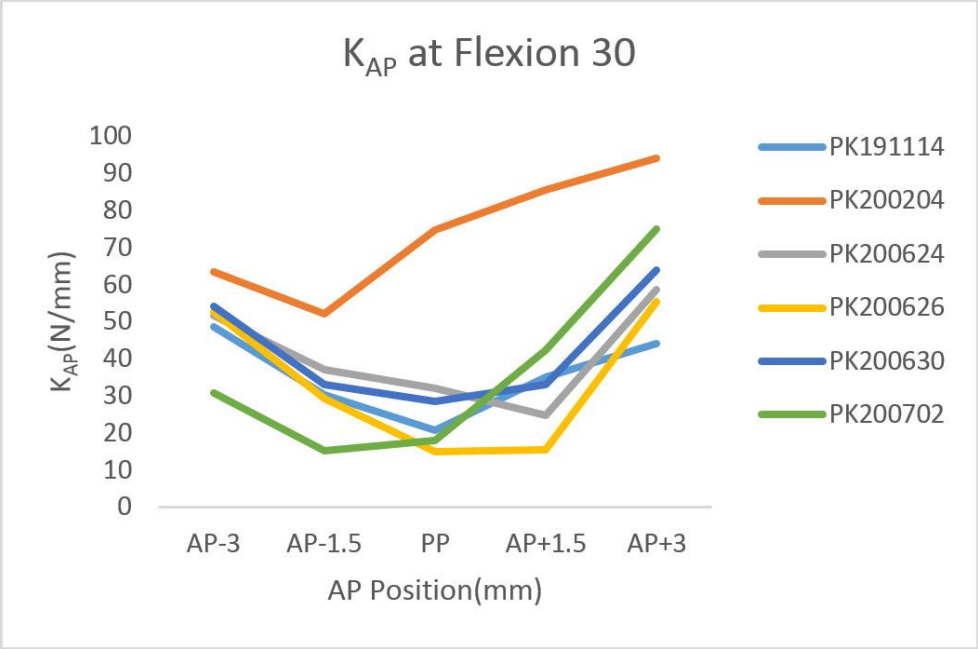

Appendix Figure 1 K_{AP} at different AP positions of different specimens at 30° flexion

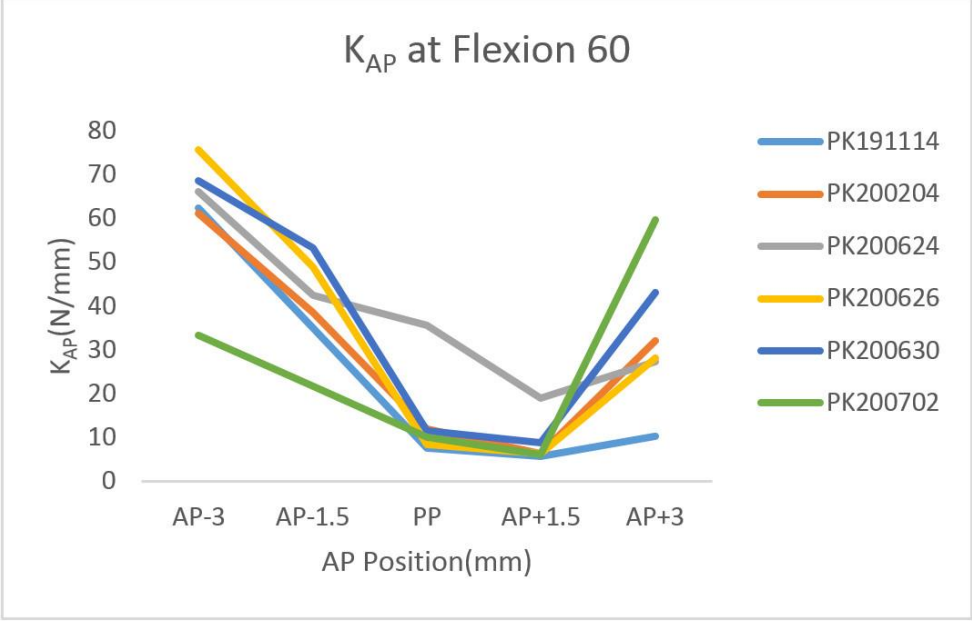

Appendix Figure 2 K_{AP} at different AP positions of different specimens at 60° flexion

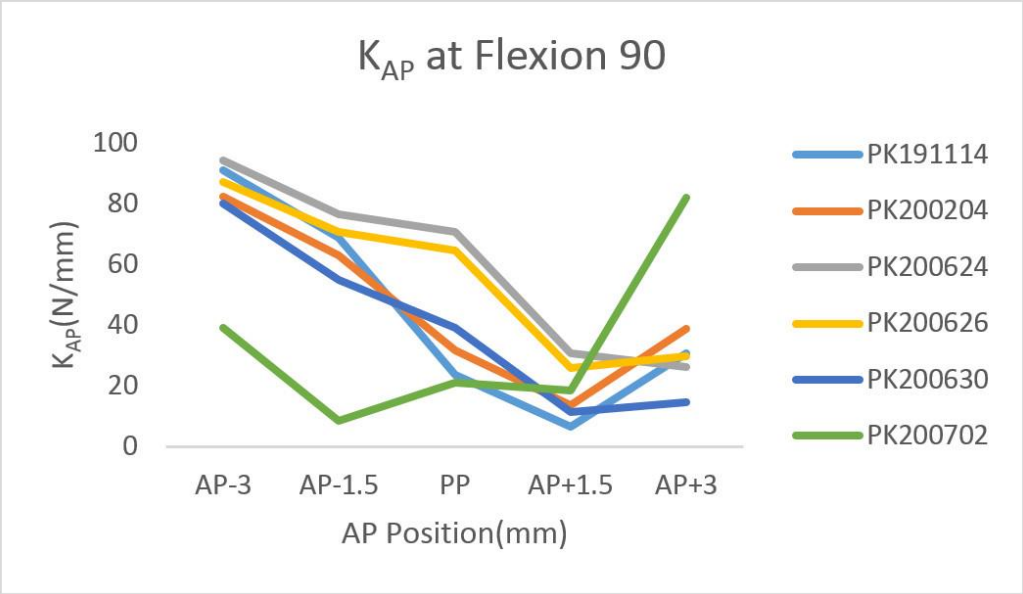

Appendix Figure 3 K_{AP} at different AP positions of different specimens at 90° flexion

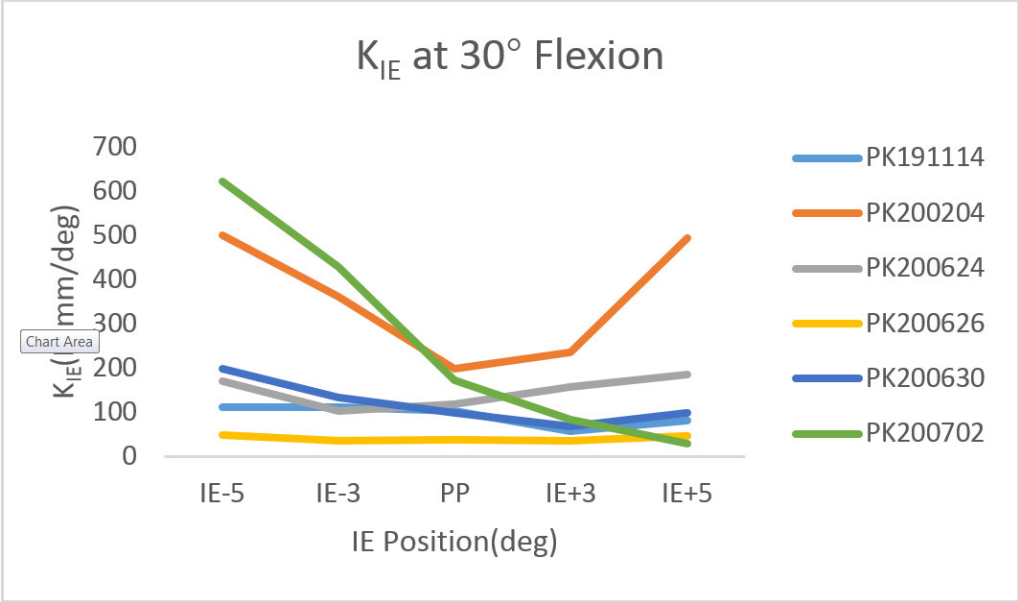

Appendix Figure 4 K_{IE} at different IE positions of different specimens at 30° flexion

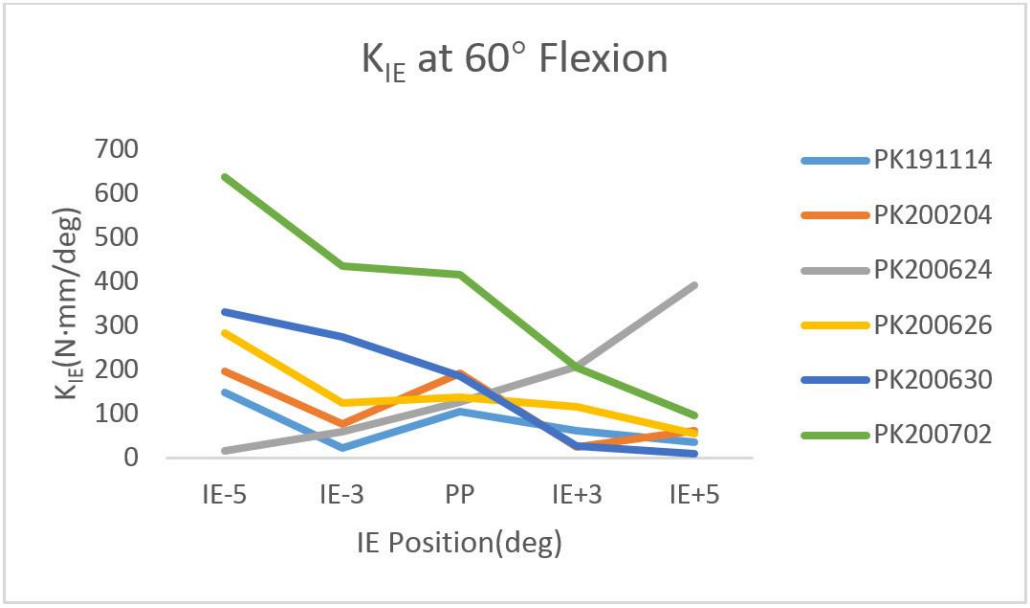

Appendix Figure 5 K_{IE} at different IE positions of different specimens at 60° flexion

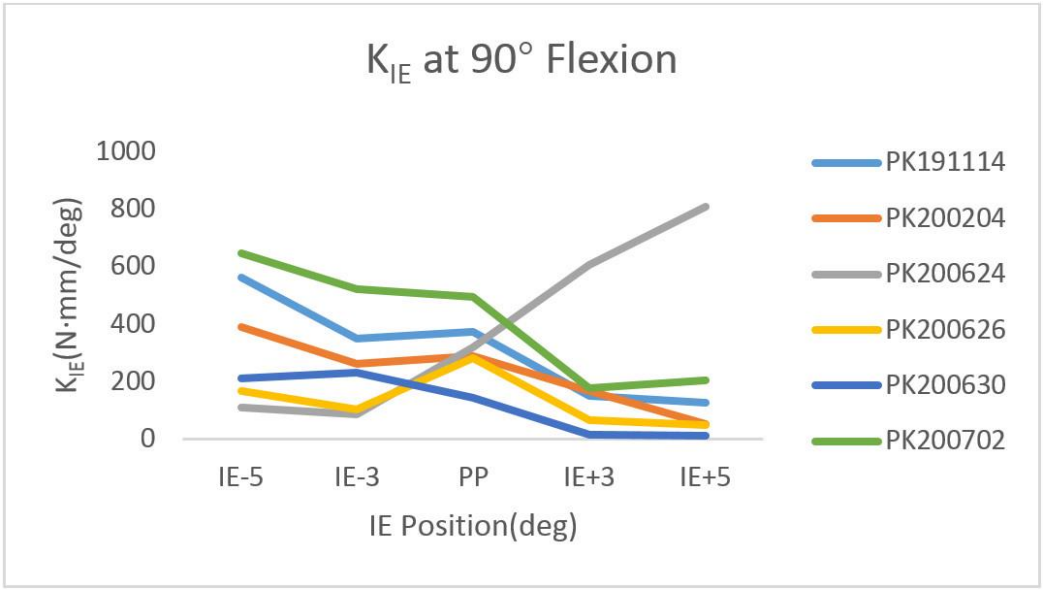

Appendix Figure 6 K_{IE} at different IE positions of different specimens at 90° flexion

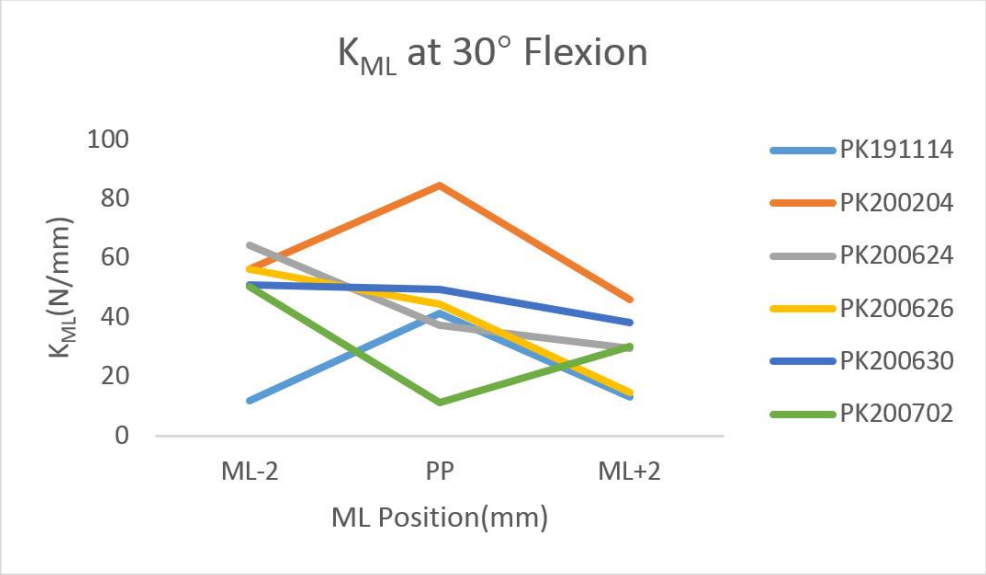

Appendix Figure 7 K_{ML} at different ML positions of different specimens at 30° flexion

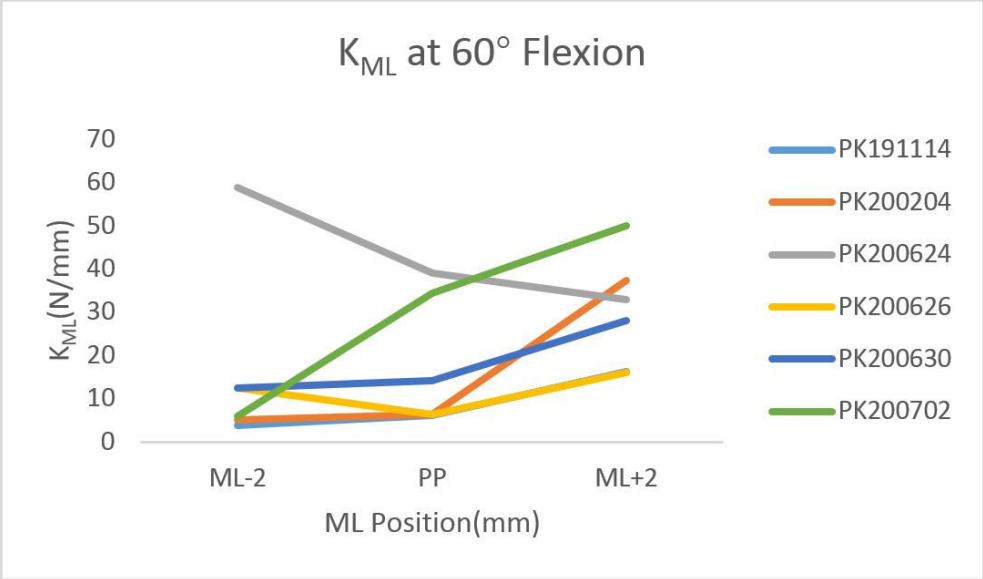

Appendix Figure 8 K_{ML} at different ML positions of different specimens at 60° flexion

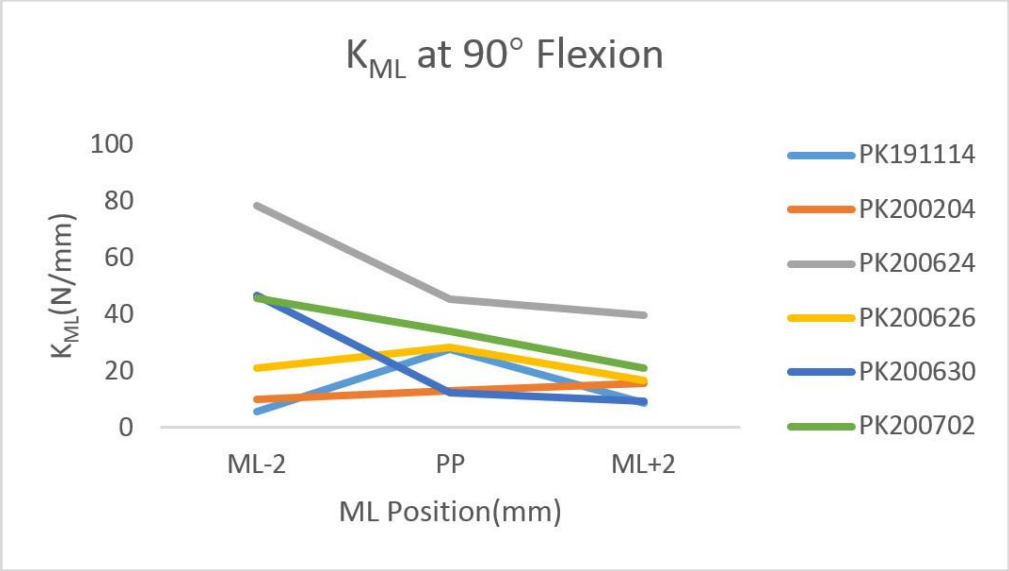

Appendix Figure 9 K_{ML} at different ML positions of different specimens at 90° flexion

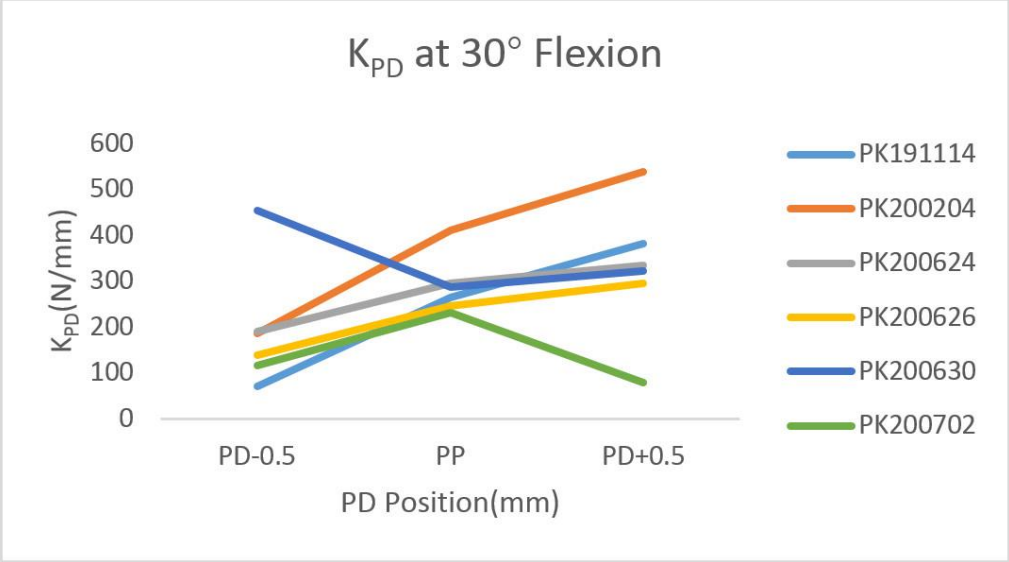

Appendix Figure 10 K_{PD} at different PD positions of different specimens at 30° flexion

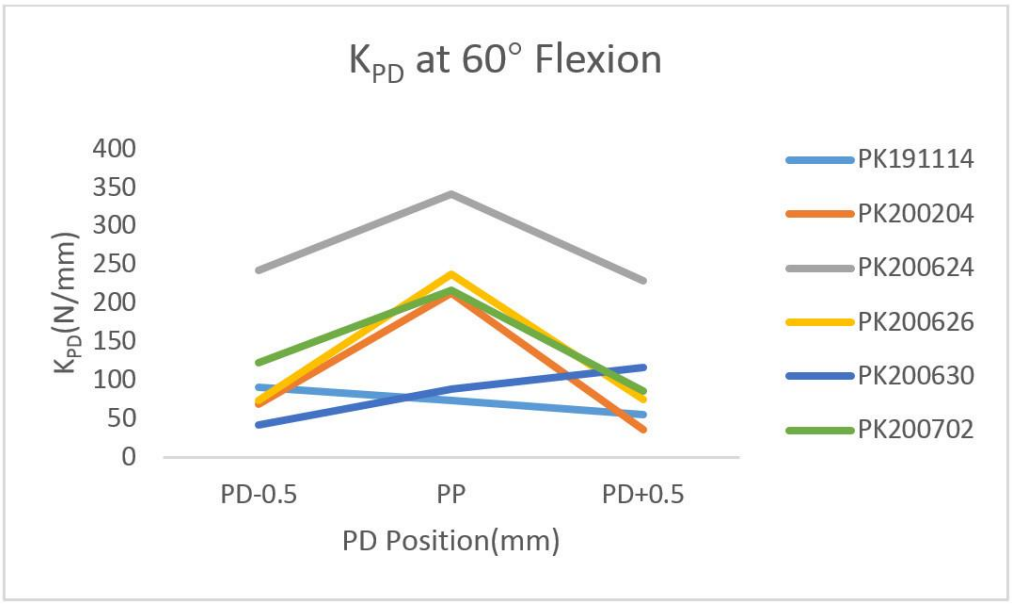

Appendix Figure 11 K_{PD} at different PD positions of different specimens at 60° flexion

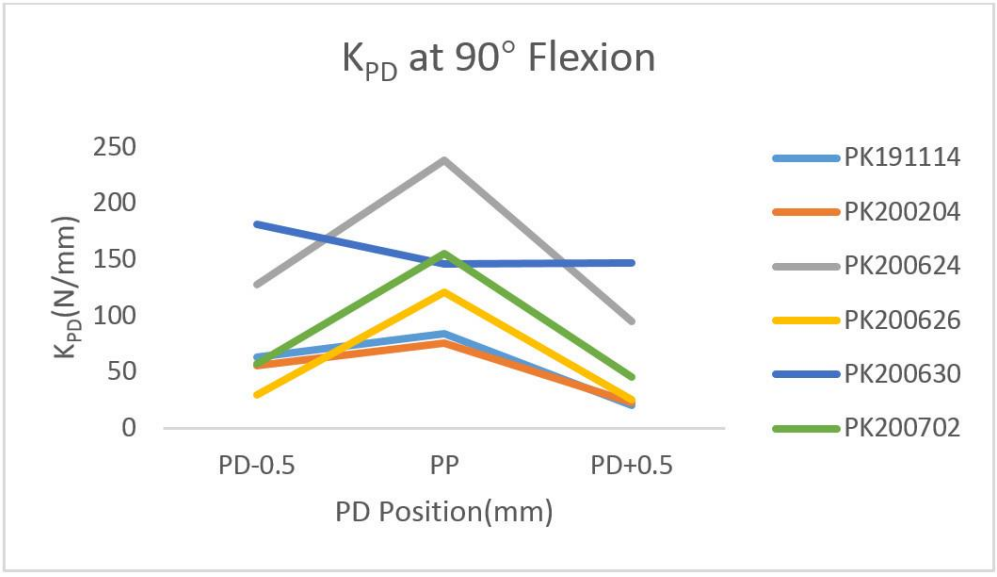

Appendix Figure 12 K_{PD} at different PD positions of different specimens at 90° flexion

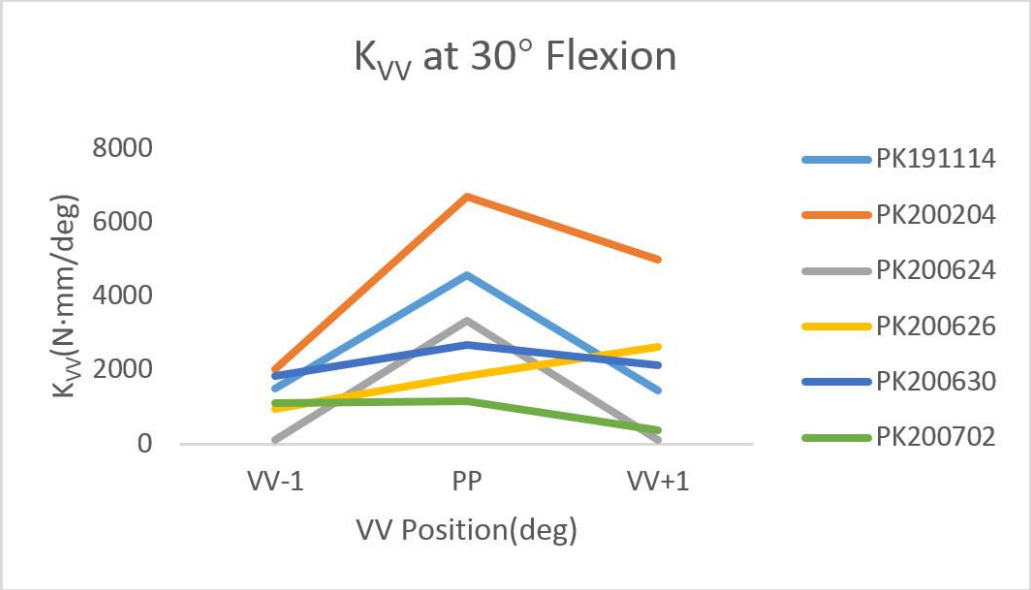

Appendix Figure 13 K_{VV} at different VV positions of different specimens at 30° flexion

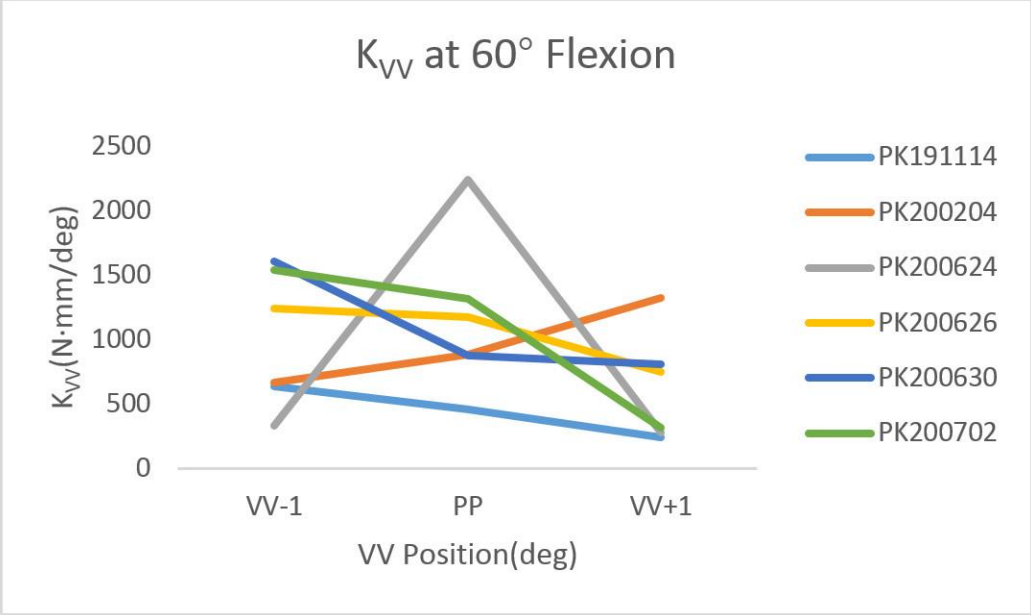

Appendix Figure 14 K_{VV} at different VV positions of different specimens at 60° flexion

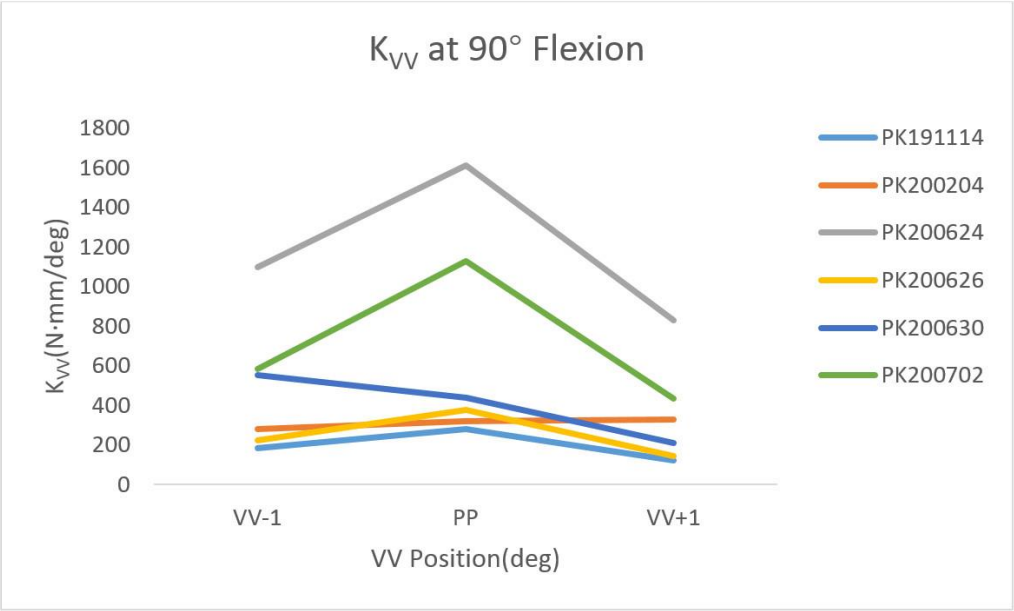

Appendix Figure 15 K_{VV} at different VV positions of different specimens at 90° flexion

Appendix C Comparison Between Both Methods

Specimen ID: PK200204

K_{AP} at Flexion 30 (N/mm)

	Passive Path	AP +1.5mm	AP+3mm	AP-1.5mm	AP-3mm
Perturbation	74.7	85.7	94.1	52.1	63.6
Continuous	26.1	47.1	98.8	27.1	45.5

K_{IE} at Flexion 30 (N·mm/deg)

	Passive Path	IE+3deg	IE+5deg	IE-3deg	IE-5deg
Perturbation	56.3	234.3	494.5	360.1	500.4
Continuous	69.1	118.7	260.0	127.7	221.5

K_{ML} at Flexion 30 (N/mm)

	Passive Path	ML+2mm	ML-2mm
Perturbation	84.6	45.9	56.3
Continuous	25.0	50.1	27.0

K_{PD} at Flexion 30 (N/mm)

	Passive Path	PD+0.5mm	PD-0.5mm
Perturbation	410.6	538.3	186.8
Continuous	237.6	481.3	180.2

K_{VV} at Flexion 30 (N·mm/deg)

	Passive Path	VV+1deg	VV-1deg
Perturbation	6695.5	4989.6	2026.9
Continuous	2233.5	4417.2	726.6

K_{AP} at Flexion 60 (N/mm)

	Passive Path	AP +1.5mm	AP+3mm	AP-1.5mm	AP-3mm
Perturbation	11.9	6.3	32.1	38.6	61.2
Continuous	1.4	1.2	20.3	21.4	61.4

K_{IE} at Flexion 60 (N·mm/deg)

	Passive Path	IE+3deg	IE+5deg	IE-3deg	IE-5deg
Perturbation	190.5	24.9	61.0	75.5	195.4
Continuous	9.3	40.6	149.1	47.3	47.4

K_{ML} at Flexion 60 (N/mm)

	Passive Path	ML+2mm	ML-2mm
Perturbation	6.4	37.4	5.1
Continuous	2.7	19.9	3.6

K_{PD} at Flexion 60 (N/mm)

	Passive Path	PD+0.5mm	PD-0.5mm
Perturbation	212.4	36.1	68.4
Continuous	11.1	54.7	22.8

K_{VV} at Flexion 60 (N·mm/deg)

	Passive Path	VV+1deg	VV-1deg
Perturbation	883.5	1325.9	669.1
Continuous	148.2	694.9	198.0

K_{AP} at Flexion 90 (N/mm)

	Passive Path	AP +1.5mm	AP+3mm	AP-1.5mm	AP-3mm
Perturbation	31.8	13.8	38.8	63.1	82.5
Continuous	0.3	2.5	45.1	36.8	82.6

K_{IE} at Flexion 90 (N·mm/deg)

	Passive Path	IE+3deg	IE+5deg	IE-3deg	IE-5deg
Perturbation	289.1	168.6	51.6	261.4	390.4
Continuous	68.8	85.4	57.4	101.3	202.6

K_{ML} at Flexion 90 (N/mm)

	Passive Path	ML+2mm	ML-2mm
Perturbation	12.9	15.6	9.8
Continuous	2.8	15.0	-1.6

K_{PD} at Flexion 90 (N/mm)

	Passive Path	PD+0.5mm	PD-0.5mm
Perturbation	75.6	23.1	55.3
Continuous	44.3	26.2	33.4

K_{VV} at Flexion 90 (N·mm/deg)

	Passive Path	VV+1deg	VV-1deg
Perturbation	321.2	327.0	279.1
Continuous	256.5	759.8	63.7

Specimen ID: PK200624

K_{AP} at Flexion 30 (N/mm)

	Passive Path	AP +1.5mm	AP+3mm	AP-1.5mm	AP-3mm
Perturbation	32.1	24.9	58.7	37.1	51.8
Continuous	21.5	13.5	56.7	23.1	17.8

K_{IE} at Flexion 30 (N·mm/deg)

	Passive Path	IE+3deg	IE+5deg	IE-3deg	IE-5deg
Perturbation	118.6	157.6	184.5	101.7	169.3
Continuous	54.8	82.7	136.2	52.2	79.7

K_{ML} at Flexion 30 (N/mm)

	Passive Path	ML+2mm	ML-2mm
Perturbation	37.3	29.6	64.2
Continuous	16.1	32.7	20.5

K_{PD} at Flexion 30 (N/mm)

	Passive Path	PD+0.5mm	PD-0.5mm
Perturbation	296.1	334.7	189.7
Continuous	88.7	433.5	101.1

K_{VV} at Flexion 30 (N·mm/deg)

	Passive Path	VV+1deg	VV-1deg
Perturbation	3338.8	99.5	101.4
Continuous	1416.1	5072.4	1249.1

K_{AP} at Flexion 60 (N/mm)

	Passive Path	AP +1.5mm	AP+3mm	AP-1.5mm	AP-3mm
Perturbation	35.7	19.0	27.3	42.5	66.3
Continuous	13.3	10.9	37.5	26.1	37.4

K_{IE} at Flexion 60 (N·mm/deg)

	Passive Path	IE+3deg	IE+5deg	IE-3deg	IE-5deg
Perturbation	127.3	207.7	392.0	58.8	16.1
Continuous	21.5	145.0	369.1	20.3	38.6

K_{ML} at Flexion 60 (N/mm)

	Passive Path	ML+2mm	ML-2mm
Perturbation	39.0	32.9	58.8
Continuous	17.8	31.9	26.6

K_{PD} at Flexion 60 (N/mm)

	Passive Path	PD+0.5mm	PD-0.5mm
Perturbation	341.2	228.9	241.7
Continuous	116.2	208.1	129.7

K_{AP} at Flexion 90 (N/mm)

	Passive Path	AP +1.5mm	AP+3mm	AP-1.5mm	AP-3mm
Perturbation	70.7	30.8	26.2	76.7	94.5
Continuous	9.9	8.3	35.3	33.5	44.2

K_{IE} at Flexion 90 (N·mm/deg)

	Passive Path	IE+3deg	IE+5deg	IE-3deg	IE-5deg
Perturbation	318.4	606.8	808.4	84.5	108.8
Continuous	32.8	232.7	653.6	56.3	68.2

K_{ML} at Flexion 90 (N/mm)

	Passive Path	ML+2mm	ML-2mm
Perturbation	45.2	39.8	78.3
Continuous	23.2	29.7	33.3

K_{PD} at Flexion 90 (N/mm)

	Passive Path	PD+0.5mm	PD-0.5mm
Perturbation	237.9	95.0	127.6
Continuous	78.1	82.8	86.4

Specimen ID: PK200626

K_{AP} at Flexion 30 (N/mm)

	Passive Path	AP +1.5mm	AP+3mm	AP-1.5mm	AP-3mm
Perturbation	14.9	15.6	55.5	29.4	52.6
Continuous	1.4	12.1	52.1	16.4	39.3

K_{IE} at Flexion 30 (N·mm/deg)

	Passive Path	IE+3deg	IE+5deg	IE-3deg	IE-5deg
Perturbation	37.4	35.4	46.5	35.6	47.7
Continuous	22.1	27.9	56.5	17.6	11.1

K_{ML} at Flexion 30 (N/mm)

	Passive Path	ML+2mm	ML-2mm
Perturbation	44.5	14.5	56.3
Continuous	13.3	27.1	27.8

K_{PD} at Flexion 30 (N/mm)

	Passive Path	PD+0.5mm	PD-0.5mm
Perturbation	245.3	296.0	137.8
Continuous	98.0	394.8	74.6

K_{VV} at Flexion 30 (N·mm/deg)

	Passive Path	VV+1deg	VV-1deg
Perturbation	1828.6	2629.6	931.5
Continuous	566.4	3580.0	1374.4

K_{AP} at Flexion 60 (N/mm)

	Passive Path	AP +1.5mm	AP+3mm	AP-1.5mm	AP-3mm
Perturbation	8.5	6.3	28.2	49.0	75.8
Continuous	0	1.7	37.1	26.4	69.3

K_{IE} at Flexion 60 (N·mm/deg)

	Passive Path	IE+3deg	IE+5deg	IE-3deg	IE-5deg
Perturbation	137.2	114.5	53.5	123.5	283.3
Continuous	73.0	30.3	89.8	108.9	133.7

K_{ML} at Flexion 60 (N/mm)

	Passive Path	ML+2mm	ML-2mm
Perturbation	6.4	16.0	12.5
Continuous	4.2	21.8	1.6

K_{PD} at Flexion 60 (N/mm)

	Passive Path	PD+0.5mm	PD-0.5mm
Perturbation	237.4	75.0	73.5
Continuous	32.7	119.3	12.3

K_{AP} at Flexion 90 (N/mm)

	Passive Path	AP +1.5mm	AP+3mm	AP-1.5mm	AP-3mm
Perturbation	64.8	25.9	29.8	70.7	87.2
Continuous	20.3	11.9	24.1	35.5	48.9

K_{IE} at Flexion 90 (N·mm/deg)

	Passive Path	IE+3deg	IE+5deg	IE-3deg	IE-5deg
Perturbation	280.5	66.3	49.1	104.7	166.4
Continuous	-474.3	2730.0	1293.8	63.3	-73.8

K_{ML} at Flexion 90 (N/mm)

	Passive Path	ML+2mm	ML-2mm
Perturbation	28.3	16.6	21.1
Continuous	1738.8	16.5	5.7

K_{PD} at Flexion 90 (N/mm)

	Passive Path	PD+0.5mm	PD-0.5mm
Perturbation	120.8	25.6	29.4
Continuous	Not applicable	121.2	18.4

Specimen ID: PK200630

K_{AP} at Flexion 30 (N/mm)

	Passive Path	AP +1.5mm	AP+3mm	AP-1.5mm	AP-3mm
Perturbation	28.5	33.2	63.9	33.0	54.2
Continuous	18.8	13.2	79.8	19.7	52.4

K_{IE} at Flexion 30 (N·mm/deg)

	Passive Path	IE+3deg	IE+5deg	IE-3deg	IE-5deg
Perturbation	97.3	67.0	97.1	132.3	197.7
Continuous	29.3	61.8	129.0	20.6	7.3

K_{ML} at Flexion 30 (N/mm)

	Passive Path	ML+2mm	ML-2mm
Perturbation	49.3	38.2	50.9
Continuous	15.0	45.4	39.9

K_{PD} at Flexion 30 (N/mm)

	Passive Path	PD+0.5mm	PD-0.5mm
Perturbation	286.2	321.7	453.4
Continuous	45.0	400.1	48.6

K_{VV} at Flexion 30 (N·mm/deg)

	Passive Path	VV+1deg	VV-1deg
Perturbation	2663.5	2127.2	1844.7
Continuous	1260.1	3417.4	1133.1

K_{AP} at Flexion 60 (N/mm)

	Passive Path	AP +1.5mm	AP+3mm	AP-1.5mm	AP-3mm
Perturbation	11.6	8.7	43.2	53.4	68.6
Continuous	0.53	1.8	48.2	29.4	56.0

K_{IE} at Flexion 60 (N·mm/deg)

	Passive Path	IE+3deg	IE+5deg	IE-3deg	IE-5deg
Perturbation	185.0	26.7	8.2	274.7	330.0
Continuous	66.3	27.8	32.0	128.9	169.3

K_{ML} at Flexion 60 (N/mm)

	Passive Path	ML+2mm	ML-2mm
Perturbation	14.2	28.1	15.6
Continuous	5.0	34.3	3.7

K_{PD} at Flexion 60 (N/mm)

	Passive Path	PD+0.5mm	PD-0.5mm
Perturbation	88.5	116.3	41.9
Continuous	54.6	149.7	-9.8

K_{VV} at Flexion 60 (N·mm/deg)

	Passive Path	VV+1deg	VV-1deg
Perturbation	878.3	806.4	1605.0
Continuous	534.7	1063.3	891.8

K_{AP} at Flexion 90 (N/mm)

	Passive Path	AP +1.5mm	AP+3mm	AP-1.5mm	AP-3mm
Perturbation	39.2	11.2	14.6	55.0	80.3
Continuous	21.2	4.8	15.0	30.1	62.3

K_{IE} at Flexion 90 (N·mm/deg)

	Passive Path	IE+3deg	IE+5deg	IE-3deg	IE-5deg
Perturbation	142.9	15.1	11.5	232.0	212.0
Continuous	87.0	32.0	30.8	74.6	93.0

K_{ML} at Flexion 90 (N/mm)

	Passive Path	ML+2mm	ML-2mm
Perturbation	12.2	9.3	46.7
Continuous	-95.4	9.28	23.1

K_{PD} at Flexion 90 (N/mm)

	Passive Path	PD+0.5mm	PD-0.5mm
Perturbation	146.0	146.9	181.4
Continuous	2588.1	240.1	79.0

K_{VV} at Flexion 90 (N·mm/deg)

	Passive Path	VV+1deg	VV-1deg
Perturbation	440.6	210.2	551.5
Continuous	826.7	434.7	463.1

Specimen ID: PK200702

K_{AP} at Flexion 30 (N/mm)

	Passive Path	AP +1.5mm	AP+3mm	AP-1.5mm	AP-3mm
Perturbation	18.0	42.3	75.0	15.3	30.9
Continuous	2.1	17.5	73.5	4.1	17.3

K_{IE} at Flexion 30 (N·mm/deg)

	Passive Path	IE+3deg	IE+5deg	IE-3deg	IE-5deg
Perturbation	171.6	83.4	27.5	427.6	622.4
Continuous	33.5	32.5	-6.4	164.9	403.7

K_{ML} at Flexion 30 (N/mm)

	Passive Path	ML+2mm	ML-2mm
Perturbation	11.3	30.2	50.4
Continuous	9.7	26.7	35.4

K_{PD} at Flexion 30 (N/mm)

	Passive Path	PD+0.5mm	PD-0.5mm
Perturbation	231.7	79.2	117.2
Continuous	25.1	173.0	32.5

K_{VV} at Flexion 30 (N·mm/deg)

	Passive Path	VV+1deg	VV-1deg
Perturbation	1166.5	362.2	1111.7
Continuous	185.8	912.9	465.3

K_{AP} at Flexion 60 (N/mm)

	Passive Path	AP +1.5mm	AP+3mm	AP-1.5mm	AP-3mm
Perturbation	10.1	6.1	59.7	21.8	33.4
Continuous	4.7	6.1	44.5	14.5	20.8

K_{IE} at Flexion 60 (N·mm/deg)

	Passive Path	IE+3deg	IE+5deg	IE-3deg	IE-5deg
Perturbation	415.5	205.1	95.2	434.0	636.8
Continuous	52.3	57.3	99.4	209.7	325.3

K_{ML} at Flexion 60 (N/mm)

	Passive Path	ML+2mm	ML-2mm
Perturbation	34.4	50.0	6.0
Continuous	22.4	33.9	13.2

K_{PD} at Flexion 60 (N/mm)

	Passive Path	PD+0.5mm	PD-0.5mm
Perturbation	216.2	86.2	122.0
Continuous	18.4	162.3	23.1

K_{VV} at Flexion 60 (N·mm/deg)

	Passive Path	VV+1deg	VV-1deg
Perturbation	1317.7	317.8	1536.3
Continuous	776.9	934.5	529.7

K_{AP} at Flexion 90 (N/mm)

	Passive Path	AP +1.5mm	AP+3mm	AP-1.5mm	AP-3mm
Perturbation	21.1	18.6	82.2	8.5	39.2
Continuous	0.5	9.6	83.6	4.9	16.7

K_{IE} at Flexion 90 (N·mm/deg)

	Passive Path	IE+3deg	IE+5deg	IE-3deg	IE-5deg
Perturbation	493.3	177.0	205.4	520.6	647.2
Continuous	107.5	90.0	217.2	200.4	360.7

K_{ML} at Flexion 90 (N/mm)

	Passive Path	ML+2mm	ML-2mm
Perturbation	34.1	20.9	45.8
Continuous	20.2	15.7	28.0

K_{PD} at Flexion 90 (N/mm)

	Passive Path	PD+0.5mm	PD-0.5mm
Perturbation	155.3	45.4	57.0
Continuous	23.2	67.9	25.4

K_{VV} at Flexion 90 (N·mm/deg)

	Passive Path	VV+1deg	VV-1deg
Perturbation	1125.9	435.9	585.6
Continuous	429.2	1380.8	166.4

Appendix D Stiffness coefficients of ACL-Deficient Knee

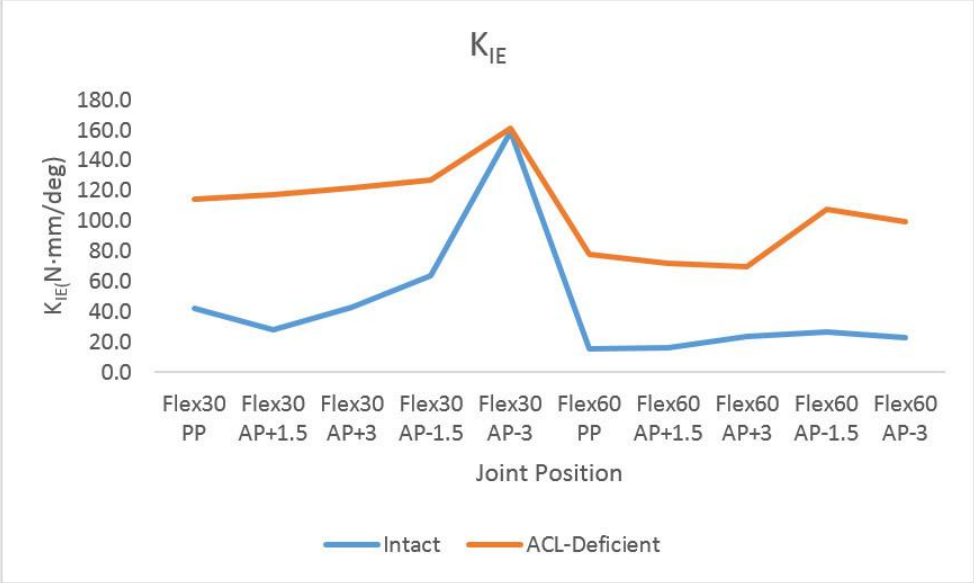

Appendix Figure 16 Primary stiffness on IE direction of both intact and ACL-deficient knee (ID: PK200702)

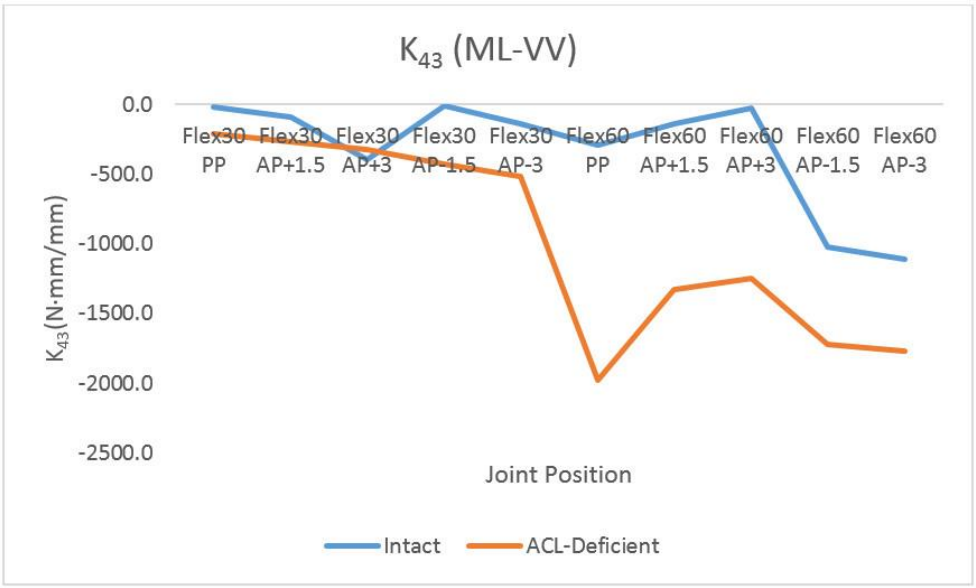

Appendix Figure 17 Secondary stiffness between ML and VV of both intact and ACL-deficient knee (ID: PK200702)

Bibliography

1. Kaneta, Y., Sasahara, N., Kusama, I., Suzuki, D., Ohkawa, H., & Hara, T. (2010). Injury Tolerance of Knee Joint Subjected to Dynamic Three-Point Bending. Journal of Biomechanical Science and Engineering, 5(2), 94-103.

2. Proffen, B. L., McElfresh, M., Fleming, B. C., & Murray, M. M. (2012). A comparative anatomical study of the human knee and six animal species. The Knee, 19(4), 493-499.

3. Takroni, T., Laouar, L., Adesida, A., Elliott, J. A., & Jomha, N. M. (2016). Anatomical study: comparing the human, sheep and pig knee meniscus. Journal of experimental orthopaedics, 3(1), 35.

4. Anyaehie, U. E., Ejimofor, O. C., Akpuaka, F. C., & Nwadinigwe, C. U. (2015). Pattern of femoral fractures and associated injuries in a Nigerian tertiary trauma centre. Nigerian journal of clinical practice, 18(4), 462-466.

5. Blankevoort, L., & Huiskes, R. (1996). A mechanism for rotation restraints in the knee joint. Journal of orthopaedic research, 14(4), 676-679.

6. Butler, D. L., Noyes, F. R., & Grood, E. S. (1980). Ligamentous restraints to anterior-posterior drawer in the human knee. J Bone Joint Surg Am, 62(2), 259-270.

7. Gollehon, D. L., Torzilli, P. A., & Warren, R. F. (1987). The role of the posterolateral and cruciate ligaments in the stability of the human knee. A biomechanical study. The Journal of bone and joint surgery. American volume, 69(2), 233-242.

8. Kaufer, H. (1971). Mechanical function of the patella. JBJS, 53(8), 1551-1560.

9. Flandry, F., & Hommel, G. (2011). Normal anatomy and biomechanics of the knee. Sports medicine and arthroscopy review, 19(2), 82-92.

10. Fox, A. J., Bedi, A., & Rodeo, S. A. (2012). The basic science of human knee menisci: structure, composition, and function. Sports health, 4(4), 340-351.

11. Grood, E. S., Noyes, F. R., Butler, D. L., & Suntay, W. J. (1981). Ligamentous and capsular restraints preventing straight medial and lateral laxity in intact human cadaver knees. JBJS, 63(8), 1257-1269.

12. Petersen, W., & Zantop, T. (2007). Anatomy of the anterior cruciate ligament with regard to its two bundles. Clinical Orthopaedics and Related Research®, 454, 35-47.

13. Fukubayashi, T., Torzilli, P. A., Sherman, M. F., & Warren, R. F. (1982). An in vitro biomechanical evaluation of anterior-posterior motion of the knee. Tibial displacement,

rotation, and torque. The Journal of bone and joint surgery. American volume, 64(2), 258-264.

14. Kohn, D., & Moreno, B. (1995). Meniscus insertion anatomy as a basis for meniscus replacement: a morphological cadaveric study. Arthroscopy: The Journal of Arthroscopic & Related Surgery, 11(1), 96-103.

15. Wascher, D. C., Markolf, K. L., Shapiro, M. S., & Finerman, G. A. (1993). Direct in vitro measurement of forces in the cruciate ligaments. Part I: The effect of multiplane loading in the intact knee. The Journal of bone and joint surgery. American volume, 75(3), 377-386.

16. Markolf, K. L., Slauterbeck, J. R., Armstrong, K. L., Shapiro, M. S., & Finerman, G. A. (1997). A biomechanical study of replacement of the posterior cruciate ligament with a graft. Part I: Isometry, pre-tension of the graft, and anterior-posterior laxity. JBJS, 79(3), 375-80.

17. Phisitkul, P., James, S. L., Wolf, B. R., & Amendola, A. (2006). MCL injuries of the knee: current concepts review. The Iowa orthopaedic journal, 26, 77.

18. Takahashi, M., Matsubara, T., Doi, M., Suzuki, D., & Nagano, A. (2006). Anatomical study of the femoral and tibial insertions of the anterolateral and posteromedial bundles of human posterior cruciate ligament. Knee Surgery, Sports Traumatology, Arthroscopy, 14(11), 1055-1059.

19. Van Dommelen, B. A., & Fowler, P. J. (1989). Anatomy of the posterior cruciate ligament: a review. The American journal of sports medicine, 17(1), 24-29.

20. Miller, M. D., & Thompson, S. R. (2014). DeLee & Drez's Orthopaedic Sports Medicine E-Book. Elsevier Health Sciences. 1047-1072

21. Race, A., & Amis, A. A. (1994). The mechanical properties of the two bundles of the human posterior cruciate ligament. Journal of biomechanics, 27(1), 13-24.

22. Parvizi, J., & Klatt, B. A. (Eds.). (2011). Essentials in total knee arthroplasty. SLACK Incorporated. 1-7

23. Warren, L. F., Marshall, J. L., & Girgis, F. (1974). The prime static stabilizer of the medial side of the knee. JBJS, 56(4), 665-674.

24. Wascher, D. C., Markolf, K. L., Shapiro, M. S., & Finerman, G. A. (1993). Direct in vitro measurement of forces in the cruciate ligaments. Part I: The effect of multiplane loading in the intact knee. The Journal of bone and joint surgery. American volume, 75(3), 377-386.

25. Zantop, T., Wellmann, M., Fu, F. H., & Petersen, W. (2008). Tunnel positioning of anteromedial and posterolateral bundles in anatomic anterior cruciate ligament reconstruction: anatomic and radiographic findings. The American journal of sports medicine, 36(1), 65-72.

26. Wilson, C. (2018). Back of knee. Knee pain explained. URL: https://www.knee-pain-explained.com/knee-ligaments.html

27. Wilson, C. (2018). Front of knee. Knee pain explained. URL: https://www.knee-pain-explained.com/knee-ligaments.html

28. Wilson, C. (2019). Tibiofemoral joint and patellofemoral joint of the knee. Knee pain explained. URL: https://www.knee-pain-explained.com/sharp-knee-pain.html

29. Piziali, R. L., Seering, W. P., Nagel, D. A., & Schurman, D. J. (1980). The function of the primary ligaments of the knee in anterior-posterior and medial-lateral motions. Journal of Biomechanics, 13(9), 777-784.

30. Seering, W. P., Piziali, R. L., Nagel, D. A., & Schurman, D. J. (1980). The function of the primary ligaments of the knee in varus-valgus and axial rotation. Journal of biomechanics, 13(9), 785-794.

31. Abulhasan, J. F., & Grey, M. J. (2017). Anatomy and physiology of knee stability. Journal of Functional Morphology and Kinesiology, 2(4), 34.

32. Andriacchi, T. P., Mikosz, R. P., Hampton, S. J., & Galante, J. O. (1983). Model studies of the stiffness characteristics of the human knee joint. Journal of biomechanics, 16(1), 23-29.

33. Bell, K. M., Rahnemai-Azar, A. A., Irarrazaval, S., Guenther, D., Fu, F. H., Musahl, V., & Debski, R. E. (2018). In situ force in the anterior cruciate ligament, the lateral collateral ligament, and the anterolateral capsule complex during a simulated pivot shift test. Journal of Orthopaedic Research®, 36(3), 847-853.

34. Butler, R. J., Crowell III, H. P., & Davis, I. M. (2003). Lower extremity stiffness: implications for performance and injury. Clinical biomechanics, 18(6), 511-517.

35. Bryant, J. T., & Cooke, T. D. V. (1988). Standardized biomechanical measurement for varus-valgus stiffness and rotation in normal knees. Journal of orthopaedic research, 6(6), 863-870.

36. Eagar, P., Hull, M. L., & Howell, S. M. (2001). A method for quantifying the anterior load–displacement behavior of the human knee in both the low and high stiffness regions. Journal of Biomechanics, 34(12), 1655-1660.

37. Fujie, H., Sekito, T., & Orita, A. (2004). A novel robotic system for joint biomechanical tests: application to the human knee joint. J. Biomech. Eng., 126(1), 54-61.

38. Hsu, W. H., Fisk, J. A., Yamamoto, Y., Debski, R. E., & Woo, S. L. (2006). Differences in torsional joint stiffness of the knee between genders: a human cadaveric study. The American journal of sports medicine, 34(5), 765-770.

39. Kang, S. H., Ren, Y., Xu, D., & Zhang, L. Q. (2014, August). Lower-limb multi-joint stiffness of knee and ankle. In 2014 36th Annual International Conference of the IEEE Engineering in Medicine and Biology Society (pp. 4009-4012). IEEE.

40. Loch, D. A., Luo, Z., Lewis, J. L., & Stewart, N. J. (1992). A theoretical model of the knee and ACL: theory and experimental verification. Journal of biomechanics, 25(1), 81-90.

41. Meleddu, A., Barrault, S., & Zysset, P. K. (2007). A rigorous method for evaluation of the 6D compliance of external fixators. Biomechanics and modeling in mechanobiology, 6(4), 253.

42. Miller, K. S., Edelstein, L., Connizzo, B. K., & Soslowsky, L. J. (2012). Effect of preconditioning and stress relaxation on local collagen fiber re-alignment: inhomogeneous properties of rat supraspinatus tendon. Journal of biomechanical engineering, 134(3).

43. Okada, Y., Teramoto, A., Takagi, T., Yamakawa, S., Sakakibara, Y., Shoji, H., ... & Yamashita, T. (2018). ACL function in bicruciate-retaining total knee arthroplasty. JBJS, 100(17), e114.

44. Panjabi, M. M., Brand Jr, R. A., & White III, A. A. (1976). Three-dimensional flexibility and stiffness properties of the human thoracic spine. Journal of biomechanics, 9(4), 185-192.

45. Piziali, R. L., Rastegar, J. C., & Nagel, D. A. (1977). Measurement of the nonlinear, coupled stiffness characteristics of the human knee. Journal of biomechanics, 10(1), 45-51.

46. Piziali, R. L., Rastegar, J., Nagel, D. A., & Schurman, D. J. (1980). The contribution of the cruciate ligaments to the load-displacement characteristics of the human knee joint.

47. Richards, D. P., Barber, F. A., & Herbert, M. A. (2005). Compressive loads in longitudinal lateral meniscus tears: a biomechanical study in porcine knees. Arthroscopy: The Journal of Arthroscopic & Related Surgery, 21(12), 1452-1456.

48. Schmitz, R. J., Ficklin, T. K., Shimokochi, Y., Nguyen, A. D., Beynnon, B. D., Perrin, D. H., & Shultz, S. J. (2008). Varus/valgus and internal/external torsional knee joint stiffness differs between sexes. The American journal of sports medicine, 36(7), 1380-1388.

49. Shamaei, K., Cenciarini, M., Adams, A. A., Gregorczyk, K. N., Schiffman, J. M., & Dollar, A. M. (2015). Biomechanical effects of stiffness in parallel with the knee joint during walking. IEEE Transactions on Biomedical Engineering, 62(10), 2389-2401.

50. Suggs, J., Wang, C., & Li, G. (2003). The effect of graft stiffness on knee joint biomechanics after ACL reconstruction—a 3D computational simulation. Clinical biomechanics, 18(1), 35-43.

51. Baumgart, F. (2000). Stiffness-an unknown world of mechanical science?. Injury-International Journal for the Care of the Injured, 31(2), 14-23.

52. Woo, S. L. Y., Orlando, C. A., Camp, J. F., & Akeson, W. H. (1986). Effects of postmortem storage by freezing on ligament tensile behavior. Journal of biomechanics, 19(5), 399-404.

53. Shultz, S. J., Shimokochi, Y., Nguyen, A. D., Schmitz, R. J., Beynnon, B. D., & Perrin, D. H. (2007). Measurement of varus–valgus and internal–external rotational knee laxities in vivo—part I: assessment of measurement reliability and bilateral asymmetry. Journal of orthopaedic research, 25(8), 981-988.

54. Ramsey, D. K., & Wretenberg, P. F. (1999). Biomechanics of the knee: methodological considerations in the in vivo kinematic analysis of the tibiofemoral and patellofemoral joint. Clinical Biomechanics, 14(9), 595-611.

55. Kato, Y., Ingham, S. J., Linde-Rosen, M., Smolinski, P., Horaguchi, T., & Fu, F. H. (2010). Biomechanics of the porcine triple bundle anterior cruciate ligament. Knee Surgery, Sports Traumatology, Arthroscopy, 18(1), 20-25.

56. Li, G., Rudy, T. W., Allen, C., Sakane, M., & Woo, S. L. Y. (1998). Effect of combined axial compressive and anterior tibial loads on in situ forces in the anterior cruciate ligament: a porcine study. Journal of Orthopaedic Research, 16(1), 122-127.

57. Kato, Y., Ingham, S. J., Kramer, S., Smolinski, P., Saito, A., & Fu, F. H. (2010). Effect of tunnel position for anatomic single-bundle ACL reconstruction on knee biomechanics in a porcine model. Knee Surgery, Sports Traumatology, Arthroscopy, 18(1), 2-10.

58. Howard, S., Zefran, M., & Kumar, V. (1998). On the 6× 6 Cartesian stiffness matrix for three-dimensional motions. Mechanism and machine theory, 33(4), 389-408.

59. Banerjee, J. R., & Fisher, S. A. (1992). Coupled bending–torsional dynamic stiffness matrix for axially loaded beam elements. International journal for numerical methods in engineering, 33(4), 739-751.

60. Ruggiu, M. (2012). Cartesian stiffness matrix mapping of a translational parallel mechanism with elastic joints. International Journal of Advanced Robotic Systems, 9(5), 195.

61. Turner, M. J., Clough, R. W., Martin, H. C., & Topp, L. J. (1956). Stiffness and deflection analysis of complex structures. journal of the Aeronautical Sciences, 23(9), 805-823.

62. Latash, M. L., & Zatsiorsky, V. M. (1993). Joint stiffness: Myth or reality?. Human movement science, 12(6), 653-692.

63. Boguszewski, D. V., Shearn, J. T., Wagner, C. T., & Butler, D. L. (2011). Investigating the effects of anterior tibial translation on anterior knee force in the porcine model: is the porcine knee ACL dependent?. Journal of Orthopaedic Research, 29(5), 641-646.

64. Xerogeanes, J. W., Fox, R. J., Takeda, Y., Kim, H. S., Ishibashi, Y., Carlin, G. J., & Woo, S. L. (1998). A functional comparison of animal anterior cruciate ligament models to the human anterior cruciate ligament. Annals of biomedical engineering, 26(3), 345-352.

65. Ohori, T., Mae, T., Shino, K., Tachibana, Y., Fujie, H., Yoshikawa, H., & Nakata, K. (2017). Varus-valgus instability in the anterior cruciate ligament-deficient knee: effect of posterior tibial load. Journal of experimental orthopaedics, 4(1), 24.

66. Inoue, M., McGurk-Burleson, E., Hollis, J. M., & Woo, S. L. Y. (1987). Treatment of the medial collateral ligament injury: I: The importance of anterior cruciate ligament on the varus-valgus knee laxity. The American journal of sports medicine, 15(1), 15-21.

67. Grood, E. S., & Suntay, W. J. (1983). A joint coordinate system for the clinical description of three-dimensional motions: application to the knee.

68. Chao, E. Y. (1980). Justification of triaxial goniometer for the measurement of joint rotation. Journal of Biomechanics, 13(12), 989-1006.

69. Keklikci, K., Yapici, C., Kim, D., Linde-Rosen, M., Smolinski, P., & Fu, F. H. (2013). The effect of notchplasty in anterior cruciate ligament reconstruction: a biomechanical study in the porcine knee. Knee Surgery, Sports Traumatology, Arthroscopy, 21(8), 1915-1921.

70. Ma, C. B., Kanamori, A., Vogrin, T. M., Woo, S. L., & Harner, C. D. (2003). Measurement of posterior tibial translation in the posterior cruciate ligament-reconstructed knee. The American journal of sports medicine, 31(6), 843-848.